REACTOR AND FUEL-PROCESSING TECHNOLOGY

A Quarterly Technical Progress Review

Prepared for DIVISION OF TECHNICAL INFORMATION, U. S. ATOMIC ENERGY COMMISSION,
by ARGONNE NATIONAL LABORATORY

Fall 1967

● VOLUME 10

● NUMBER 4

TECHNICAL PROGRESS REVIEWS

The United States Atomic Energy Commission publishes the Technical Progress Reviews to meet the needs of industry and government for concise summaries of current nuclear developments. Each journal digests and evaluates the latest findings in a specific area of nuclear technology and science. *Nuclear Safety* is a bimonthly journal; the other three are quarterly journals.

Isotopes and Radiation Technology
P. S. Baker, A. F. Rupp, and Associates
Isotopes Information Center, Oak Ridge National Laboratory

Nuclear Safety
Wm. B. Cottrell, W. H. Jordan, J. P. Blakely, and Associates
Nuclear Safety Information Center, Oak Ridge National Laboratory

Reactor and Fuel-Processing Technology
Argonne National Laboratory

Reactor Materials
E. M. Simons and Associates
Battelle Memorial Institute

All are available from the U. S. Government Printing Office. See the back cover for ordering instructions.

Availability of Reports Cited in This Review

United States Atomic Energy Commission (USAEC) reports are available at USAEC depository libraries and are sold by the Clearinghouse for Federal Scientific and Technical Information (CFSTI), National Bureau of Standards, U. S. Department of Commerce, 5285 Port Royal Road, Springfield, Va. 22151. All reports sold by CFSTI are $3.00 for printed copy and $0.65 for microfiche. Each separately bound part of a report is priced as a separate report. Some reports may not be available because of their preliminary nature; however, the information contained in them will generally be found in later progress or topical reports on the subject.

Other U. S. Government agency reports identified in this journal generally are available from CFSTI.

Private-organization reports should be requested from the originator.

United Kingdom Atomic Energy Authority (UKAEA) and Atomic Energy of Canada Limited (AECL) reports are available at USAEC depository libraries. UKAEA reports are sold by Her Majesty's Stationery Office, London; AECL reports are sold by the Scientific Document Distribution Office, Atomic Energy of Canada Limited, Chalk River, Ontario, Canada. UKAEA and AECL reports issued after March 1, 1967, are sold by CFSTI to purchasers in the United States and its territories.

Contents

Reactor and Fuel-Processing Technology
Vol. 10, No. 4, Fall 1967

Issued quarterly by the U. S. Atomic Energy Commission. Use of funds for printing this publication approved by the Director of the Bureau of the Budget on July 8, 1966.

Reactor and Fuel-Processing Technology

is a quarterly review of developments in reactor and reactor fuel technology. As such, this journal reports and interprets progress in the reactor field in terms of its significance to the reactor designer, operator, and fuel-cycle specialist. Articles either summarize and critically evaluate recently reported developments or review the "state of the art" of a particular topic. Both types of articles reference reports and publications that merit study; readers are urged to consult the references for additional information and the judgments of the original authors. If a reader has information that causes his evaluation to reinforce, modify, or contradict the opinions of our reviewers, he is encouraged to write to the Editor.

The scope of the journal encompasses:

CONCEPTS and APPLICATIONS: Progress in evaluating the applicability and economics of various reactor types and systems (including unconventional approaches), as well as of fuel resources and cycles, for utility central-station generation of electricity, auxiliary power, process radiation and heat, desalting, and propulsion—and for terrestrial, undersea, aerospace, and other advanced uses.

ANALYSIS and EXPERIMENTATION: Advancements in the techniques of reactor physics, fluid and thermal technology, energy conversion, fuel elements, materials, mechanics, control and dynamics, and reactor safety.

SYSTEMS and COMPONENTS: Experience as reflected in design and construction practice, components, systems technology, and operating performance of various specific types of reactors—including pressurized- and boiling-water reactors, molten-salt, organic-, gas-, and liquid-metal-cooled reactors, as well as generally applicable aspects of research and test reactors.

FUEL PROCESSING: Recent research and development on fuel aqueous processing, nonaqueous processing, waste disposal, and processing safety.

This journal is prepared by Argonne National Laboratory at the request of the Division of Technical Information of the U. S. Atomic Energy Commission. At Argonne, the Reactor Engineering Division (L. J. Koch, Director) and the Chemical Engineering Division (R. C. Vogel, Director) have the principal responsibility for the preparation of *Reactor and Fuel-Processing Technology*, with the regular assistance of the Reactor Physics Division (R. A. Avery, Director) and the Idaho Division (M. Novick, Director) and the occasional assistance of other divisions (Metallurgy, Chemistry, and Reactor Operations). Thus, unless noted otherwise, the reviewers and authors of articles are Laboratory staff members. The editors welcome interpretive review articles contributed by authors outside the Laboratory.

Letter to the Editor

Progressive Hydrogen Embrittlement

The article entitled "Hydrogen Embrittlement: A Reactor Safety Problem?" in *Power Reactor Technology and Reactor Fuel Processing*, 10(2): 102-110, describes—among other things—the progressive development of stress-induced cracks in hydrogenated steel specimens. A descriptive figure was included, but because of a production error, it may have been (and should have been) confusing. Darker gray rings were eliminated from cross sections in the figure. In fact, these darker rings are quite significant.

The correct illustration is shown here (courtesy of A. R. Troiano). It includes a curve—applied stress vs. fracture time—and three cross-sectional views. The curve is meant to be typical for identical test specimens of a high-strength steel that have been charged with hydrogen and should be interpreted as follows:

1. Below a certain stress level (the lower critical stress) the test specimens should not fail as a result of hydrogen embrittlement.
2. Above a certain stress level (the upper critical stress) failure should be rapid, the reduction in notch tensile strength being due to the presence of hydrogen.
3. At constant stress levels between the upper and lower critical stresses, delayed failure should result from hydrogen embrittlement.
4. Failure due to hydrogen embrittlement begins with a crack that occurs an "incubation time" after stress is applied; cracking proceeds in steps until the specimen fails.

(Letter continues on the next page.)

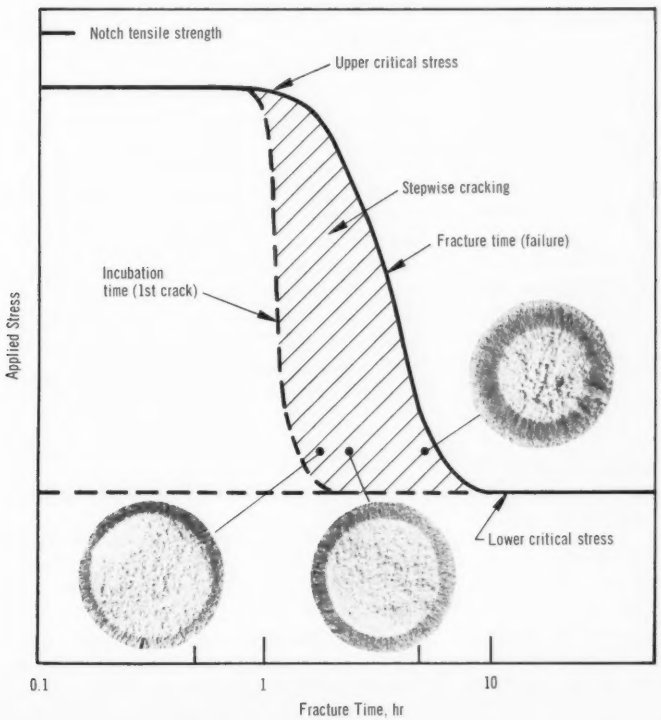

The steps to failure in a typical hydrogenated high-strength steel. Specimens of high-strength steel, all precharged in the same internal concentration of hydrogen, show a dependence of time to failure on the applied stress level. Under stress the hydrogen concentration in a specimen builds up locally near the root of a notch by preferential diffusion. A crack begins when a critical combination of stress and hydrogen concentration is achieved. The cross sections show three tests at equal stress levels which were stopped at different times before failure and then broken to show progressive hydrogen embrittlement.

The incubation period, the time required for preferential diffusion to build a critical hydrogen concentration in the stressed specimen, can be measured with equipment that detects a change in the electrical resistance through the specimen. Usually this initial crack is small, but a new (and more intense) peak stress situation is set up near its root, preferential diffusion takes place, and another step in the crack follows quickly. The process is repeated (sometimes a sequence of clicks is clearly audible) until the cross section is reduced to the point where the breaking stress is reached, and the specimen fractures.

The three cross sections are of identically charged specimens that have been stressed at one level for various times, then fractured and photographed. In the cross section, the change in fracture surface is apparent between the outer darker-gray section, broken because of critical hydrogen concentration, and the inner section, where fracturing was caused by stress alone. Equally apparent — from the increasing size of the darker-gray rings — is the progressive nature of hydrogen embrittlement.

A. David Rossin
Adlai Stevenson Institute
of International Affairs

The Evolution of Hot-Channel Factors for Shippingport Reactor Cores

By Richard Atherton, Westinghouse Electric Corporation

Each thermal designer of reactor cores has his own convictions as to what hot-channel factors he should use (to account for unfavorable phenomena in the thermally limiting coolant channel), what the magnitude of his various factors should be, and what mathematical method he should use to obtain an overall factor. This article is concerned not with changing that situation, but rather with illustrating the evolution of hot-channel factors over a period of about 10 years for one particular operating power reactor.

The hot-channel factors of the first reactor core at the Shippingport Atomic Power Station, PWR Core 1 Seed 1, were established and used by the methods described in Ref. 1. In the intervening decade the kinds of hot-channel factors needed and the methods of calculating and using hot-channel factors have changed as core thermal-design techniques have evolved from hand calculations to complex computer programs. Increased understanding of boiling flow has permitted relaxation of thermal limitations which, in turn, has changed the emphasis on the various hot-channel factors. In addition, by describing certain phenomena explicitly in the design analyses, some hot-channel factors have been eliminated. The result of these developments has been a significant contribution to the overall technical effort that more than doubled core power level [from 231 to 505 Mw(t)] and density.

Station Background

The Shippingport Atomic Power Station, at Shippingport, Pa., was first operated at full 231-Mw(t) power in December 1957. The uprated 505-Mw(t) seed-and-blanket cores operate in pressurized water without bulk boiling in the steady state. The highly enriched fuel in the seed of a seed-and-blanket core provides neutrons for the fissioning of the natural-uranium fuel of the blanket by the leakage of the neutrons across the boundary of the seed. Four seeds were used with the blanket of PWR Core 1 between 1957 and 1964. The blanket of PWR Core 2, currently in operation with its first seed, was designed to operate for two seed lifetimes. However, Core 2 seed lives are expected to be about twice those of Core 1.

Operating experience with PWR Core 1 is summarized in Refs. 2 to 4. Operating experience with PWR Core 2 is discussed in Ref. 5. Core cross sections and fuel-element assemblies are shown in Figs. 1 to 6.

Hot-Channel Factors for Core 1

The original hot-channel factors for design of the first seed (PWR Core 1 Seed 1) are given in Table 1 for the seed and in Table 2 for the blanket. These factors are applied to the heat flux, coolant temperature or enthalpy rise, or fluid-film temperature rise as appropriate, in the coolant channel of the core designated as most limiting thermally.[6] The symbol F in Tables 1 and 2 represents a hot-channel factor with the subscripts ΔT, θ, and q identifying the factors as applying to coolant temperature rise, fluid-film temperature rise, and heat flux. It is assumed that all the unfavorable phenomena occur simultaneously in the hot channel, and at the same location (the "hot spot"), unless it can be proven otherwise.

ENGINEERING FACTORS FOR THE SEED

Phenomena for which the factors of Table 1 were devised to account include flow distribution, dimensional variations, and thermal effects.

Flow Distribution. The factor for flow distribution accounted for the possibility that the hot channel might have less flow than the average channel because of nonuniformities of flow in the inlet plenum to the reactor vessel; the result would be an increase in the temperature rise of both coolant and film.

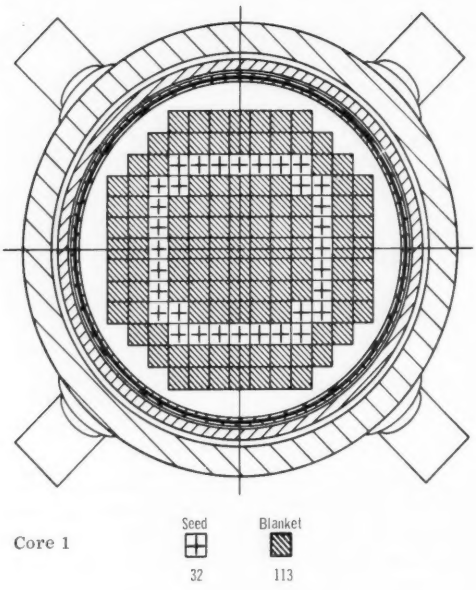

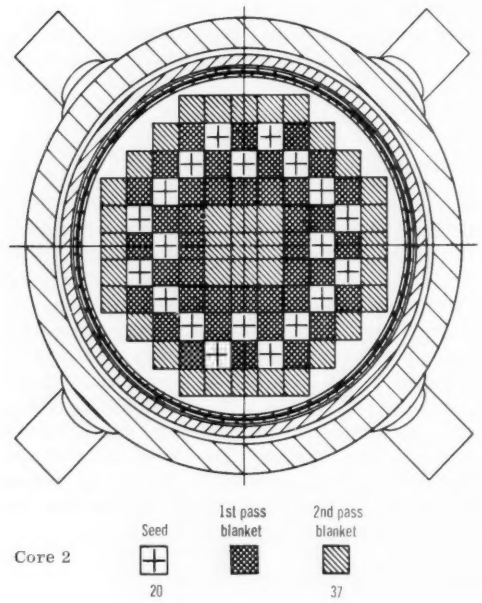

Fig. 1 Core cross sections for the Shippingport PWR. Core 1, at top, has a 6-in. square pitch and contains 145 fuel assemblies and 32 control rods. Core 2, at bottom, has a 7.5-in. square pitch and contains 97 fuel assemblies and 20 control rods.

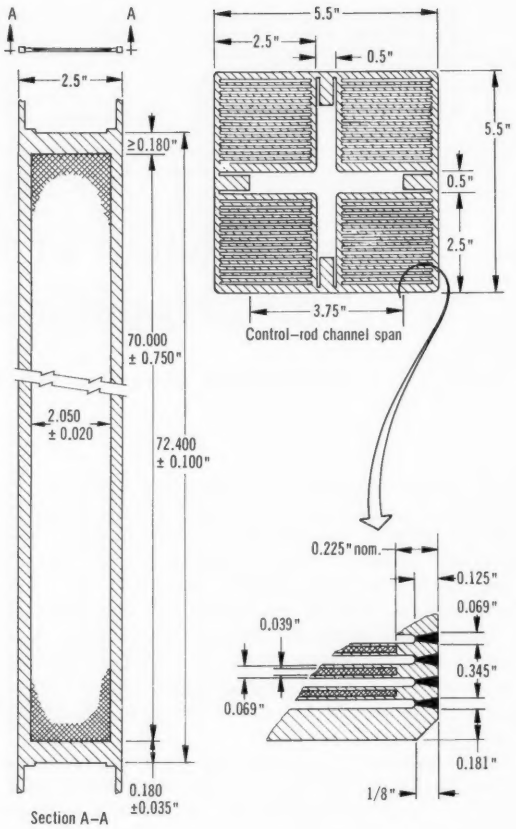

Fig. 2 Fuel cluster for PWR Core 1 Seed 1 has plates that contain highly enriched uranium dioxide within 0.039-in.-thick zirconium-alloy walls.

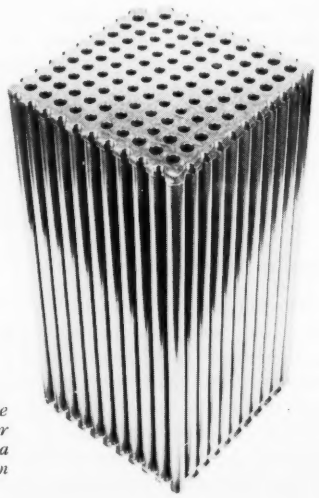

Fig. 3 Fuel bundle for PWR Core 1 blanket has 120 rods. One corner position in each bundle houses a failed-element detection and location (FEDAL) system.

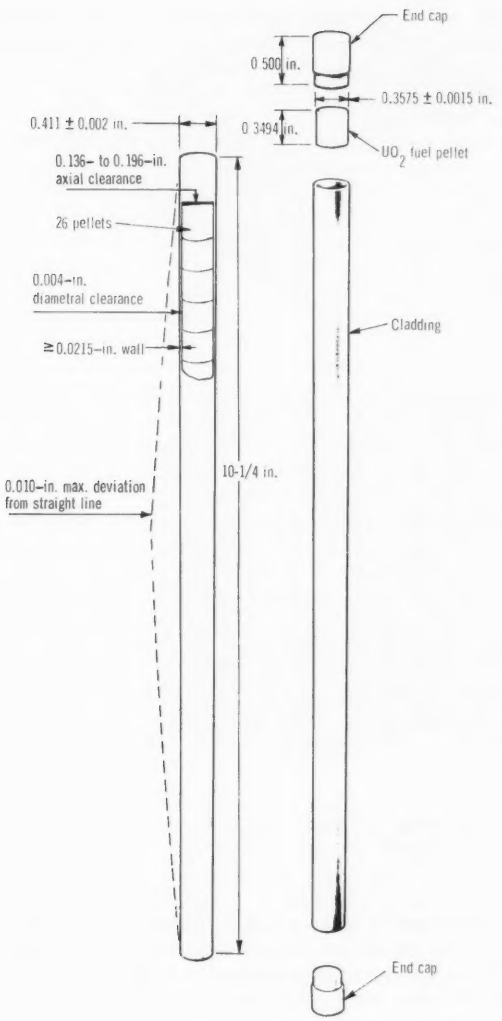

Fig. 4 Rods for the blanket of PWR Core 1 were made from zirconium-alloy tubes and natural uranium dioxide pellets.

Dimensional Variations. The next four factors listed in Table 1 all account for the effects of having dimensions at the maximum or minimum values permitted by manufacturing tolerances. If the "meat," the fuel alloy sandwiched between the two pieces of cladding, is at the maximum thickness, all three hot-channel parameters (ΔT, θ, and q) will be increased by the additional heat generated as compared to a plate with nominal-thickness meat. The same is true with a maximum concentration of enriched uranium in the meat. In addition, meat can become eccentrically located in the plate if the hot-channel-side cladding is at the minimum thickness while the cladding adjacent to the neighboring channel is at the maximum thickness; thus more than half of the heat generated would be forced into the hot channel.

Thermal Effects. The last three engineering factors of Table 1 apply to both plates forming the hot-channel boundaries. If the channel thickness is at the minimum value, the flow in the hot channel will be reduced with consequent increases in coolant and film temperature rises. The factor for "heat-transfer correlation" accounted for the scatter in the data establishing the correlation by which the film coefficient of heat transfer was calculated. The favorable factors (i.e., those having values less than unity) accounted for the effect of heat leakage from the end of the fuel plate into the subassembly (of plates) box structure, and for the fact that the end channel would cool the second plate more than an average amount because the end (first) plate was a structural member which contained no fuel (Fig. 2). "End conduction" is based on knowledge that the peak heat generation was at the edge of the fuel plate, whereas "end coolant channel" requires that the hot channel be the one adjacent to the end channel.

NUCLEAR FACTORS FOR THE SEED

The first two nuclear factors in Table 1 were the conventional radial and axial nuclear peaking factors applied to the average power generated in the core to obtain the local maximum. In addition to these, a separate local factor was applied for water-hole peaking because the peak would shift from the control-rod channel water (control rod out) to the inter-cluster water gap (control rod in). Thus two values of the water-hole peaking factor would be applied at one radial location, one above the control-rod tip and one below it. The blanket-rod end cap was made of unfueled zirconium alloy; the absence of fuel would therefore cause a local flux peak which would affect the adjacent seed cluster at the locations of the six interfaces between the seven blanket fuel bundles in an assembly.

ENGINEERING FACTORS FOR THE BLANKET

In Table 2 the first five factors account for the same effects as in Table 1 with the fuel-pellet diameter replacing meat thickness because of the different kind of fuel element (natural uranium dioxide pellets contained in tubes, as seen in Figs. 3 and 4). The factor for pitch, bowing, and rod diameter is equivalent to that for channel thickness in the seed. The blanket "channel" model used in thermal and hydraulic analysis was all the coolant space inside a boundary formed by connecting the centers of four adjacent rods by straight lines, the rods being on a square pitch. The bundles contained 120 rods in an 11 by 11 array.

One corner rod was omitted from each bundle to provide space for tubing which was part of the Failed

Element Detection and Location (FEDAL) system. The absence of fuel again caused local power peaking. The factor for cooling effectiveness accounted for that amount of coolant not inside the channel boundary described above. This coolant flowed around the periphery of the fuel bundles and between the bundles and the zirconium-alloy shell which supported them in the core.

The factor for differential orificing accounted for the increased flow at the thermally limiting locations arranged for by providing larger orifices in the flow paths to those locations. In a typical blanket fuel bundle, the two outer rows of orifices on all four sides are larger in diameter than the other orifices.

NUCLEAR FACTORS FOR THE BLANKET

The nuclear factors for the blanket accounted for the same effects as in the seed. Blanket assemblies were orificed at the inlets to provide four distinct flow regions consistent with the variation in power generation throughout the blanket; therefore different nuclear factors were applied in these regions. The fact that the radial peaking factor in Region 4 was less than unity was a consequence of the much lower than average power generation in Region 4, so that even the peak power in Region 4 was lower than the average power of the blanket as a whole.

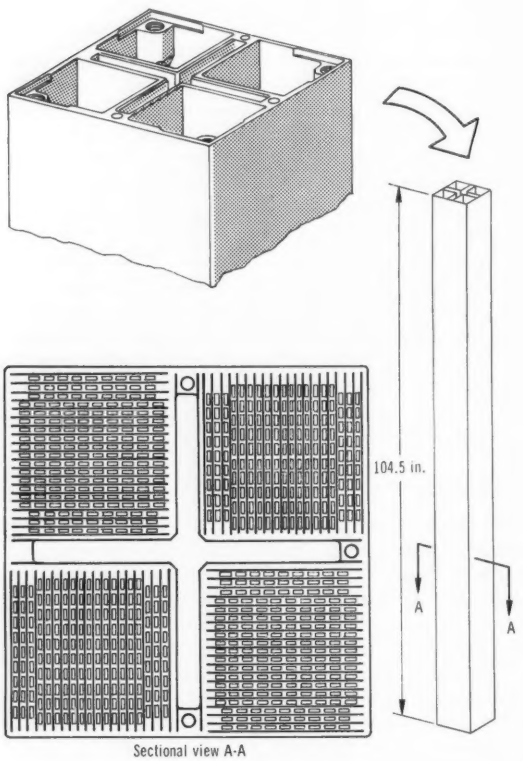

Fig. 5 Seed fuel clusters for PWR Core 2 are made of zirconium-alloy plates that contain 1.5- by 0.25- by 0.1-in. fuel wafers in separate compartments. Each seed wafer is a mixture of enriched uranium dioxide and zirconium dioxide.

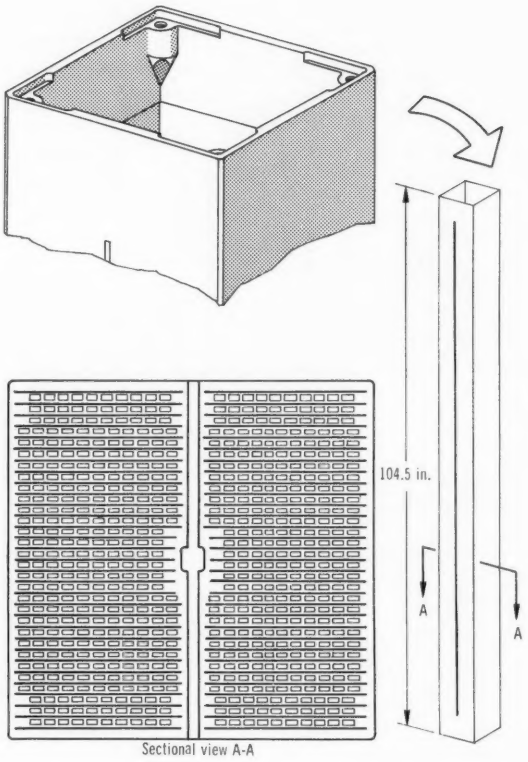

Fig. 6 Blanket fuel clusters for PWR Core 2 contain plates similar to those for the seed, but blanket wafers are natural uranium dioxide.

Design Changes

During the period 1957 to 1959, which coincided with the startup and operation[2] of PWR Core 1 with Seed 1, a number of changes occurred in design techniques and new experimental information became available in both the nuclear- and thermal-design disciplines. Both disciplines improved their analytical models and programmed the analyses for computer solutions.

NUCLEAR REFINEMENTS

In nuclear design, one of the advances was a three-dimensional description of the core power distribution which included all the nuclear factors listed in

Tables 1 and 2. These power distributions were and are input to the thermal-design calculation at nominal values, since all identified perturbations that cause power peaks are already included in the nuclear code output. These calculations are verified by critical experiment for the beginning-of-life power distributions within the accuracy of the instrumentation.

During core lifetime, observations of the nuclear characteristics of the operating reactor are used to make any necessary modifications to the predictions of power distributions. Observations made during operation of the reactor with in-core thermocouples and flowmeters verify, within the accuracy of the instrumentation, that the modified nuclear-design calculations describe the core power distributions without significant bias.[2–5] Therefore the nominal nuclear power distributions as modified by observations during operation are considered to be the proper values for use as input to the thermal-design calculation. Adequate conservatism with respect to thermal margin is provided by the use of the hot-channel concept.

THERMODYNAMIC REFINEMENTS

Programming of the thermodynamic equations of the core for steady-state and transient operation resulted in the elimination of three hot-channel factors for phenomena which could now be easily described explicitly in the calculation, namely, those for channel thickness, flow distribution, and heat-transfer correlation.

Channel Thickness. Channel thickness is now entered directly as code input, the hot-channel value being either the minimum of the tolerance range specified on the design drawing or the minimum as-measured value. The latter is preferred when it becomes available. Channel thickness measurements are made and recorded for all core fuel assemblies used at Shippingport. Refinements can and have been made in the calculation by evaluating local as-measured narrowings of channels at the specific elevation or radial position at which they occur. For example, local axial narrowings can be selectively assembled so that the thermal consequence is minimized. The usual result is that the fuel assembly is inserted in the core so that the local narrowing is near the bottom of the core, an arrangement that minimizes boiling in the narrowest portion of the channel and thus reduces the effect of two-phase pressure drop. In other words, since boiling is most prevalent in the upper part of the core (coolant flows upward), it would then occur in the wider part of the channel and thus cause less friction pressure drop than if it occurred in the narrower part of the channel. Radial selective assembly can be accomplished by rotating the fuel assembly so that the narrowed channel is in the position of lowest power generation. Hence the use of the channel thickness explicitly permits increased

Table 1 HOT-CHANNEL FACTORS FOR THE SEED AT THE BEGINNING OF CORE 1 LIFE

Type of factor	Coolant temp. rise, $F_{\Delta T}$	Fluid-film temp. rise, F_θ	Heat flux, F_q
Engineering			
Flow distribution	1.07	1.06	1.00
Meat thickness variation	1.05	1.13	1.13
Fuel concentration	1.02	1.04	1.04
Meat eccentricity	1.05	1.14	1.14
Channel thickness	1.10	1.11	1.00
Heat-transfer correlation	1.00	1.25	1.00
End conduction from fuel	0.95	0.95	0.95
End coolant channel	0.97	0.95	0.95
Product	1.22	1.77	1.21
Nuclear			
Maximum to average, radial	1.25	1.25	1.25
Maximum to average, axial		2.00	2.00
Maximum to average, water hole	1.29	1.29	1.29
Blanket end-cap effect		1.09	1.09
Product	1.61	3.51	3.51

Table 2 HOT-CHANNEL FACTORS FOR THE BLANKET AT THE BEGINNING OF CORE 1 LIFE

Type of factor	Coolant temp. rise, $F_{\Delta T}$	Fluid-film temp. rise, F_θ	Heat flux, F_q
Engineering			
Flow distribution	1.07	1.06	1.00
Fuel diameter	1.01	1.01	1.01
Fuel concentration (1.01 density, variation, 1.002 concentration variation)	1.01	1.01	1.01
Meat eccentricity	1.02	1.03	1.03
Heat-transfer correlation	1.00	1.25	1.00
Pitch, bowing, and rod diameter	1.11	1.14	1.00
Absence of one fuel rod (for FEDAL system)	1.01	1.01	1.01
Cooling effectiveness	1.06	1.05	1.00
Differential orificing	0.87	0.89	1.00
Product	1.16	1.49	1.06
Nuclear			
Maximum to average,* radial			
Region 1	1.24	1.24	1.24
Region 2	1.94	1.94	1.94
Region 3	1.82	1.82	1.82
Region 4	0.90	0.90	0.90
Maximum to average,* axial			
Region 1		1.77	1.77
Region 2		2.00	2.00
Region 3		2.00	2.00
Region 4		1.77	1.77
Maximum to average,* bundle depression, all regions	1.24	1.28	1.28
End-cap peaking, all regions		1.18	1.18
Product			
Region 1	1.54	3.33	3.33
Region 2	2.40	5.85	5.85
Region 3	2.25	5.49	5.49
Region 4	1.11	2.41	2.41
Overall factors			
Region 1	1.78	4.95	3.52
Region 2	2.77	8.71	6.19
Region 3	2.60	8.17	5.80
Region 4	1.29	3.58	2.54

*Average of the entire blanket region.

design flexibility as compared to use of a hot-channel factor.

Flow Distribution. The factor for flow distribution has been replaced by entering a reduced flow or pressure drop for the hot channel into the code input. For steady-state calculations this has almost the same effect as the use of a hot-channel factor, but during transients a more exact description of the channel parameters is obtained. Once boiling begins in the hot channel (with the average channel still in one-phase liquid flow), the hot-channel-flow coastdown following pump failure is more rapid than the average-channel-flow coastdown, with an increasing rate of divergence. The hot-channel factor for flow distribution thus becomes a variable once boiling starts. Using a lower initial flow or pressure drop in the hot channel eliminates the need for evaluating the variable hot-channel factor.

Heat Transfer. The factor for heat-transfer correlation has been replaced by entering the film coefficient into the program as a conventional equation with a conservative value of the constant coefficient which is applied to the product of the fractional powers of the Reynolds and Prandtl numbers. In this way the film coefficient of heat transfer can be calculated for each hot-channel meshpoint at each time step, a considerable refinement over the use of a hot-channel factor.

CRITICAL-HEAT-FLUX CORRELATIONS

During this same period (1957 to 1959), reliable correlations for CHF (Critical Heat Flux, also referred to as "departure from nucleate boiling" and "burnout") and friction pressure drop in two-phase flow became available and permitted extension of the thermal limitation past the initiation of boiling into boiling conditions during accidental transients.

Extended Limits. The new limitation, replacing the avoidance of bulk boiling, became avoidance of CHF, as described by a design limit curve. The design limit curves for CHF are expressed in terms of heat flux and enthalpy with a parametric effect of mass flow rate and were the lower bounds of the data points on which the correlation was based. Similarly, a design limit curve expressing the two-phase friction factor as a multiplier of the isothermal liquid-phase friction factor was used to compute pressure drop for the flowing steam–water mixture. This design limit curve was the upper bound of the data on which the correlation was based. Thus two-phase flow could be predicted conservatively, as could the margins in flow, heat flux, and enthalpy to CHF. These correlations were included directly into the core thermodynamic computer codes. Since the correlations were conservatively stated, and were included directly in the calculation, there was no need of additional hot-channel factors for heat-transfer correlations.

Channel-Temperature Rise. The new limitations changed the relative importance of the hot-channel factors and of the explicit calculations which have replaced some of them. For example, if consideration is limited to channel coolant conditions (assuming fuel-element temperatures prior to CHF are satisfactorily low), the emphasis in avoiding bulk boiling is on the factors affecting total channel coolant temperature rise, and the local factors for heat flux become relatively unimportant. The integral under the axial flux shape determines the total coolant temperature rise, and so the axial flux peak is not of concern, again assuming no fuel temperature problems there.

The Importance of Flux Shape. In two-phase flow the friction factor is much higher than in liquid-phase flow, so that the longer the length of boiling in the channel the higher will be the pressure drop, or, if channel pressure drop is fixed, the lower will be the flow.

For the same integral power, the axial shape with a peak low in a core with upflow of coolant will cause boiling sooner than an axial shape with a peak high in the core. Boiling occurs in both cases at the same fraction of the integrated power, but this fraction occurs lower if the power is concentrated lower in the core. Then a longer length of channel will be subject to the high two-phase friction factor, rather than to the low single-phase factor, and flow, for a fixed pressure drop, is much smaller (than for the case where the power is concentrated in the upper part of the core). Thus the axial flux shape became highly significant to the calculation of coolant exit conditions. Since the CHF correlations are flux dependent, and the location of CHF is usually near the channel exit, a peak low in the core is more favorable from a flux viewpoint than one high in the core, in contrast to the boiling consideration. This is usually a lesser effect than the reduction of flow due to length in boiling.

Testing and Evaluation Techniques. Concurrently with the development of correlations, other modifications of the hot-channel factors were in progress. During the design of a core, the numerical values of the hot-channel factors are usually set on the basis of limit calculations which provide assurance that the actual values are not greater than those selected. By "limit" calculation is meant a simple approximation based on assumptions that assure that the most limiting possible value results. Thus the hot-channel factors tend to have conservative values. This degree of conservatism is established by tests that are frequently run to evaluate sensitive parameters.

Model Tests of Conservatism. A test aimed at establishing the value of the factor for flow distribution

(or the fraction of average cluster flow which is input to the code as hot cluster flow) is reported in Ref. 7; this flow-distribution test, which was performed on a scale model of PWR Core 1 utilizing air as a test fluid, showed that the maximum variation in flow of any seed cluster from average cluster flow was 2% of the average, as compared with the 7% allowed in Table 1. However, during this period, other tests had shown that distribution of flow from channel to channel within a cluster was not negligible, although less than 3% of the total flow for the PWR Core 1 seeds.

Applying Statistics. Another conservatism in the hot-channel concept is the method which specifies that the product of all the individual factors should form the overall hot-channel factor. Methods of statistically combining hot-channel factors are conventionally sought to reduce this conservatism. The problem here is to find an acceptable probability of an event that leads to acceptable consequences.

In the Shippingport program the acceptable probability was established at 0.0001 for the acceptable event that was the simultaneous combination of the most unfavorable tolerance of the fuel-element dimensions within a single fuel element, namely, enriched-uranium concentration in the meat, thickness of the meat, and eccentricity of the meat. For operation of Core 1 with Seeds 2, 3, and 4, these values had been increased (above those in Table 1) because of a reduction in seed fuel-element thickness, while the same manufacturing tolerances were retained, so that the tolerance became a larger percentage of the fuel-element dimensions. The product of these three individual hot-channel factors in the seeds subsequent to Seed 1 was 1.18. However, the probability that a value greater than 1.05 would occur was established at less than 0.0001.

Fuel-element failure was not an expected consequence of this event which might occur no more than once in 10,000 fuel elements (about 2200 in each seed). It was judged that there was sufficient conservatism in the remainder of the calculation method to assure core safety despite a direct combination of these factors. For example, the probability that this event (maximum concentration and thickness in fuel with maximum eccentricity) would occur in the narrowest channel and at the peak power location in the core was much smaller than 0.0001.

Other examples of the conservatisms are the utilization as a design limit of the bounds of the data forming both the CHF and two-phase pressure-drop correlations, and the assumption that the reactor was operating with the worst possible combination of instrument errors and at the worst control-band positions. More conservatisms occur in the ways in which designers construct their analytical models and the ways in which manufacturing data are reported. The designer, at a point of choice, will always choose the more conservative alternative, as a detailed review of design models will disclose. Many manufacturing dimensions are also reported conservatively and include the maximum inaccuracy of the measuring device.

Results. As a consequence of the air flow test and the statistical analysis, for operation of PWR Core 1 with Seeds 3 and 4, the fraction of average channel flow rate in the seed hot channel was increased from 0.93 to 0.95, and the combined hot-channel factor for fuel-element parameters was decreased from 1.17 to 1.05.

Hot-Channel Factors for Core 2

Seed and blanket hot-channel factors for PWR Core 2 which are comparable to those of PWR Core 1 are given in Table 3. The values in Table 3 for *average* heat flux can be seen to be significantly smaller than the $F_{\Delta T}$ factors in Tables 1 and 2 for PWR Core 1, to which the Core 2 "average flux" factors are equivalent. In fact, the fourth significant figure has become a significant percentage of the effect accounted for and is therefore included. The reason for the small values lies in the nature of the fuel elements, Figs. 5 and 6; these elements are particularly susceptible to statistical analysis.

Table 3 CORE 2 HOT-CHANNEL FACTORS FOR BLANKET AND SEED

Factors	Blanket		Seed	
	Average heat flux, $F_{\phi av.}$	Local heat flux, $F_{\phi loc.}$	Average heat flux, $F_{\phi av.}$	Local heat flux, $F_{\phi loc.}$
Seed 1				
Fuel thickness	1.003	1.025	1.030 (loading factor)	1.050 (loading factor)
Fuel concentration	1.021	1.031		
Fuel eccentricity	1.019	1.027	1.016	1.025
Combined factors	1.043	1.085	1.046	1.076
Seed 2				
Fuel thickness	1.003	1.025	1.034 (loading factor)	1.050 (loading factor)
Fuel concentration	1.021	1.031		
Fuel eccentricity	1.019	1.027	1.016	1.025
Combined factors	1.043	1.085	1.050	1.076

CORE 2 FUEL

A Core 2 fuel element is fabricated by machining a zirconium-alloy plate into compartments into which are placed wafers made from natural uranium dioxide (for the blanket), or enriched uranium dioxide combined with zirconium dioxide as a diluent (for the seed). The individual wafers, 1.5 in. long by 0.25 in. wide by 0.1 in. thick in the blanket and 1 in. long by 0.25 in. wide by 0.036 in. thick in the seed, are separated from each other in the compartment by zirconium-alloy shims placed at the ends of the wafers. A zirconium-alloy cover plate is placed over the top of the receptacle plate containing compartments loaded with wafers and is bonded to the receptacle by gas pressure (10,000 psi at ~1500° F). The result is that each wafer is, in effect, individually compartmented.

Fuel Thickness and Concentration. Individual compartmenting makes each wafer independent of every other wafer with respect to fuel thickness and fuel concentration, provided that there is no manufacturing bias. Therefore it is no longer necessary to assume that all the wafers in both plates bounding the hot channel have the maximum thickness and fuel concentration permitted by the design tolerances on these parameters.

Statistical analysis can be used to determine the maximum probable average thickness of the wafers in a plate, as well as the maximum average fuel concentration. These dimensions, which are significantly smaller than those permitted by tolerance, are then used to calculate hot-channel factors for average heat flux. The hot-channel average heat flux is used only to calculate the hot-channel enthalpy rise. Since this is an integrated effect of heat flux, local individual wafers can still be at the maxima allowed by the tolerances without affecting the results. The statistical analysis accounts for the effect on enthalpy of those wafers which are not at the maxima as well. By the same reasoning, this type of statistical analysis does not apply to hot-channel factors for local heat flux. Local heat flux is defined for CHF evaluation as the heat flux averaged over one-quarter of a wafer; the probability that a quarter wafer has maximum dimensions is high.

If there is a normal distribution of wafer dimensions in either seed or blanket, the most probable deviation (of the dimensions of a sample of these wafers) from nominal (also most probable) over the length of a single fuel element can be obtained by conventional statistical methods. This most probable deviation in the unfavorable direction was taken as the average dimension used to establish the hot-channel factors for average heat flux. Again, the fact that individual wafers may have larger deviations does not matter, since as many will have smaller deviations if the distribution is normal. The as-built distributions of the wafers were found to be normal.

Calculating Average-Heat-Flux Factors. A single approach was applied to all the factors for average heat flux in the seed and the blanket. To illustrate: a typical blanket fuel element (Fig. 5) contains 620 wafers in 10 rows of 62 wafers. Because the thermal analysis of Core 2 considers each of the 10 rows and the coolant flow adjacent to each row as independent subchannels, with coolant interchange between subchannels, the 62 wafers in a row were used as the sample population on which a statistical analysis was based. The plate forming the other channel boundary was ignored, so sample size was reduced. This procedure was conservative because the dimensional deviation from nominal decreases as sample size increases.

In retrospect, the statistical analysis used in Core 2 to evaluate the hot-channel factors for average heat flux could have been applied to the fuel pellets in the blanket of Core 1 for the effect on enthalpy rise ($F_{\Delta T}$) of the pellet diameter and fuel concentration. It would probably not be desirable to apply statistics to the eccentricity factor, since it is not improbable that pellets in a stack are all eccentric in the same direction.

CORE 2 VS. CORE 1 FACTORS

The factors for average fuel thickness and concentration listed in Table 3 for Core 2 (blanket and first seed) are based on as-built manufacturing data, rather than design, and thus include the effects of manufacturing biases, which generally caused lower hot-channel factors. The hot-channel factors for *local* heat flux listed in Table 3 are comparable to those equivalent factors for the Core 1 blanket in Table 2. The factors for thickness (diameter) are lower than the corresponding seed factors for *Core 1* (Table 1) because the oxide pellet and wafer dimensions are more closely controlled than are those of the fuel alloy of the Core 1 seed. The factors for eccentricity with the oxide are lower because the contact conductance between oxide and cladding, rather than the cladding thermal resistance, controls the distribution of heat flux to the two sides of the plate and is not significantly affected by eccentricity if the oxide is in contact with the cladding, as is the case of operating temperatures for PWR cores at Shippingport.

Seed and Blanket Differences. Table 3 shows that the factors for fuel thickness and fuel concentration are combined in the seed into a "loading factor." This combining occurred because the required specification for fuel loading of individual fuel assemblies could not be met by the tolerances on thickness and fuel concentration of individual wafers. Therefore the wafers are weighed to determine fuel loading. The factor on local heat flux consists of 1.03 for weighing and 1.02 for fuel concentration. Since the blanket wafers were so much thicker (0.100 in.) than the seed wafers (0.036 in.) and were made to the same

tolerance, this problem did not arise in the manufacture of the blanket. This characteristic also contributed to the very low blanket factor for average heat flux based on wafer thickness.

As has already been stated, the Core 2 factors are applied to average heat flux rather than coolant temperature or enthalpy rise. The end result on the coolant parameters would be the same for steady-state operation, but during a transient the coolant parameters can now be calculated directly, not obtained by applying a factor. The factors for film temperature rise do not appear in Table 3 because this quantity is now calculated directly as a function of space and time in the hot channel where the factors for local heat flux have been applied.

End Effects. Comparison of Table 3 with Table 1 reveals that two hot-channel factors with values less than unity were used for Core 1 but were not used for Core 2. Both these factors were eliminated for specific design reasons. The factor for end conduction into the structure was applied directly in the nuclear-design calculation to minimize the local power peaking of the edge track of wafers. In other words, the nuclear power peaking factor at the edge of the outermost wafer is converted into a thermal peaking factor of lower value because of end conduction effects that can be demonstrated by validated analytical techniques for evaluation of two-dimensional heat conduction. The factor for the effect of the end channel did not apply to Core 2 because, in the pursuit of high performance, the end channel was made narrower than the internal channels, in contrast to Core 1 in which all seed channels had the same dimensions. The narrowing, combined with subsequent discoveries that having one wall of a channel relatively unheated reduced the average cooling effectiveness of the coolant in the end channel, resulted in equal heat fluxes from both sides of the first fuel plate with a resultant factor of 1.00 for the end-channel effect.

Flow. The allowances required for flow maldistributions for PWR Core 2 were determined by tests.[8,9] Among the results of the tests described in Ref. 8 is that all the fuel assemblies of a given flow region have flows within 1% of the average flow for that region. Prior to the test, the design value of the factor for flow maldistribution had been calculated to be 1.04, meaning that flow in the fuel assembly containing the hot channel was established at 96% of average fuel-assembly flow. The results of the tests verified the design selection of 1.025 as the hot-channel factor for flow maldistribution channel-to-channel; i.e., the hot channel has 97.5% of the flow of the average channel in the fuel assembly containing the hot channel.[9] The total design flow-maldistribution factor of 1.065, including both the foregoing effects, thus contained some conservatism, as was the case in Core 1.

AID FROM "PENALTY AND MARGIN" CALCULATIONS

Experience during the design, manufacture, and operation of the cores for Shippingport has disclosed a number of other parameters affecting the thermal design, which initially are treated by the "penalty-and-margin" concept.

The penalty-and-margin concept is akin to the hot-channel factor concept in providing a convenient means for evaluating the effects of deviations from nominal input parameters of the thermal-design process. The specific parameter is evaluated in terms of its effect on the core power capability. For example, a flow reduction of 1% of full flow corresponds to a "penalty" of 1% of full power, but, if the as-measured hot channel were larger than the minimum design value by 0.001 in., a "margin" of 2% of full power would be available. Evaluating these effects as perturbations on an existing thermal design, rather than performing the full-scale thermal-design calculation with the penalties and margins as input, is rapid and convenient.

Linearity. Within a small range of perturbation, most of the input parameters are quite linear in their effect on power level. For example, a postulated 10% reduction in steady-state flow rate through the core has been found to reduce the core power capability by 9.7% of full power, as limited by a loss-of-flow transient. This result was obtained by a series of full-scale thermal-design calculations of the transient with initial flow reductions of 1 to 10% of full flow. The maximum deviation from linearity was found in the result for the maximum (10%) flow reduction.

Penalties. Typical penalties arise through fuller understanding of the design and operation. For example, manufacturing results show that fuel-element lateral misalignment may be significant. Specifically, it is postulated that one fuel edge in the hot channel extends the maximum distance toward the water-hole gap (looking at a radial core cross section as in Fig. 5), whereas the two or more adjacent fuel edges on either side are displaced a maximum distance in the opposite direction. The resultant power peak has been evaluated as a penalty of 2% of full power. Another example is the deposition of corrosion product on the heat-transfer surfaces in the fuel coolant channels; operating experience shows that this can also lead to significant penalties.[5]

Margins. Typical margins arise from measured values of core parameters. Examples are: (1) core coolant flow, which is expected to be higher when measured at Shippingport because of known conservatisms in the design calculations; (2) control-rod scram delay time (1% power per 0.025 sec reduction in time); and (3) measured flow-coastdown characteristic which permits a margin of 5% of full power above the capability calculated using the design flow coastdown.

When a deviation has a confirmed maximum value, it is generally more accurate to include it explicitly in the detailed design procedure rather than use either the penalty-and-margin concept or hot-channel factors. However, this decision depends on weighing the gain in accuracy against the additional complexity added to the calculational procedure.

The author acknowledges the assistance of P. A. Bickel, D. L. Crum, Jr., and P. S. Marinkovich of the Bettis Atomic Power Laboratory, PWR Reactor Thermal and Hydraulic Design, in providing facts and reasons from a decade of records.

The Shippingport reactor was designed and developed by the Bettis Atomic Power Laboratory under the direction of, and in technical cooperation with, the Division of Naval Reactors, U. S. Atomic Energy Commission.

References

1. B. W. LeTourneau and R. E. Grimble, Engineering Hot Channel Factors Useful in the Thermal Design of Nuclear Power Reactors, *Nucl. Sci. Eng.*, 1(5): (October 1956).
2. Duquesne Light Co., Shippingport Operations from Start-Up to First Refueling, December 18, 1957, to October 7, 1959, USAEC Report DLCS-364.
3. Duquesne Light Co., Shippingport Operations from Power Operation After First Refueling to Second Refueling, May 6, 1960, to August 16, 1961, USAEC Report DLCS-36402.
4. Duquesne Light Co., Shippingport Operations from Power Operation After Second Refueling to Power Operation After Third Refueling, October 24, 1961, to January 30, 1963, USAEC Report DLCS-36403.
5. Westinghouse Electric Corporation, Bettis Atomic Power Laboratory, Pressurized Water Reactor Project, Technical Progress Report, April 24, 1965–July 23, 1965, USAEC Report WAPD-MRP-113.
6. *Shippingport Pressurized Water Reactor*, written by personnel of the Naval Reactors Branch, Division of Reactor Development, U. S. Atomic Energy Commission; Westinghouse Electric Corporation, Bettis Plant; and Duquesne Light Company; Addison-Wesley Publishing Company, Inc., Reading, Mass., 1958.
7. L. J. Flanigan and H. R. Hazard, Supplementary Model Studies of Flow Distribution in the Core of the PWR Reactor, USAEC Report BMI-1229, Battelle Memorial Institute, Oct. 7, 1957.
8. L. J. Flanigan, G. R. Whitacre, and H. R. Hazard, Studies of Flow and Mixing in a 0.4-Scale Model of the PWR Core 2 Reactor, USAEC Report BMI-1582, Battelle Memorial Institute, June 26, 1962.
9. L. J. Flanigan, C. L. Coffin, and W. D. Beck, Model Studies of Flow in PWR Core 2 Fuel Assemblies, USAEC Report BMI-1720, Battelle Memorial Institute, Mar. 30, 1965.

Current Values of Fundamental Fission Parameters

By Alexander De Volpi

Fission parameters fundamental to nuclear reactor design are being systematically organized into evaluated compilations based on "standardized" cross sections, reference energies, and uniform corrections for secondary effects. However, there are conspicuous discrepancies in the latest compilations. The discrepancies are generally associated with difficult absolute measurements or with techniques most susceptible to systematic error. From the cross-section disparities that currently exist, it is clear that the needs of the reactor designer are not yet fulfilled. But it is also apparent that experimental results are converging — a trend revealed in this review of measured and average values of the following basic fission parameters:

σ_a, absorption cross section

σ_s, scattering cross section

η, ratio of neutrons emitted to neutrons absorbed

α, capture-to-fission ratio

σ_γ, nonfission capture cross section

σ_f, fission cross section

ν, average total neutrons/fission

Information on these parameters has been collected in this survey primarily for ^{235}U and ^{233}U and for ^{239}Pu and ^{241}Pu. In general, references that provide ^{235}U data also contain data for other isotopes of uranium and for plutonium isotopes. Information for ^{233}U is not quite as precise as for ^{235}U; plutonium cross sections have even poorer accuracy. Many of the values deduced for isotopes other than ^{235}U are based on ratio measurements of different parameters compared to ^{235}U samples under similar conditions. Limited quantities and poor assessment of isotopic constituents are largely responsible for the greater errors generally found for fissionable materials tested against the ^{235}U standard. Sometimes, the widely varying shape response of the isotope (such as resonance shielding) causes additional uncertainties in a comparison. Data for ^{241}Pu have only recently been brought up to sufficient quality to yield a comparable fit. The latest computations by Westcott[1] are summarized in Table 1.

Inasmuch as the basic fission constants are best compared at accessible reference energies, the energy dependence of the various parameters in the range of thermal and fast reactor interest is considered only briefly. Instead, the view is taken that certain key quantities serve as underpinnings in the structure of fission data. For example, measurements of ^{235}U neutron yield at energies above thermal are, in all cases, relative to ^{235}U production at 2200 m/sec; and $\nu(E)$ for all other fissile materials are normalized to either ^{235}U or ^{252}Cf yields. Because of such relations, emphasis on certain thermal cross sections becomes justified.

Table 1 RECOMMENDED VALUES FOR FISSION PARAMETERS[1,19]

(2200 m/sec)

	^{233}U	^{235}U	^{239}Pu	^{241}Pu	^{252}Cf
σ_a, barns	576.3 ± 2.3	679.9 ± 2.3	1008.1 ± 4.9	1371 ± 18	
σ_f, barns	527.7 ± 2.1	579.5 ± 2.0	742.4 ± 3.5	1011 ± 9	
σ_γ, barns	48.6 ± 1.5	100.5 ± 1.4	265.7 ± 3.7	360 ± 15	
α	0.0921 ± 0.0029	0.1734 ± 0.0025	0.3580 ± 0.0054	0.356 ± 0.015	
η	2.284 ± 0.008	2.071 ± 0.007	2.114 ± 0.010	2.189 ± 0.030	
ν	2.494 ± 0.009	2.430 ± 0.008	2.871 ± 0.014	2.969 ± 0.023	3.772 ± 0.015

The use of 2200 m/sec as a standard neutron velocity is common practice; this should not obscure the fact that few measurements are actually made with neutrons of that velocity. In fact, many of the

basic parameters for ^{235}U and especially for other fissionable isotopes are based partly or entirely on data taken in Maxwellian neutron spectra.

Some questions immediately arise. What input data are available; what data are needed? Do the existing contradictions display some systematic tendencies, and how can the required cross-section accuracy be achieved? In partial response this article examines the uses of the data, notes the role of various compiling centers, tabulates the latest thermal values, and analyzes the experimental input data in search of possible systematic errors, weaknesses, or limitations of the measurements. The greatest attention is focused on ν and σ_f—parameters that display the largest inconsistencies. Finally, reliability and attainable precision are estimated.

Data Utilization

Judgment that data are adequate requires knowledge of utilization in reactor design and other applications. Indications of requirements (or of deficiencies arising from existing inadequate data) have been given by Persiani[2] and in a number of papers at recent conferences.[3-14]

For criticality considerations, errors of $\leq 0.5\%$ either for ν and σ_f or for σ_a and η are generally desired by reactor designers even though small-scale mockups of specific designs are made in critical facilities.[12,13] Although critical experiments are likely to remain essential for all major variations in reactor conditions, extrapolation to power-reactor size still requires precise knowledge of cross sections.

A further long-term need for high-quality data is connected with the burnup limits for natural (or very low enrichment)-uranium reactor fuels.

Anticipated fissile-fuel-inventory depletion spurs the growing effort in fast breeder reactor technology. This trend increases the requirements for cross-section data in the kev region.

Accurate cross-section values for fast reactors are required not only for simple criticality consideration[2] but also for reasons of breeding gain[6] and nuclear safety.[7] In addition, the extra hazard of plutonium and the problems associated with liquid sodium make fast critical experiments less convenient and more expensive; thus future extensions of computation techniques become necessary. Although the sodium-void and Doppler effects are currently subjects of major international interest, the great number of Doppler-broadened resonances makes theoretical extensions difficult in the absence of detailed experimental nuclear data.

Compilations

In addition to the well-established "barn book"[15] (now available with supplements to the second edition) and related studies by the Brookhaven Sigma Center,[16] there are a number of newer summaries of data on fission parameters. Foremost are the CINDA indexes,[17] which contain a reference to every available measurement or report concerning nuclear data. These indexes are updated with supplements published jointly by the USAEC and the European Nuclear Energy Agency (ENEA) and by newsletters from the Neutron Data Compilation Centre. The collection of most nuclear data in the United States is centered about the evaluated nuclear data file (ENDF) maintained at Brookhaven National Laboratory.[18] *Nuclear Data*—a journal devoted to compilation and evaluation of experimental and theoretical results in nuclear physics—is published by Academic Press Inc. and carries submissions from the Nuclear Data Group and from readers at large.

Studies specifically directed toward fission constants have been made by the IAEA.[19] At the Washington Conference on Cross Section Technology[20] and the Paris Conference on Nuclear Data—Microscopic Cross Sections and Other Data Basic for Reactors,[21] additional measurements and data summaries were reported. (Hereafter in this article these conferences are referred to as the Washington and Paris Conferences.) The combined Paris paper by Parker, Goldman, and Wallin[22] lists available evaluations of neutron cross sections as of Sept. 1, 1966.

A comprehensive analysis of $\sigma_f(E)$ from 1 kev to 10 Mev for 11 fissionable actinides has been developed by Davey,[23] and Drake[24] has made a study of ^{233}U alone. The evaluation by Davey has been modified by Hart[25] with the addition of new experimental data and extended to 14 Mev. Fillmore[26] has recently carried out an examination of data for $\nu_p(E)$.

RECOGNIZED THERMAL FISSION PARAMETERS

The results obtained from least-squares analyses of two major study groups are reproduced in Tables 1 and 2 (Refs. 16 and 19). Table 1 contains recently upgraded data. There are a number of conspicuous discrepancies which are discussed in this review. In both tables, data have been referred to 2200 m/sec.

Table 2 SIGMA CENTER SUMMARY OF FISSION PARAMETERS[16] DERIVED THROUGH 1965

(2200 m/sec)

	^{235}U	^{233}U	^{239}Pu
σ_f, barns	577.1 ± 1.9 (582.6 ± 4.1)*	524.5 ± 1.9 (518 ± 5)*	740.6 ± 3.5
σ_a, barns	678.2 ± 2.2	573.1 ± 2.1	1014.5 ± 4.2
ν	2.442 ± 0.006 (2.438 ± 0.004)*	2.504 ± 0.008	2.898 ± 0.011
η	2.078 ± 0.005 (2.076 ± 0.006)*	2.292 ± 0.006	2.116 ± 0.009
α	0.175 ± 0.002	0.0926 ± 0.0027	0.370 ± 0.006
$1 + \alpha$	1.1756 ± 0.0022 (1.1738 ± 0.0010)*	1.0926 ± 0.0027 (1.0937 ± 0.0004)*	

*Average of measured values; the adjacent numbers are least-square values.

For the Brookhaven report[16] (Table 2), little effort was made to determine and correct systematic errors, except that a normalizing value of $\nu(^{252}Cf) = 3.779 \pm 0.010$ was adopted and relative ν measurements were renormalized to that value. As a result, it represents a passive average of published data.

On the other hand, the IAEA work included a thorough search for systematic errors combined with extensive renormalization procedures. All measurements were examined for consistency; where possible, fission cross sections were tied to the "gold standard" (98.7 ± 0.2 barns). Various spectral index corrections were made to obtain uniform criteria for evaluation.

Analysis of Experimental Data

The neutron-generation process in a reactor is related to either of two combined parameters, $\nu\sigma_f$ or $\eta\sigma_a$. Neither of these pairs is sufficient information because of structural effects, but each is a basis of calculational procedures. In order of decreasing measurement precision, the fission parameters are σ_a, η, σ_f, and ν. This implies that greater reliance in present calculations and compilations should be on $\eta\sigma_a$. There are several reasons: (1) absorption cross sections, σ_a, are readily derived from transmission measurements, especially if the scattering component is small as in the case of the thermally fissionable isotopes, and (2) η results from a relative measurement of neutrons; but, on the other hand, (3) the fission cross section, σ_f, introduces the specific measurement of fragments which have an extremely short range and which are strongly oriented with the accompanying prompt fission radiation, and (4) the neutron yield, ν, contains the result of two absolute measurements—fast neutrons and fission fragments—that are both rather difficult to detect accurately and are both connected through angular correlations.

VALUES FOR ^{235}U

As previously noted, the most precise values of fission parameters are those for ^{235}U. Tables 3 to 9 summarize these experimental data as adjusted by Westcott,[19] except for the inclusion of some more recent results.

σ_a, the Absorption Cross Section. The accepted absorption cross-section values in Table 3 were derived from total cross sections found primarily at four laboratories: Columbia,[27] Oak Ridge,[28] Phillips[29] (now Idaho Nuclear Corp.), and Argonne.[30] Since scattering from ^{235}U is only 2.1% of the total cross section, reliable transmission measurements of the total cross section can be rather accurately reduced to provide the absorption fraction. As improved samples and better beam-energy definition have become available, the reported values have converged to better than 0.5%. There is little likelihood of systematic error in this quantity.

η, Neutrons Emitted/Neutron Absorbed. Reports that give values of η should be carefully scrutinized because the value of η is heavily weighted in all fitting procedures used to deduce the remaining set of overdetermined fission parameters. Such scrutiny has been done by Westcott[19] and resulted in the selection of three experiments (after spectral and cross-section normalization) as input to the weighted mean. The three experiments (listed in Table 4) followed essentially different approaches.

Table 3 ABSORPTION CROSS-SECTION MEASUREMENTS* FOR ^{235}U
(σ_a at 2200 m/sec)

Investigators	Ref.	Date	σ_a, barns	Neutron source, ev	Fission source				Thermal-neutron detector	
					Type	Thickness, cm	Enrichment %	Uniformity, %	Type†	Error, %
Saplakoglu	30	1961	679.5 ± 3.4	Fast chopper, 0.003 to 0.5	Rolled metal	0.046	93	1	^{10}B	2‡
Block, Slaughter, and Harvey	28	1960	678.5 ± 5.5	Fast chopper, 0.02 to 0.20	Rolled metallic foil	~0.0625 and ~0.033	93.36	1	BF_3	4‡
Simpson, Moore, and Simpson	29	1960	675.5 ± 10	Fast chopper, 0.02 to 0.08	Metal	3 × 0.025	93.15 ± 0.05	±12	BF_3	10‡
Safford and Havens	98	1959	680.5 ± 2.8	Crystal spectrometer with mechanical monochromator	Liquid§	1	99.76	0.1	BF_3	
Safford, Havens, and Rustad	27	1959	684.2 ± 5.9	Crystal spectrometer with mechanical monochromator	Rolled metal (4 samples)	0.005	99.7	6	BF_3	

*All accomplished by transmission methods with scattering component subtracted.
†Proportional counter.
‡Dead time.
§Uranyl nitrate in D_2O.

Although the Oak Ridge data[31,32] agree within 0.5%, the meticulous measurement by the Phillips organization[33] was reported with a mean value slightly higher but with comparable error limits. The results of this direct experiment were not complete for the original Westcott analysis, so the Phillips data can be expected to increase the weighted mean by perhaps a few tenths of a percent.

There is room for concern in interpretation of the Macklin experiment from evidence not in the published report.[31] An informal memorandum[34] indicates that the combined reactor background and epicadmium contribution to the fission rate was ~15%, whereas the beam itself produced a 25% background and epicadmium component. In view of the low cadmium ratio (3) and the strong energy dependence of η, it is not clear that the high nonthermal beam content can be properly treated.

α, *the Capture-to-Fission Ratio.* Most experiments for α have involved irradiation in a reactor spectrum, and thus they require corrections to 2200 m/sec. Measurements made in well-thermalized media were reported at the Paris Conference[35,36] (Table 5), but, instead of clarifying the value, these measurements raised additional questions. Errors quoted for both experiments (about 1%) are similar prior to inclusion of errors for conversion to 2200 m/sec; yet the results disagree by 3%, whereas their mean value coincides with Westcotts's estimation of α. Durham[36] believes the explanation for this variation lies not in the conversion to 2200 m/sec but either in unsuspected experimental errors or in differences between actual and assumed neutron spectra. Curiously, a lower value of α would be consistent with a lower value of ν.

σ_s, *the Scattering Cross Section.* The scattering cross section has, in general, been estimated from a few direct measurements, from high- to low-energy extrapolations of potential cross sections, and from multilevel fits. The most reliable values are drawn from 0.27 ev, the lowest energy experimental point, and the result is a 15% error in σ_s. Fortu-

Table 4 NEUTRON YIELD PER NEUTRON ABSORBED IN ^{235}U

(η at 2200 m/sec)

Investigators	Ref.	Date	η	Method	Source	Neutron detector	Comments
Smith, Reeder, and Fluharty	33	1966	2.079 ± 0.010	Fission absorption ratio in beam	Crystal spectrometer	Large manganese bath	
Gwin and Magnuson	32	1962	2.071 ± 0.0140	Criticality	Aqueous uranium solutions	Reactor instrumentation	
Macklin, de Saussure, Kington, and Lyon	31	1960	2.071 ± 0.0117	Fission absorption ratio in beam	Reactor core spectrum	Large manganese bath	See text concerning epicadmium effects

Table 5 EXPERIMENTAL CAPTURE-TO-FISSION RATIOS IN ^{235}U

(α Corrected to 2200 m/sec)

Investigators	Ref.	Date	α ratios		Method	Source	Analysis
			Corrected	Measured			
Cabell	35	1966	0.1716 ± 0.0033	0.1786 to 0.1901	Irradiation	Reactor core spectrum (10 samples)	Mass spectrometer
Durham, Hannah, Lounsbury, Bigham, Hart, and Jones	36	1966	0.1765 ± 0.0015	0.179	Irradiation	Highly thermalized spectrum in reactor core	Mass spectrometer
Lisman, Maeck, Rein	99	1966	0.1716 ± 0.0015	0.177	Irradiation	Reactor core	Mass spectrometer, isotope dilution
Okazaki, Lounsbury, Durham, and Crocker	100	1964	0.1718 ± 0.0015	0.1753 ± 0.0006	Irradiation	NRU reactor spectrum	Mass spectrometer, chemical and isotope dilution
Safford and Melkonian	101	1959	0.171 ± 0.009	1.171 ± 0.009 ($1 + \alpha$)	Transmission/fission ratio (σ_t/σ_f)	Crystal spectrometer (0.00291 ev)	Boron flux monitor
Cocking	102	1958	0.172 ± 0.022		Transmission/fission ratio (σ_t/σ_f)	Cold neutrons (0.0011 ev)	^{197}Au transmission/capture

nately, the 12-barn scattering effect is of relatively minor interest in reactor design and, as mentioned, is small compared to the total cross section.

One problem associated with measurements of the coherent scattering cross section arises from possible preferred orientation produced by rolling or other manufacturing processes for commonly used metallic foils.[27]

σ_γ, *the Nonfission Capture Cross Section.* Values of the capture cross section (Table 1) and the related resonance integral are all based on measurements of the capture-to-fission ratio α.

σ_f, *the Fission Cross Section.* Although fission cross sections for ^{235}U have been reported with accuracies of 1%, the numbers quoted since 1953 (in Table 6) have varied by as much as 5%. One source of this divergence, as recognized by Maslin,[37] is possibly related to the strong angular correlation between fission-fragment and associated fast-neutron emission. This potential systematic error can also

Table 6 MEASURED FISSION CROSS SECTIONS FOR ^{235}U

(σ_f at 2200 m/sec)

Investigators	Ref.	Date	σ_f, barns	Method	Source	Normalization, barns	Comments
Fraysse, Prosdocimi, Netter, and Samour	103	1965	582 ± 10	Absolute fission and absolute flux	Crystal spectrometer	$B^{nat.}(n,\alpha) = 761 \pm 2$	Investigators report 588 ± 10 barns in Ref. 106
Maslin, Moore, Reichelt, and Crowde	37	1965	572 ± 7	Absolute fission and absolute flux	Fast chopper		Corrected for angular correlation between fission fragment and fission neutrons; method similar to Saplakoglu (Ref. 42)
Deruytter	104	1961	590 ± 8	Absolute fission and absolute flux	Slow chopper	$\sigma_a(Au) = 97.7 \pm 0.5$ ($1/v$ part)	
Raffle	105	1959	586 ± 18	Absolute fission and absolute flux	Slow chopper, thermal and reactor core beam	$\sigma_a(Au) = 98.7$	
Safford and Melkonian	101	1959	586.2 ± 8.0	$\sigma_t/\sigma_f = 1 + \alpha$	Crystal spectrometer	Requires $\sigma_a(^{235}U)$ to determine σ_f	Redundant in a least-squares fit of fission parameters; should be excluded from σ_f averages
Saplakoglu	42	1958	602.6 ± 10.3	Absolute fission and absolute flux	Fast chopper	None required owing to coincidence calibration	Angular correlation of fission neutrons and fragments; evaluated indirectly; fission detector extrapolation modified; errors expanded by internal inconsistency
Friesen, Leonard, and Seppi	41	1956	555 ± 14	Absolute fission and absolute flux	Crystal spectrometer	$\sigma[^{197}Au(n,\gamma)] = 50.9$ barns at 0.10 ev	Erroneous foil assay possible; documentation sparse

Investigators	Fission detector				Thermal-neutron detector	
	Type	ϵ_f	Coating thickness	Efficiency calibration	Type	Efficiency calibration
Fraysse, Prosdocimi, Netter, and Samour	Gas scintillator and low-geometry semiconductor	94% for 140 $\mu g/cm^2$	60 to 400 $\mu g/cm^2$	Extrapolation	Boron-gridded ionization	Extrapolation
Maslin, Moore, Reichelt, and Crowde	Parallel-plate ionization	92%	500 $\mu g/cm^2$	Coincidence with liquid scintillator	Boron counter	Coincidence with NaI
Deruytter	4π ionization	89 to 98%	1 to 0.1 mg/cm^2	Extrapolation	2π boron counter	^{197}Au absolute β/γ coincidence counting
Raffle	Ionization	97 to 98%	0.5 mg/cm^2	Extrapolation to zero bias	Boron-gridded ionization	^{197}Au foil activation
Safford and Melkonian	Fission ionization	93.36%	0.492 mg/cm^2	Extrapolation to zero bias	^{10}B-plated ionization	Calculated
Saplakoglu	Fission counter	98.89%	0.5% of booster	Coincidence with liquid scintillator	^{10}B counter + boron-slab and NaI	Coincidence with NaI 10% chance coincidences
Friesen, Leonard, and Seppi	Mass spectrometric isotopic dilution				^{197}Au foil	Calibrated by absolute β/γ coincidence

Table 7 URANIUM-235 FISSION-COUNTER EFFICIENCIES DETERMINED BY INTEGRAL-BIAS EXTRAPOLATION

Investigators	Ref.	Counting thickness, mg/cm²	Chamber efficiency, %
Knoll and Pönitz	80	1.203 ± 0.03	91.25
Porges and De Volpi	44	0.3	87 ± 1
Fraysse and Prosdocimi	103	0.14	94
Maslin et al.	37	0.5	91.8
Perkin et al.	75	0.5 to 1.0	≥97 ± 0.5*
Deruytter	104	1	92 ± 1
		0.1	97.5 ± 0.3
		0.661 ± 0.003	88.8 ± 0.5
Raffle	105	0.5	97 to 98
Safford	101	0.492	93.36
Kenward, Richmond, and Sanders	57	0.8	94

*Separation of 1 to 4% was made for self-absorption of fission fragments.

Table 8 SURVEY OF TOTAL NEUTRON YIELDS FROM THERMAL FISSION OF ^{235}U

Value	ν, neutrons per fission	Ref.	Comments
A	2.44 ± 0.12	38	Relative to calibrated Ra–Be source
B	2.47 ± 0.15	107	Relative to spontaneous fission $\nu(^{238}U) = 1.59 \pm 0.09$
C	2.5 ± 0.1	108	Relative to calibrated neutron source
D	2.43 ± 0.07	50	Liquid scintillator calibrated by $n-p$ scattering (value rejected by experimenter)
E	2.420 ± 0.037	57	Relative to ^{240}Pu source for neutron efficiency
F	2.418 ± 0.039	109	Relative to ^{240}Pu source used in Ref. 57
G	2.331 ± 0.053	110	Relative to $\nu(^{252}Cf) = 3.64$
H	2.37 ± 0.07	47	Critical mass of ^{235}U sphere
I	2.446 ± 0.041	51	Normalized to $\nu(^{252}Cf) = 3.779$
J	2.443 ± 0.029	111	Normalized to $\nu(^{252}Cf) = 3.779$ (Ref. 109)
K	2.430 ± 0.033	61	Normalized to $\nu(^{252}Cf) = 3.779$
L	2.438 ± 0.004	16	Average of values A, E, I, J, and K
M	2.370 ± 0.014	62	Value E revised by authors (source recalibrated)
N	2.430 ± 0.008	19	10-parameter least-squares fit
O	2.385 ± 0.015	54	Boron-pile gated measurement
P	2.417 ± 0.030	48	Absolute neutron rate with manganese bath; absolute fission rate by coincidence counting

occur in ν measurements. Another opportunity for systematic error resides in the use of extrapolation methods for fission-fragment counting efficiency.

ν, Neutrons/Fission. Since ν inherently requires two absolute measurements—a fast-neutron emission rate and a fission-fragment rate—it is most susceptible to systematic errors in fully independent measurements. Historically the first measurements were made by comparing the neutron rate against calibrated neutron sources.[38] Table 8 indicates that there have been few ν measurements that were entirely independent of secondary calibration. (Absolute values of ν are collected in Table 9.) Most measurements were relative either to calibrated or recalibrated neutron sources or normalized to ν of ^{252}Cf. As a result, present averages derived from least-squares fits are deduced mostly from the relation $\nu = \eta(1 + \alpha)$.

MEASURING THE FISSION CROSS SECTION

To find the fission cross section, most experiments involve some method of fission-fragment counting and thermal-flux evaluation, both of which require efficiency calibration for particle detection. Sometimes the thermal-neutron detector is normalized against a standard cross section such as ^{197}Au or ^{10}B. Additional problems of precise isotopic content[39] and quantitative determination of the fissile mass[40] are encountered in σ_f measurements. For example, according to Westcott,[19] erroneous foil assay may be responsible for the very low value of Friesen, Leonard, and Seppi.[41]

The relatively high value of Saplakoglu[42] should be compared to the recent measurement by Maslin,[37] who used a similar technique. To calibrate a parallel-plate fission counter, Saplakoglu required coincidences with a liquid scintillator that had a large exit aperture.

Angular Correlations. Since about 90% of the fission neutrons from ^{235}U are boiled off from the moving fission fragments, much of the fission-neutron kinetic energy appears to be derived from the momentum of the fragments.[43] As depicted in Fig. 1, this correlation in direction means that most of the neutrons are in an emission cone surrounding the direction of fragment movement. Fragment pairs with large velocity components perpendicular to the foil plane have the highest probability of ionization, whereas those emitted parallel to the foil plane have the highest probability of being absorbed in the foil coating.

If the neutron detectors used for coincidence calibration of these fission counters were truly 4π, the correlation effect would vanish. However, in practice, the necessity for beam tubes through the neutron detector means that escape apertures range from 10 to 30%. In addition, the exit solid angle for fast neutrons may be as much as double the optical solid angle.

The degree of correlation is highly dependent on the coating thickness. A thick coating leads to a reduced average coincidence rate and, thus, a fission-fragment efficiency that is too low. Maslin et al.[37] noted a 12% decrease in coincidence efficiency when orientation to the beam of their 0.5 mg/cm² fission counter was changed from 45 to 90°. After evaluating this discrepancy with foils of 0.5, 0.1, and 0.14 mg/cm², they report a final error of 1% in σ_f.

A small correction for angular correlations was applied by Saplakoglu,[42] although this was determined indirectly rather than by angular traverses. In addition, Westcott[19] found it necessary to modify Sap-

Table 9 MEASUREMENTS OF TOTAL NEUTRON YIELD PER FISSION IN ^{235}U

(2200 m/sec)

Investigators	Ref.	Date	Method	ν, neutrons per fission	
				Values	Comments
De Volpi and Porges	48	1966	Independent absolute neutron and fission rates	2.417 ± 0.030	
Colvin and Sowerby	54	1965	Gated boron pile	2.385 ± 0.015	Revised[109] from 2.418 ± 0.039 which was based on ^{240}Pu source subsequently recalibrated (Ref. 62)
Engle, Hansen, and Paxton	47	1960	Critical mass of ^{235}U spheres	2.37 ± 0.07	2 σ_f measured
Kenward, Richmond, and Sanders	57	1958	Gated wax castle	2.370 ± 0.014	Value reduced from 2.420 ± 0.037 after recalibration of source in 1966
Diven, Martin, Taschek, and Terrell	50	1956	Gated scintillator	2.41 ± 0.07	Value rejected by experimenter in favor of normalization of data using $\nu(^{235}U) = 2.46 \pm 0.03$; a corresponding value of $\nu(^{252}Cf)$ would have been 3.80

Investigators	Neutron detector					
	Type	Size	Aperture	Calibration	ϵ_n, %	Errors
De Volpi and Porges	Manganese bath	1.06-m-diameter sphere	*	Absolute 4π β/γ coincidence (corroborated with NBS-II source)	†	0.3% Mn/H absorption; 1 to 1.3% neutron rate
Colvin and Sowerby	Graphite with 240 BF_3 detectors	220-cm cube	5.5° (core)	$d(\gamma,n)p$ reaction in ionization counter	64 (^{252}Cf)	0.2% anisotropy; 0.1% gating effects
Engle, Hansen, and Paxton						
Kenward, Richmond, and Sanders	12 BF_3 counters in paraffin	45-cm-long 40-cm-diameter cylinder	30°	Standard ^{240}Pu source	1.7 to 2.2	
Diven, Martin, Taschek, and Terrell	Cadmium-loaded liquid scintillator	76-cm-long 73-cm-diameter cylinder	10°	(n,p) scattering in plastic scintillator	83	1.5% in calibration

Investigators	Fission detector			
	Type	ϵ_f	Calibration	Errors
De Volpi and Porges	Two hemispherical ionization counters	90%+ (0.3 mg/cm^2)	Fragment/neutron coincidence	0.3 to 0.8% fission rate
Colvin and Sowerby	Parallel-plate ionization counter	(1 mg/cm^2)		0.1% ion-counter efficiency
Engle, Hansen, and Paxton				
Kenward, Richmond, and Sanders	Parallel-plate ionization counter	94% (0.8 mg/cm^2)		
Diven, Martin, Taschek, and Terrell	Parallel-plate ionization counter			

*Neutron leakage: 1%.
†σ(Mn)/σ(H): 0.0251, Ref. 67.

lakoglu's fission-counter extrapolation and to expand his reported errors due to poor internal consistency.

Additional evidence concerning angular-correlation effects on coincidence measurements has been provided by Porges and De Volpi.[44] More recent data (Fig. 2) indicate that even a fission foil with 99.0% fragment efficiency leads to a 1% 0°/90°/180° effect for a neutron detector with 60% of 2π solid angle.[45]

Efficiencies. The extrapolation of fission-fragment count rate to zero bias is subject to a number of errors for efficiencies <100%. These problems have been discussed by Maslin,[37] White,[46] and by Porges and De Volpi.[44] Comparison in Table 7 of fission-counter efficiencies against reported coating thickness indicates wide latitude in practice. Whether or not a distinct adjustment has been made for self-absorption is often not clear in published reports.

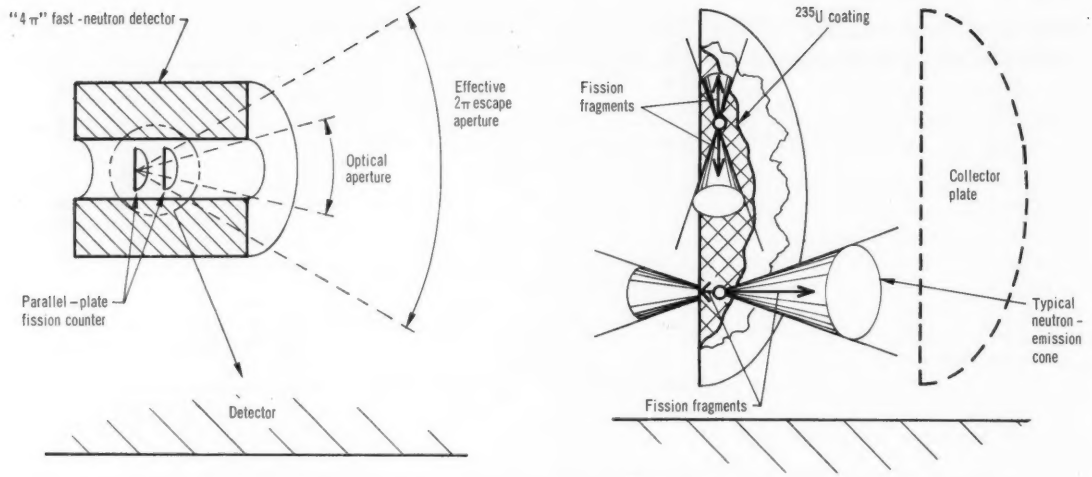

Fig. 1 Schematic of coincidence losses caused by angular correlation of fission fragments and fission neutrons, most of which will travel within emission cones surrounding the direction of fission-fragment movement. Coincidence losses will increase as the fission-fragment efficiency decreases and as the effective escape aperture increases.

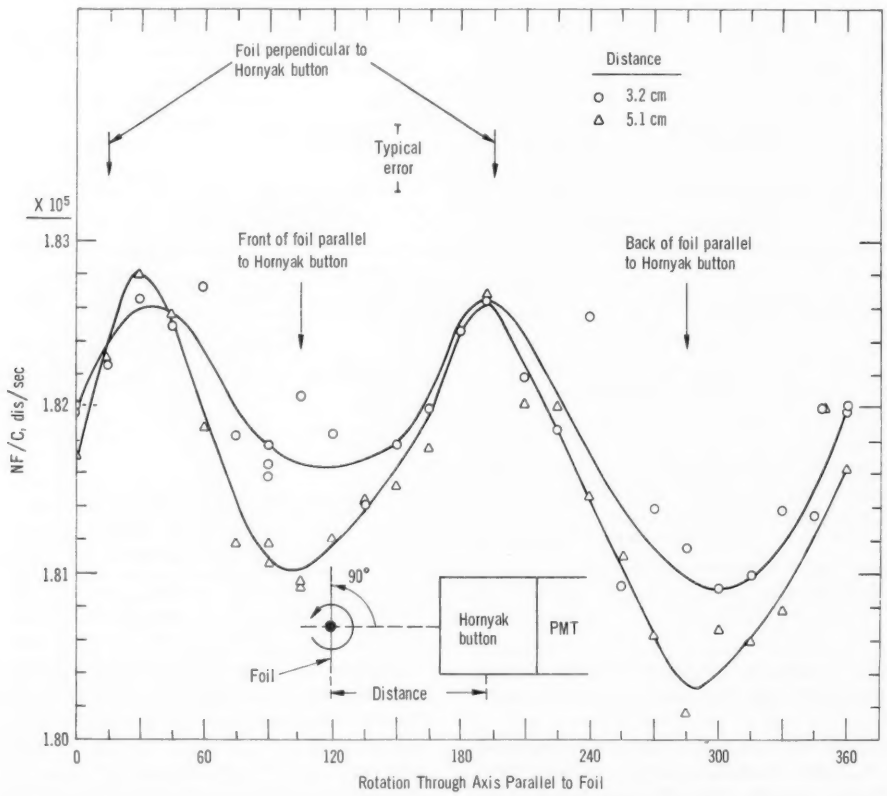

Fig. 2 Clear evidence for angular dependence of coincidence rate for a fission-fragment counter with 99.0 ± 0.5% efficiency viewed by a fast-neutron detector with 60% of a 2π solid angle. A front/back correlation due to heavy- and light-fragment neutron emission is also noticeable.

The problem is compounded by different techniques used for deposition, by varying oxidation states, and by degree of achievement in uniformity.

MEASURING NEUTRONS/FISSION

Absolute values of ν may be obtained by (1) evaluation of the critical mass in good geometry, (2) direct, ungated measurements of the separate neutron rates and fission rates, and (3) gated methods in which the product $\nu\epsilon_n$ is the quantity derived with neutron-detection efficiency ϵ_n determined in an absolute experiment.

A precise measurement of critical mass in good geometry was published[47] in 1960. Aside from questions that arise concerning the status of multiplication theory, the experiment is effectively an evaluation of the product $\nu\sigma_f$.

There has been only one result in the second category — ungated direct measurements. It was reported at the Paris Conference;[48] supplementary details were described at the Vienna Symposium.[44,49] The fission rates from two hemispherical ^{235}U counters were calibrated by a coincidence method using a low-efficiency neutron detector to find the fission-fragment counting efficiency. The neutron emission rates from the calibrated counters were determined in a manganese-bath system located in identical geometry at the reactor thermal column. Precision of 1.25% was obtained; the limiting factor was the inconsistency in the two averaged values. Subject to assumptions of uniformity and reproducibility of flux pattern, the hemispherical geometry should eliminate the angular-correlation effects expected from fission counters with less than 100% fragment detection. The manganese-bath neutron efficiency was found from application of the $4\pi\beta/\gamma$ coincidence technique and use of the well-known hydrogen/manganese cross-section ratio. The neutron calibration was confirmed by comparison with the U. S. National Bureau of Standards source NBS-II.

Most measurements of neutron yield have used gated methods.

Gated Measurement Methods. Gated ν measurements require a fission counter, a fast-acting neutron detector, and electronic circuitry to record the number of single-channel and coincidence counts. In simplified form the fission-counter rate F is proportional to the source rate S:

$$F = \epsilon_f S \tag{1}$$

where ϵ_f is the fission-counter efficiency. The neutron-channel rate N may contain the desired quantity ν in the form

$$N = \sum_{\nu} [1 - (1 - \epsilon_n)^{\nu}] P(\nu)\, S \tag{2}$$

where $P(\nu)$ is the neutron multiplicity distribution (if the neutron detector can count only one neutron per fission event) and ϵ_n is the detection efficiency per neutron. The summation is over all discrete values of ν.

At the other extreme, if the neutron detector can accumulate every possible neutron count per fission event, then the neutron rate is simply

$$N = \nu\epsilon_n S \tag{3}$$

For the latter case, the coincidence rate is

$$C = \nu\epsilon_n\epsilon_f S \tag{4}$$

and the coincidence/fission ratio gives

$$C/F = \nu\epsilon_n \tag{5}$$

Thus, if the neutron-detector efficiency can be found (over the fission-neutron energy spectrum), ν can be determined.

Detectors for Gated Measurements. Whether Eq. 2 or 3 applies depends on the nature of the neutron detector. If the neutrons from a single fission event can be sufficiently separated in time by slowing down in a moderator, then it is possible to detect nearly all neutrons of an event and Eq. 3 is used. Two types of detectors satisfy this requirement: the large liquid scintillators[50–53] and the boron pile.[54]

Equation 2 is appropriate when the neutron detector responds to a maximum of one neutron per fission — e.g., prompt-neutron detectors of small physical size, where the first detectable reaction initiates a dead time that prevents the remaining neutrons from producing multiple counts. This type of detector was used for fission-counter calibration by Porges and De Volpi.[44] If the neutron-detector efficiency is low, Eq. 2 approaches $\nu\epsilon_n\,(1 - \epsilon_n/2)$. It is not unusual for a prompt-neutron detector of small volume to be less than 0.1% efficient.

Although Eq. 2 is primarily valid for small neutron detectors, it is also partially true for large detectors that have sufficient dead time or ungated duration — relative to the neutron lifetime — to exclude some neutrons from a given fission event. If uncompensated, a reported ν value would be too low. Neither the $\nu = 1$ nor the standard source-calibration techniques adjust for this effect.

Interactions. Validity of the coincidence equations requires that interactions between fission fragments and emitted neutrons be negligible. Two of the three recognized interactions[55] are certainly negligible — (1) the connection between ν and fission energy (e.g., fission-counter bias)[50,56] and (2) the relation between the direction of incident fission-inducing low-energy neutrons and the resulting fission; but it is not clear that the third interaction, (3) the orientation in direction between the fission fragment and its boiled-off neutron progeny, can be readily dismissed.

The strong correspondence between emitted fragment and associated neutrons was illustrated and discussed earlier in connection with fission cross-section measurements. In the usual equipment arrangement for the gated coincidence measurements of ν, a parallel-plate fission counter is placed perpendicular to the beam in a tube at the center of a "large" neutron detector. Sometimes these beam tubes have been several inches in diameter, resulting in escape apertures of up to 30° in one direction. If, at the same time, the fission-fragment counter has an efficiency significantly less than unity, it is possible for a small bias to be introduced into the experiment.

Kenward reported a direct measurement of the prompt-neutron yield using the coincidence technique.[57] The neutron detector consisted of a paraffin-wax cylinder containing 12 BF_3 counters with a through hole for the fission counter. A set of four neutron sources was used for calibration of the neutron detector, whose efficiency ranged from 1.7 to 2.2% over the neutron-energy range 24 kev to 5 Mev. A cadmium liner excluded thermal neutrons. A fission foil, mounted in a parallel-plate counter, was quite thick, 0.8 mg/cm^2; thus it presented a strong likelihood of problems in angular correlation even though the efficiency claimed was 94%. Normalization of neutron efficiency was based on a ^{240}Pu source calibrated by Richmond and Gardner.[58] Although the strength was quoted with an error of 1.5%, its value was derived from comparisons with other sources that typically have 3% standard errors. This indirect procedure was required because of the low emission rate of the ^{240}Pu source.

"Boron-Pile" Experiments. Colvin and Sowerby[59] have applied a boron pile as the neutron detector in a prompt coincidence-type neutron-yield experiment. The boron pile is a stack of graphite in which 240 BF_3 counters were implanted. This type of detector has nearly the same neutron efficiency (60%) as large liquid scintillators but is rather insensitive to gamma rays. The boron pile can be located next to a reactor, with a through hole used for location of a fission counter. Gates of 4 msec are required for foreground and background measurements owing to the long slowing-down times of neutrons in graphite. The efficiency of this neutron detector has been found by using a reaction with ν known to be 1, namely, photodisintegration of the deuteron. This type of calibration is quite difficult, and the lowest calibration energy is 200 kev. Because of the detector-channel arrangement, there is a small anisotropy in neutron-detection efficiency.

Liquid-Scintillator Experiments. A large liquid scintillator was first calibrated with an n-p scattering experiment originated by Diven.[50] A 300-liter cadmium-loaded tank was used; neutron efficiency was roughly 80%. Values finally reported for the experiment are based on efficiency normalized by $\nu = 2.46 \pm 0.03$ (for ^{235}U) even though independent calibration was made through n-p scattering. The results of this latter calibration were rejected in favor of normalization because of lack of confidence in the precision of the method. If the result had been accepted, a ^{235}U neutron yield of 2.41 could have been obtained.

Diven[50] used a plastic scintillator for n-p scattering to provide essentially $\nu = 1$. There are several objections to this technique. One trouble is that so little energy from the incident neutron is left in the plastic scintillator (which detects the proton recoil) that there is serious competition with intrinsic noise and gamma-ray background. In addition, it is necessary to know the energy of a (single) scattering in the recoil, and this is subject to difficulties even above noise levels. Furthermore, a reasonably monochromatic beam is required, as is a capability to simulate neutrons over the fission-energy spectrum. Also, it is necessary, a priori, to have adequate knowledge of the fission spectrum,[56,60] which in itself is poorly known, especially in the region below 0.5 Mev. However, the larger liquid scintillators have high efficiencies, ~80%, that are reasonably uniform over the entire energy range; thus the weaknesses attributed must be weighted by this higher efficiency.

NEUTRON YIELD FROM ^{252}Cf

Because the neutron yield from the spontaneous-fission isotope ^{252}Cf can be determined in the absence of a reactor-connected background, it has been used rather extensively in evaluation of ν for ^{235}U. A number of measurements relying on both the gated and ungated techniques have been listed in Tables 10 and 11.

Most of the basic requirements of the measurements for ^{252}Cf are similar to those outlined for ^{235}U. Tables 10 and 11 contain recent summaries of measurements and evaluations. As with ^{235}U, there are two groupings of values; some are around 3.78 and some about 3.70. The low ^{252}Cf values are associated with experimenters who derived low ^{235}U results.

A report by Moat[52] describes an evaluation of ^{235}U and ^{252}Cf neutron-yield values. The ^{252}Cf results follow from separate experiments using calibrated ^{240}Pu as a neutron standard (somewhat similar to the work of Kenward[57] and finding the fission rate by extrapolation to zero bias. The value obtained in this experiment, 3.70 ± 0.07, was revised in 1964 to 3.78 ± 0.07 by the same authors[61] who administered a correction for fission-neutron spectral differences of ^{252}Cf and ^{240}Pu. This result has again been revised downward to 3.683 following the 1966 recalibration of the ^{240}Pu source.[62] After finding a value of $\bar{\nu}$ for ^{252}Cf, the authors proceeded to calibrate a 100-liter cad-

Table 10 SURVEY OF TOTAL NEUTRON YIELDS FROM SPONTANEOUS FISSION OF ^{252}Cf

Value	ν, neutrons per fission	Ref.	Comments
A	3.53 ± 0.15	112	Manganese bath calibrated by mock fission source
B	3.82 ± 0.12	113	Relative to $\nu(^{240}\text{Pu}) = 2.257 \pm 0.046$
C	3.52 ± 0.16	114	Relative to calibrated Ra−γ−Be source (National Bureau of Standards)
D	3.70 ± 0.07	52	Relative to ^{240}Pu source used by Ref. 57 (value later revised to 3.77 ± 0.07)
E	3.77 ± 0.05	115	Revised value based on $\nu(^{235}\text{U}) = 2.414$
F	3.763 ± 0.048	116	Based on $\nu(^{235}\text{U}) = 2.414$
G	3.780 ± 0.031	51	Liquid scintillator calibrated by $n-p$ scattering
H	3.780 ± 0.053	117	Unpublished value circulated by private communication[117]
I	3.808 ± 0.034	53	Liquid scintillator calibrated by $n-p$ scattering
J	3.77 ± 0.07	61	Upgrading of data in value D
K	3.782 ± 0.024	118	Best weighted mean of values G, H, I, and J
L	3.779 ± 0.010	16	Weighted average of values G, H, I, and J
M	3.772 ± 0.015	19	10-parameter least-squares fit
N	3.713 ± 0.015	54	Boron-pile gated measurement (revised)
O	3.683 ± 0.040	62	Revised value of J based on recalibration of ^{240}Pu source
P	3.750 ± 0.028	48	Absolute neutron rate by manganese bath; absolute fission rate by coincidence counting
Q	3.798 ± 0.033	66	Preliminary value; absolute neutron rate by manganese bath; absolute fission rate by small-solid-angle counting

mium-loaded liquid-scintillation counter for comparative measurements with ^{235}U.

Key Measurements. One of the few internally consistent experiments reported with an absolute yield is by Hopkins and Diven[51] They used an 800-liter cylindrical scintillation system to reduce fission escape to a nominal level. Efficiency for ^{252}Cf was about 85% following calibration by n-p scattering from 0.6-cm-thick NE-102 plastic scintillator. The d-d and d-t reactions were used to provide incident neutrons of 0 to 2, 3.9, and 6 to 8 Mev. The authors believe that a pile-up correction is the limiting factor in accuracy (contributing 0.6% uncertainty to ν). The ^{252}Cf neutron spectrum reported by Bonner[63] was used for integration. (Compare with recent experiments by Meadows[64] and Condé and During.[60]) Relative values for ^{235}U and other nuclides were also obtained by Hopkins and Diven.[51]

Another key measurement was by Asplund-Nilsson.[53] One improvement this absolute measurement incorporated over similar prompt coincidence-type experiments was the use of pulse-shape discrimination to separate pulses due to recoil protons from those due to gamma rays. A spherical neutron counter containing 110 liters of cadmium-loaded scintillator was calibrated with d-d and d-t neutrons. It was possible to discriminate against Compton electrons down to 0.8-Mev proton-recoil energy. Neutron efficiency ranges from a little over 70% in the low-energy range down to 50% at 10 Mev. A parallel-plate fission counter providing a little more than 1 fission/sec was mounted in the beam tube.

An independent efficiency determination of the boron pile for ^{252}Cf was carried through by several methods; subsequent support for the single-neutron-detection efficiency was obtained with calibration of the Harwell ^{240}Pu neutron source.[62]

The gated methods for determination of the neutron yield were examined at the Paris Conference by Colvin and Sowerby.[65] Although the boron-pile system has been dismantled, Colvin and Sowerby have been studying various effects that could lead to systematic errors in the different experiments, gated and ungated, as well as their own. They did not find any clear-cut symptoms; however, they did not up to then have an opportunity to examine thoroughly the two effects of neutron multiplicity and angular correlations mentioned by others at the conference.[21]

Two new reports of ν by the ungated method were made at the Paris conference. The most extensive data were given by De Volpi and Porges[48] who derived an intermediate result with a precision of 0.75%. For their measurements, two ^{252}Cf counters, one with parallel-plate geometry and the other with hemispherical geometry, were calibrated for fragment efficiency by a prompt-coincidence method. Studies were made of a rather large 4 to 15% angular-correlation effect that was taken into account. These calibrated counters were placed in a manganese-bath system which, besides being independently standardized, was also compared with the U. S. National Bureau of Standards neutron source.

A second measurement quoted with similar precision has been reported by White and Axton.[66] One fission counter was calibrated for fission rate by small solid-angle fragment counting. Despite several initial problems in fission and neutron assay, high confidence has been realized because of the well-established manganese-bath system developed by Axton.[67]

A study made by Condé[68] highlights some additional features of the neutron-yield experiments which may tend to explain the lack of internal consistency.

CROSS SECTIONS AT 24 kev

Fission parameters and underlying cross sections are being measured or referred to the nominal energy of 24 kev for two reasons. First, a sizable share of fissions in fast breeders occurs in the kev range. Second, the energy of the convenient ^{124}Sb−^{9}Be photoneutron source is about 24 kev. Actually, recent spectroscopy of ^{124}Sb combined with the beryllium(γ,n) threshold (1665.1 ± 0.6 kev) indicates that Sb−Be neutrons originate at less than 24 kev. Ryves and Beale[69] find the ^{124}Sb gamma to be 1690.7 ± 0.4 kev, and thereupon they calculate a neutron distribution

centered at 22.8 ± 1.0 kev. White and Groves[70] have since reported the ^{124}Sb line to be 1691.24 ± 0.08, which implies a centroid at 23.3 ± 0.9 kev. (I compute 22.7 ± 0.6 and 23.2 ± 0.5 kev, respectively.)

Neutrons emerging from Sb–Be sources are distributed, according to angle relative to the photon, with a full width at half maximum of about 1.3 kev. A low-energy tail is also produced from moderation effects in the beryllium. Thin shells (0.76 mm) such as those used by Schmitt[71] for a number of nonfission absorption cross sections are likely to be nominally unaffected by this degradation. However, since the absorption cross sections follow a $1/v$ slope, the moderated neutrons have a high importance.

Table 11 MEASUREMENTS OF TOTAL NEUTRON YIELD FROM SPONTANEOUS FISSION OF ^{252}Cf

Investigators	Ref.	Date	Method	ν, neutrons per fission
De Volpi, Porges, and Armani	48	1966	Independent absolute neutron and fission rates	3.750 ± 0.028
White and Axton	66	1966	Independent absolute neutron and fission rates	3.796 ± 0.030
Colvin and Sowerby	54	1965	Gated boron pile	3.713 ± 0.015
Asplund-Nilsson, Condé, and Starfelt	53	1963	Gated scintillator	3.808 ± 0.034
Hopkins and Diven	51	1963	Gated scintillator	3.780 ± 0.031
Moat, Mather, and McTaggert	52	1961	Independent neutron fission rates	3.70* ± 0.07

Investigators	Neutron detector					
	Type	Size	Aperture	Calibration	ϵ_n, %	Errors
De Volpi and Porges	Manganese bath	1.06-m-diameter sphere	†	Absolute 4π β/γ coincidence (corroborated with NBS-II	‡	0.3% Mn/H absorption
White and Axton	Manganese bath	0.98-m-diameter sphere	†	Absolute 4π β/γ coincidence (corroborated with NPL standard source)	‡	0.2% Mn/H absorption
Colvin and Sowerby	Graphite with 240 BF_3 counters	220-cm cube	5.5° (core)	$d(\gamma,n)p$ reaction in ionization counter	64	0.2% anisotropy; 0.1% gating effects
Asplund-Nilsson, Condé, and Starfelt	Cadmium-loaded liquid scintillator	60-cm-diameter sphere	11.5°	(n,p) scattering in anthracene	69	0.5% (^{252}Cf) fission spectrum
Hopkins and Diven	Cadmium-loaded liquid scintillator	1-m-long 1-m-diameter cylinder	9°	(n,p) scattering in plastic scintillator	86	0.6% pileup
Moat, Mather, and McTaggert	Paraffin wax castle with BF_3 counters	Two 75-cm-long, 38- and 100-cm-diameter cylinders	85° and 30°	^{240}Pu standard neutron source	1	0.3% neutron spectrum; 0.4% self-multiplication

Investigators	Fission detector			
	Type	ϵ_f, %	Calibration	Errors
De Volpi and Porges	Parallel-plate and hemispherical ionization counter	60, 90	Fragment/neutron coincidence	0.4% fission rate
White and Axton	Parallel-plate ionization counter	99	Small solid-angle counter	0.8% fission counting
Colvin and Sowerby	Parallel-plate ionization counter			0.1% ion-counter efficiency
Asplund-Nilsson, Condé, and Starfelt	Parallel-plate fission counter	(80 fissions/min)		
Hopkins and Diven	Parallel-plate ionization counter			
Moat, Mather, and McTaggert	Parallel-plate ionization counter	98.5	Extrapolation	0.3% fission rate

*Revised value based on recalibration of ^{240}Pu source [revised to 3.78 ± 0.07 (Ref. 61) in 1964 and reduced in 1966 to 3.684 ± 0.010 (Ref. 62)].
†Neutron leakage: 1%.
‡σ(Mn)/σ(H): 0.0251, Ref. 67.

Because the very important ^{235}U fission cross section exhibits fluctuations in the 24-kev region, it is not clear that (1) 24 kev is a good energy for a standard measurement or (2) that only thin beryllium shells should be used. A good case can be made for a series of measurements in which the line width is intentionally broadened in order to average over the microstructure.

In any event, Sb–Be represents the only opportune monoenergetic source in this crucial region; in addition, there remain a number of other important cross sections that do not display strongly varying characteristics at 24 kev.

Capture Cross Sections. Some cross-section data are based on either the gold or boron cross sections at this energy. A measurement and thorough evaluation of the ^{197}Au (n,γ) cross section at 30 kev has been reported by Pönitz.[72] Considerable spread is noted in reported measurements, but Pönitz believes he can reconcile these with his own experimental value of 0.598 ± 0.012 barns at 30 kev. Ryves[73] reports 640 ± 25 mb at the Sb–Be energy in fair agreement with an extrapolation of Pönitz's value.

A large number of absorption cross sections using Sb–Be sources have been provided by Belanova.[74] The Russian group finds σ_a = 2.91 ± 0.17 barns for ^{235}U and σ_a = 2.69 ± 0.17 barns for ^{239}Pu at the Sb–Be energy. The Russian work is generated from beryllium shells 2 to 4 mm thick.

Fission Cross Sections. Fission cross sections derived by Perkin et al.[75] for nine isotopes include σ_f = 2.36 ± 0.06 barns for ^{235}U and σ_f = 1.66 ± 0.07 barns for ^{239}Pu. Their thorough experiment included absolute neutron-source calibration by the manganese bath, a 3-mm beryllium shell, extrapolation of fission-fragment efficiency, and careful examination of neutron-scattering effects. Comparisons with other published data are made by the authors.

Large Discrepancies. There are discrepancies up to 30% in various kev capture cross-section values. It has been emphasized by Bogart[76] that some of this disagreement may result from the ^{10}B standard. Because many of the gold and other cross sections are based on ^{10}B normalization, both the absolute value and the shape of the cross section should be examined. Bogart indicates that the boron cross section departs significantly from $1/v$ variation above 80 kev. In addition, a Monte Carlo study of sphere transmission experiments has been made by Bogart[77] that further demonstrates the incoherence of nonstandardized cross sections at 24 kev.

An area of special concern has been the 20% gulf between the kev fission cross sections reported by White[46] and the higher values previously accepted.[78] White has taken special precautions to account for room-scattered background.[79] White's data extrapolated to 24 kev are consistent with the Sb–Be measurements of Perkin,[75] and these values are quoted to less than 3%. Measurements by Knoll and Pönitz[80] linearly extended to 24 kev likewise support the lower values within a 3% band.

CROSS SECTIONS AS ENERGY FUNCTIONS

A number of groups are making broad spectrum measurements of the various fission parameters at energies going up to the top of the fission-energy distribution. Some of these were reported at the Paris Conference. A group at Harwell[22] has been accumulating data for η, α, and σ_f for ^{239}Pu from the resonance region into the kev region, based on the thick-sample method that requires normalization through η. A major advantage of this method is that it does not depend on any coincidence requirement (with its attendant angular-correlation problems). Similar experiments have been conducted at Rensselaer Polytechnic Institute.[81] Another prolific source of cross sections as functions of energy has been the time-of-flight data resulting from underground nuclear explosive tests.[82]

Various aspects of these techniques were surveyed at the Washington Conference and critically reviewed at the Paris Conference.[21]

P. H. White at Aldermaston has contributed a number of papers containing essential fission cross-section data over a wide span of reactor interest. Underlying most of his work is measurement to an accuracy of about 3% of the ^{235}U fission cross section relative to the n-p scattering cross section at a number of points in the interval from 40 kev to 14 Mev.[46] Upon this foundation the fission cross sections have been ascertained for a variety of fissionable materials from 40 to 500 kev (Ref. 83) and from 1 to 14 Mev (Ref. 84).

VALUES FOR BORON, LITHIUM, AND HYDROGEN

The $^{10}B(n,\alpha)$ cross section for thermal neutrons is considered one of the best known values of all cross sections.[85] It is believed that 0.1% precision is assignable to the total absorption (3834 ± 5 barns for one standard deviation)[86] and that the branching ratio $(n,\alpha_0)/(n,\alpha)$ = 0.06303 ± 0.00006 at thermal is good to 0.2% or better;[85] however, above thermal there are significant discrepancies, especially in the kev region, which provide only 5% agreement in absorption and 10% in branching.[87] More measurements of the absorption and elastic cross sections and angular distributions are needed to bring these values down to an objective of 1%.

Because of poor knowledge of the isotopic composition of natural lithium, the thermal $^{6}Li(n,\alpha)$ cross section is only known to an accuracy of ±3% (Ref. 85). Measurements of the ratio of ^{6}Li to ^{10}B cross sections in the thermal and epithermal region have been recommended.[85]

As a nuclear standard supporting a number of fission measurements, the hydrogen absorption and

scattering cross sections deserve comment. The BNL-325 absorption cross section is recommended as 332 ± 2 mb. The suitability of the n-p cross section above 100 kev was examined by Hopkins,[88] who indicates that 2% confidence may be attached presently to the total cross section, whereas Spaepen[89] believes 1% is generally more appropriate. Bennett[90] has shown that proton recoils can also be detected well below 100 kev; thus the range required for precise scattering data is extended.

PROMPT-NEUTRON YIELDS AS ENERGY FUNCTIONS

A recent examination by Fillmore[26] brings the prompt-neutron yield as a function of energy $\nu_p(E)$ up-to-date with the latest data tabulations and graphs for the four fissionable isotopes. All data were renormalized to ^{252}Cf $\nu_p = 3.764$, which is a convenient choice if there should be changes in the underlying standard. Condé[91] has submitted additional ^{239}Pu and ^{241}Pu data for publication.

Attainable Precision

Certain general limitations in cross-section accuracy must be recognized. Attainable precision for average quantities such as nuclear cross sections is bounded by proved techniques. This implies replication by other experimenters and critical scrutiny of measurement procedures, or at least cooperative exchange of samples, sources, equipment, or personnel. Attainable precision also is constrained by fitting processes currently applied to published data. At present, diverse experimeters located at distant laboratories, often applying different methods of measurement, must reconcile the data.

LIMITING FACTORS

In addition to the above general limits, precision depends on sample composition, neutron-energy resolution, and counting and calibration techniques.

Sample Composition. For accuracies of ~0.5%, the ingredients, in general, must be known to 0.1% (e.g., chemical composition, isotopic constituents, and gravimetric analysis or alpha assay). Owing to the efforts of such broad-based laboratories as the Central Bureau of Nuclear Measurements,[85] many of the problems associated with sample composition are converging to the 0.1% level of confidence.

Energy Resolution. The neutron-energy definition usually need not be precise. An exception to this is the effort to establish some reference cross sections in the resonance and kev span. Improved energy resolution is emerging from proton-recoil spectrometers recently developed with nearly 2-kev resolving power and reduced gamma-ray sensitivity due to pulse-shape discrimination.[90] The existence of some useful monoenergetic neutron reference sources is helpful on occasion.

Counting. There were indications at the Vienna Symposium on Standardization of Radionuclides[92] that counting facilities are in some selected cases approaching the 0.1% objective. This is true for small-solid-angle counting of alpha emitters and particularly true for coincidence counting. Various physical effects requiring small corrections in the coincidence data have been thoroughly studied,[93] and instrumental effects have been assimilated into available computer programs.[94] International calibrations of certain standard radioisotopes have been organized and analyzed by the International Bureau of Weights and Measures; 0.5% agreement has been obtained by a large number of laboratories in the past few years.[95]

Calibrations. Absolute neutron-measurement techniques are also progressing. Despite only 1% agreement in source calibration for a dozen national laboratories[96] through 1965, improved manganese-bath calibration and monitoring methods[67] promise to reduce the error by an order of magnitude.

The various reference cross sections, especially $^{10}B(n,\alpha)$, $^{197}Au(n,\gamma)$, and $^{1}H(n,\gamma)$, continue to be reevaluated by both old and new methods, especially with improved samples and better knowledge of supporting parameters such as half-life, branching ratios, and ancillary cross sections.

VALUES AT THERMAL ENERGIES

As a consequence of these developments, it is reasonable to expect uncertainties in the fission parameters to be reduced to 0.5% or less. Values for ^{235}U are more precise than for other fissile materials, a condition that will change as sufficiently pure samples of other materials become available.

σ_a, *the Absorption Cross Section.* The absorption cross section is derived from the most elementary experimental process; precision approaching 0.1% can be foreseen as carefully assayed samples are traded among users.

η, *Neutrons Emitted/Neutron Absorbed.* Measurements of the number of neutrons emitted per neutron absorbed are more difficult because they involve detection of both high- and thermal-energy neutrons. Experiments in a well-thermalized reactor spectrum have not yet been performed; in principle, the new manganese-bath systems making use of on-line counting[49,67,97] are well-suited for this application. A precision of 0.33% ultimately may be attained.

α, *the Capture-to-Fission Ratio.* Direct values of the capture-to-fission ratio are beginning to benefit from several years of irradiation. Despite the present unexpected deviations, precisions approaching 0.2% should be obtainable as better knowledge of irradiation spectra is attained.

σ_f, *the Fission Cross Section.* Some sources of discord in the fission cross-section data are being

recognized, particularly the effect of angular correlations for experiments relying on neutron/fission coincidence techniques. It is also somewhat circumspect that those experiments which have reported relatively low values of ν for ^{235}U and ^{252}Cf have more than one of the following characteristics: low fission-counter efficiency, large escape aperture, low neutron-detector efficiency, or relatively long gating time.

ν, Neutrons/Fission. Determination of the neutron yield per fission requires absolute counting measurements, which are avoided in other fission-parameter determinations. However, reduced specifications for sample composition and for incident-neutron texture offset this liability. There also have been a number of improvements in neutron detection which are applicable to neutron-yield evaluation. Both British[66] and American[48] groups are pursuing better data and better agreement. Because the yields may be determined by two widely different experimental methods, and because ^{252}Cf can be established as a convenient reference standard, it is likely that 0.33% accuracy is attainable in ν as well as in σ_f.

VALUES AT ENERGIES ABOVE THERMAL

The requirements for precision in fission quantities at high energies may not be as severe as at thermal energies; this is good because the only energy point at which the slope of the energy dependence can be conveniently fixed at present is based on Sb–Be photoneutrons. At 24 kev the fission cross section is a factor of 100 lower than at thermal energy, thus raising additional problems that are likely to limit precision for all parameters to 1% in the immediate future. Even that precision necessitates a factor of 3 improvement in technique.

With the addition of another calibration point of ~200 kev, the foundations will at least be established for an effort to adequately meet acknowledged fast reactor design objectives.

A number of people—C. H. Westcott, H. Condé, M. G. Sowerby, W. P. Pönitz, and J. Spaepen—were kind enough to provide recent data or forthright comments concerning an early draft; even though I was unable to comply with all suggestions, the manuscript benefited greatly from their advice. Some mistakes in the draft were graciously brought to my attention by L. Bollinger, A. Moat, B. S. Mather, D. W. Colvin, and P. H. White. Compilation of this survey was suggested by R. Gold.

References

1. C. H. Westcott, Atomic Energy of Canada Ltd., personal communication, May 29, 1967.
2. P. J. Persiani, R. R. Smith, and D. Okrent, Physics Measurements in an Operating Fast Breeder Power Reactor, in *Physics Measurements in Operating Power Reactors*, Seminar Proceedings, Rome, 1966, pp. 73–118, OECD, European Nuclear Energy Agency, 1966.
3. M. Segev and S. Yiftah, Basic Nuclear Data for Fast Reactor Calculations, in *Nuclear Data for Reactors*, Conference Proceedings, Paris, 1966, International Atomic Energy Agency, Vienna, 1967 (STI/PUB/140); Paper 23/14.
4. R. L. Hellens, Sensitivity of Reactor Characteristics to Cross Section Uncertainties Below 100 ev, in Proceedings of Conference on Neutron Cross Section Technology, March 22–24, 1966, Washington, D. C., USAEC Report CONF-660303, p. 3.
5. R. C. Liikala, W. L. Purcell, and J. R. Worden, Sensitivity of Reactor Multiplication Values to Cross Section Uncertainties for Thermal Systems, in Proceedings of Conference on Neutron Cross Section Technology, March 22–24, 1966, Washington, D. C., USAEC Report CONF-660303, p. 75.
6. P. Greebler and B. A. Hutchins, User Requirements for Cross Sections in the Energy Range from 100 ev to 100 kev, in Proceedings of Conference on Neutron Cross Section Technology, March 22–24, 1966, Washington, D. C., USAEC Report CONF-660303, p. 357.
7. D. Okrent, Cross Section Uncertainties and Reactor Safety, in Proceedings of Conference on Neutron Cross Section Technology, March 22–24, 1966, Washington, D. C., USAEC Report CONF-660303, p. 430.
8. G. E. Hansen, Criticality Dependence on Neutron Cross Sections Above 100 kev, in Proceedings of Conference on Neutron Cross Section Technology, March 22–24, 1966, Washington, D. C., USAEC Report CONF-660303, p. 557.
9. W. G. Davey, A Critical Evaluation of Fast Fission Cross Sections, in Proceedings of Conference on Neutron Cross Section Technology, March 22–24, 1966, Washington, D. C., USAEC Report CONF-660303, p. 796.
10. H. H. Hummel, Sensitivity of Fast Reactor Parameters to Cross Section Uncertainties, in Proceedings of Conference on Neutron Cross Section Technology, March 22–24, 1966, Washington, D. C., USAEC Report CONF-660303, p. 809.
11. T. M. Snyder, Future Cross Section Needs of the Nuclear Power Industry, in Proceedings of Conference on Neutron Cross Section Technology, March 22–24, 1966, Washington, D. C., USAEC Report CONF-660303, p. 1025.
12. R. D. Smith, Nuclear Data Requirements for Fast Reactor Design and Operation, in *Nuclear Data for Reactors*, Conference Proceedings, Paris, 1966, International Atomic Energy Agency, Vienna, 1967 (STI/PUB/140); Paper 23/52.
13. G. H. Kinchin, Nuclear Data Requirements for Thermal Reactor Design and Operation, in *Nuclear Data for Reactors*, Paris, International Atomic Energy Agency, Vienna, 1967 (STI/PUB/140); Paper 23/117.
14. Proceedings of the International Conference on Fast Critical Experiments and Their Analysis, Argonne, Ill., Oct. 10–13, 1966, USAEC Report ANL-7320.
15. Neutron Cross Sections, Sigma Center, Brookhaven National Laboratory, USAEC Report BNL-325 and supplements.
16. R. Sher and J. Felberbaum, Least Squares Analysis of the 2200 m/sec Parameters of ^{233}U, ^{235}U, and ^{239}Pu, USAEC Report BNL-918, Brookhaven National Laboratory, March 1965.
17. H. Goldstein and D. W. Colvin (Eds.), CINDA, An Index to the Literature on Microscopic Neutron Data, ENEA Neutron Data Compilation Center and USAEC, July 1, 1966; also CINDA 67, 2 Vols., Oct. 1, 1967.
18. H. C. Honeck, ENDF/B, Specifications for an Evaluated Nuclear Data File for Reactor Applications, USAEC Report BNL-50066, May 1966, Brookhaven National Laboratory (Revised July 1967 by S. Pearlstein).

19. C. H. Westcott et al., A Survey of Values of 2200 m/s Constants for Four Fissile Nuclides, *At. Energy Rev.*, 3(2): 3 (1965).
20. Proceedings of Conference on Neutron Cross Section Technology, March 22–24, 1966, Washington, D. C., USAEC Report CONF-660303, Books 1 and 2.
21. *Nuclear Data for Reactors*, Conference Proceedings, Paris, 1966, International Atomic Energy Agency, Vienna, 1967 (STI/PUB/140).
22. K. Parker et al., A Survey of Neutron Cross-Section Evaluations Available at June 1, 1966, in *Nuclear Data for Reactors*, Conference Proceedings, Paris, 1966, International Atomic Energy Agency, Vienna, 1967 (STI/PUB/140); Paper 23/28.
23. W. G. Davey, Analysis of the Fission Cross Sections of ^{232}Th, ^{233}U, ^{234}U, ^{235}U, ^{236}U, ^{237}Np, ^{238}U, ^{239}Pu, ^{241}Pu, and ^{242}Pu from 1 kev to 10 Mev, *Nucl. Sci. Eng.*, 26: 149-169 (1966). Also to be published in *Nucl. Sci. Eng.* (1968).
24. M. K. Drake, Neutron Cross Sections for ^{233}U, USAEC Report GA-7076, General Atomic Division, General Dynamics Corp., Sept. 15, 1966.
25. W. Hart, Fission Cross Section Data Files for ^{232}Th, ^{233}U, ^{234}U, ^{235}U, ^{236}U, ^{238}U, ^{237}Np, ^{239}Pu, ^{241}Pu, and ^{242}Pu in the Energy Range 1 kev to 14 Mev, UKAEA Report AHSB(S)R-124, 1967.
26. F. L. Fillmore, Recommended Values for the Number of Neutrons per Fission, submitted to *J. Nucl. Energy* (1967), in preparation.
27. G. J. Safford, W. W. Havens, and B. M. Rustad, A Precise Determination of the Total Cross Section of Uranium-235 from 0.000818 ev to 0.0918 ev, *Nucl. Sci. Eng.*, 6: 433-440 (1959).
28. R. C. Block, G. G. Slaughter, and J. A. Harvey, Thermal Neutron Cross-Section Measurements of ^{233}U, ^{235}U, ^{240}Pu, ^{234}U, and ^{129}I with the ORNL Fast Chopper Time-of-Flight Neutron Spectrometer, *Nucl. Sci. Eng.*, 8: 112 (1960).
29. O. D. Simpson, M. S. Moore, and F. B. Simpson, Total Neutron Cross Sections of ^{233}U and ^{235}U from 0.02 to 0.08 ev, *Nucl. Sci. Eng.*, 7: 187 (1960).
30. A. Saplakoglu, Precision Measurements of the Neutron Total Cross Section of ^{235}U, *Nucl. Sci. Eng.*, 11: 321 (1961).
31. R. L. Macklin, G. de Saussure, J. D. Kington, and W. S. Lyon, Manganese Bath Measurements of η of ^{233}U and ^{235}U, *Nucl. Sci. Eng.*, 8: 210-220 (September 1960).
32. R. Gwin and D. N. Magnuson, The Measurement of Eta and Other Nuclear Properties of ^{233}U and ^{235}U in Critical Aqueous Solutions, *Nucl. Sci. Eng.*, 12: 364-380 (1962).
33. J. R. Smith, S. D. Reeder, and R. G. Fluharty, Measurement of the Absolute Value of Eta for ^{233}U, ^{235}U, and ^{239}Pu Using Monochromatic Neutrons, USAEC Report IDO-17083, Phillips Petroleum Company, February 1966.
34. R. L. Macklin, G. de Saussure, J. D. Kington, and W. S. Lyon, Manganese Bath Measurements of η of ^{233}U and ^{235}U, USAEC Report CF-60-2-84, Oak Ridge National Laboratory, Mar. 15, 1960.
35. M. J. Cabell, Harwell Mass Spectrometric Measurements of the Ratio of Neutron Capture to Fission for ^{233}U, ^{235}U, ^{239}Pu, and ^{241}Pu, in Reactor and Maxwellian Neutron Spectra, in *Nuclear Data for Reactors*, Conference Proceedings, Paris, 1966, International Atomic Energy Agency, Vienna, 1967 (STI/PUB/140); Paper 23/21.
36. R. W. Durham et al., The Ratio of Capture to Fission in ^{235}U and ^{239}Pu, in *Nuclear Data for Reactors*, Conference Proceedings, Paris, 1966, International Atomic Energy Agency, Vienna, 1967 (STI/PUB/140); Paper 23/2.
37. E. E. Maslin et al., Absolute Fission Cross Section of ^{235}U for 2200-m/sec Neutrons, *Phys. Rev.*, 139: B852 (1965).
38. T. M. Snyder and R. W. Williams, Number of Neutrons per Fission for 25 and 49, USAEC Report LA-102, Los Alamos Scientific Laboratory, 1944.
39. P. G. Aline, The Role of Isotopic Composition Measurements in Cross Section Evaluation, in *Nuclear Data for Reactors*, Conference Proceedings, Paris, 1966, International Atomic Energy Agency, Vienna, 1967 (STI/PUB/140); Paper 23/92.
40. H. L. Smith and J. P. Balagna, A Method of Assay of ^{235}U, ^{238}U, and ^{237}Np Fission Foils, in Proceedings of Conference on Neutron Cross Section Technology, March 22–24, 1966, Washington, D. C., USAEC Report CONF-660303, p. 1013.
41. W. J. Friesen, B. R. Leonard, and E. J. Seppi, Comparison of a ^{235}U Fission Cross Section and ^{197}Au Capture Cross Section, in Nuclear Physics Research Quarterly Report, July, August, September 1956, USAEC Report HW-47012, Hanford Atomic Products Operation, November 1956.
42. A. Saplakoglu, Absolute Thermal Fission Cross Section Measurements of ^{235}U by a New Method, in *Proceedings of the Second United Nations International Conference on the Peaceful Uses of Atomic Energy, Geneva, 1958*, Vol. 15, p. 103, United Nations, New York, 1958.
43. J. C. D. Milton and J. S. Fraser, The Energies, Angular Distributions, and Yields of the Prompt Neutrons from Individual Fragments in the Thermal Neutron Fission of ^{233}U and ^{235}U, Canadian Report AECL-2163, March 1965.
44. K. G. Porges and A. De Volpi, Absolute Determination of Fission Fragment Emission Rates with a Prompt Neutron-Fission Coincidence Method, in *Standardization of Radionuclides*, Symposium Proceedings, Vienna, 1966, International Atomic Energy Agency, Vienna, 1967, p. 693 (STI/PUB/139).
45. K. G. Porges and A. De Volpi, letter submitted in September 1967 to Nuclear Cross Section Advisory Group (they are AEC-sanctioned and print intermittent reports with contributions from various laboratories).
46. P. H. White, Measurements of the ^{235}U Neutron Fission Cross Section in the Energy Range 0.04–14 Mev, *J. Nucl. Energy, Parts A & B*, 19: 325 (1965).
47. L. B. Engle et al., Reactivity Contributions of Various Materials in Topsy, Godiva, and Jezebel, *Nucl. Sci. Eng.*, 8: 543 (1960).
48. A. De Volpi and K. G. Porges, Direct and Absolute Measurements of Average Fission Neutron Yield from Uranium-235 and Californium-252, in *Nuclear Data for Reactors*, Conference Proceedings, Paris, 1966, International Atomic Energy Agency, Vienna, 1967, Vol. 1, pp. 297-306 (STI/PUB/140).
49. A. De Volpi, K. G. Porges, and R. J. Armani, Absolute Calibrations of Fission Neutron Source Strength Relying upon an Improved Manganese Bath Technique and Absolute Beta–Gamma Coincidence Counting, in *Standardization of Radionuclides*, Symposium Proceedings, Vienna, 1966, International Atomic Energy Agency, Vienna, 1967, p. 717 (STI/PUB/139).
50. B. C. Diven et al., Multiplicities of Fission Neutrons, *Phys. Rev.*, 101: 1012 (1956).
51. J. C. Hopkins and B. C. Diven, Prompt Neutrons from Fission, *Nucl. Phys.*, 48: 433 (1963).
52. A. Moat et al., Some Experimental Determinations of the Number of Prompt Neutrons from Fission, *J. Nucl. Energy, Parts A & B*, 15: 102 (1961).
53. I. Asplund-Nilsson et al., An Absolute Measurement of $\bar{\nu}$ of ^{252}Cf, *Nucl. Sci. Eng.*, 16: 124 (1963).
54. D. W. Colvin and M. G. Sowerby, Boron Pile $\bar{\nu}$ Measurements, in *Physics and Chemistry of Fission*, Symposium Proceedings, Salzburg, 1965, International Atomic Energy Agency, Vienna, 1965, Vol. II, p. 25 (STI/PUB/101).
55. J. Terrell, Prompt Neutrons from Fission, in *Physics and Chemistry of Fission*, Symposium Proceedings,

Salzburg, 1965, International Atomic Energy Agency, Vienna, 1965, pp. 3-22 (STI/PUB/101).
56. H. Condé, Average Number of Neutrons from a Fission of ^{235}U, *Ark. Fys.*, 29: 293-299 (1965).
57. C. J. Kenward, R. Richmond, and J. E. Sanders, A Measurement of the Neutron Yield in Thermal Fission of ^{235}U, British Report AERE-R/R-212 (Rev.), October 1958.
58. R. Richmond and B. J. Gardner, Calibration of Spontaneous Fission Neutron Sources, British Report AERE-R/R-2097, 1957.
59. D. W. Colvin and M. G. Sowerby, Precision Measurements of the Mean Number of Neutrons per Fission by the Boron Pile, in *Proceedings of the Second United Nations International Conference on the Peaceful Uses of Atomic Energy, Geneva, 1958*, Vol. 16, p. 121, United Nations, New York, 1958.
60. H. Condé and G. During, Fission-Neutron Spectra of ^{235}U, ^{239}Pu, and ^{252}Cf, in *Physics and Chemistry of Fission*, Symposium Proceedings, Salzburg, 1965, International Atomic Energy Agency, Vienna, 1965, p. 93 (STI/PUB/101).
61. D. S. Mather, Average Number of Prompt Neutrons from ^{235}U Fission Induced by Neutrons from Thermal to 8 Mev, *Phys. Rev.*, 133: B1403 (1964).
62. P. Fieldhouse et al., Revision of the Harwell ^{240}Pu Source Strength and for $\bar{\nu}$ for ^{235}U and ^{252}Cf, *J. Nucl. Energy, Parts A & B*, 20: 549-555 (July 1966).
63. T. W. Bonner, Measurements of Neutron Spectra from Fission, *Nucl. Phys.*, 23: 116 (1961).
64. J. W. Meadows, ^{252}Cf Fission Neutron Spectrum from 0.003 to 15.0 Mev, *Phys. Rev.*, 157: 1076-1082 (1967).
65. D. W. Colvin, M. G. Sowerby, and R. I. McDonald, Confirmatory Experimental Data on the Harwell Boron Pile $\bar{\nu}$ Values, in *Nuclear Data for Reactors*, Conference Proceedings, Paris, 1966, International Atomic Energy Agency, Vienna, 1967 (STI/PUB/140); Paper 23/33.
66. P. H. White and E. J. Axton, Measurement of the Number of Neutrons per Fission for ^{252}Cf, submitted for publication to *J. Nucl. Energy*, 1967.
67. E. J. Axton, P. Cross, and J. C. Robertson, Calibration of the NPL Standard Ra–Be Photoneutron Sources by an Improved Manganese Sulphate Bath Technique, *J. Nucl. Energy, Parts A & B*, 19: 409 (1965).
68. H. Condé, $\bar{\nu}$ of ^{252}Cf, presented at the Panel of International Atomic Energy Agency on Nuclear Standards Needed for Neutron Cross Section Measurements, Brussels, May 8–12, 1967.
69. T. B. Ryves and D. W. Beale, An Estimate of the Energy of Sb–Be Photoneutrons from a Measurement of the ^{124}Sb Gamma-Ray Energy, *Int. J. Appl. Radiat. Isotop.*, 18: 204-205 (1967).
70. D. H. White and D. J. Groves, Precision Measurements of Standard Gamma-Ray Energies, *Nucl. Phys.*, A91: 453-459 (1967).
71. H. W. Schmitt and C. W. Cook, Absolute Neutron Absorption Cross Sections for Sb–Be Photoneutrons, *Nucl. Phys.*, 20: 202 (1960)
72. W. P. Pönitz, An Absolute (n,γ)-Cross-Section Measurement for Gold at 30 kev and Its Application in Normalization of Other Data, in *Nuclear Data for Reactors*, Conference Proceedings, Paris, 1966, International Atomic Energy Agency, Vienna, 1967 (STI/PUB/140); Paper 23/6.
73. T. B. Ryves et al., The Radiative Capture Cross Section of Gold at the Energy of Sb–Be Photoneutrons, *J. Nucl. Energy, Parts A & B*, 20: 249-260 (1966).
74. T. S. Belanova, A. A. Van'kov, F. F. Mikhailas, and Yu. Ya. Stavisskii, Measurements of Absorption Cross Sections for Neutrons with Energy of 24 kev in Spherical Geometry, in *Nuclear Data for Reactors*, Conference Proceedings, Paris, 1966, International Atomic Energy Agency, Vienna, 1967 (STI/PUB/140); Paper 23/96.
75. J. L. Perkin et al., The Fission Cross Sections of ^{233}U, ^{234}U, ^{235}U, ^{236}U, ^{237}Np, ^{239}Pu, and ^{241}Pu for 24-kev Neutrons, *J. Nucl Energy, Parts A & B*, 19: 423 (1965).
76. D. Bogart, Boron Cross Sections as a Source of Discrepancy for Capture Cross Sections in the kev Region, in Proceedings of Conference on Neutron Cross Section Technology, March 22–24, 1966, Washington, D. C., USAEC Report CONF-660303, p. 486.
77. D. Bogart and T. T. Semler, A Monte Carlo Interpretation of Sphere Transmission Experiments for Average Capture Cross Sections at 24 kev, in Proceedings of Conference on Neutron Cross Section Technology, March 22–24, 1966, Washington, D. C., USAEC Report CONF-660303, p. 502.
78. W. D. Allen and A. T. Ferguson, The Fission Cross Sections of ^{233}U, ^{235}U, ^{238}U, and ^{239}Pu for Neutrons in the Energy Range 0.030 Mev to 3.0 Mev, *Proc. Phys. Soc. (London)*, A70: 573 (1957).
79. P. H. White, The Room Scattered Background Produced by a Neutron Source in a Laboratory with Concrete Walls, *Nucl. Instrum. Methods*, 39: 256-260 (1966).
80. G. F. Knoll and W. P. Pönitz, A Measurement of the ^{235}U Fission Cross Section at 30 and 64 kev, *J. Nucl. Energy*, 21(8): 643-652 (1967).
81. G. de Saussure et al., Measurement of the Neutron Capture and Fission Cross Sections and Their Ratio, α, for ^{233}U, ^{235}U, and ^{239}Pu, in *Nuclear Data for Reactors*, Conference Proceedings, Paris, 1966, International Atomic Energy Agency, Vienna, 1967 (STI/PUB/140); Paper 23/48.
82. A. Hemmendinger, New Time-of-Flight Measurements Made with an Intense Source, in *Nuclear Data for Reactors*, Conference Proceedings, Paris, 1966, International Atomic Energy Agency, Vienna, 1967 (STI/PUB/140); Paper 23/42.
83. P. H. White, J. C. Hodgkinson, and G. C. Wall, Measurement of Fission Cross Sections for Neutrons of Energies in the Range 40–500 kev, in *Physics and Chemistry of Fission*, Symposium Proceedings, Salzburg, 1965, International Atomic Energy Agency, Vienna, 1965, Vol. 1, p. 219 (STI/PUB/101).
84. P. H. White and G. P. Warner, The Fission Cross Sections of ^{233}U, ^{234}U, ^{236}U, ^{238}U, ^{237}Np, ^{239}Pu, ^{240}Pu, and ^{241}Pu Relative to that of ^{235}U for Neutrons in the Energy Range 1 to 14 Mev, *J. Nucl. Energy*, 21: 671-679 (1967).
85. J. Spaepen, Standard Data and Standard Samples in Nuclear Energy, in *Nuclear Data for Reactors*, Conference Proceedings, Paris, 1966, International Atomic Energy Agency, Vienna, 1967 (STI/PUB/140); Paper 23/19.
86. G. H. Debus and P. J. De Bievre, Thermal Neutron Absorption Cross Section of Boron, *J. Nucl. Energy*, 21: 373 (1967).
87. R. L. Macklin and J. H. Gibbons, A Study of $^{10}B(n,\alpha)^7Li$, $^7Li^*$ for $30 < E_n(\text{kev}) < 500$, submitted for publication in *Phys. Rev.* (1967).
88. J. C. Hopkins, The $^1H(n,n)$ Cross Section as a Nuclear Standard, a paper presented at the International Atomic Energy Agency Panel on Nuclear Standards Needed for Neutron Cross Section Measurements, Brussels, May 8–12, 1967.
89. J. Spaepen, Central Bureau Neutron Measurements, Geel, Belgium, personal communication, Aug. 21, 1967.
90. E. F. Bennett, Fast Neutron Spectroscopy by Proton-Recoil Proportional Counting, *Nucl. Sci. Eng.*, 27: 16-27 (1967).
91. H. Condé et al., Prompt $\bar{\nu}$ in Neutron-Induced Fission of ^{239}Pu and ^{241}Pu, submitted for publication to *J. Nucl. Energy* (1967).
92. *Standardization of Radionuclides*, Symposium Proceedings, Vienna, 1966, International Atomic Energy Agency, Vienna, 1967 (STI/PUB/139).
93. A. P. Baerg, Measurement of Radioactive Disintegra-

tion Rate by the Coincidence Method, *Metrologia*, 2: 23 (1966).
94. A. De Volpi, K. G. Porges, and G. Jensen, Computer Code for Reduction of Coincidence Counting Data, *Int. J. Appl. Radiat. Isotop.*, 17: 277 (1966).
95. Bureau International des Poids et Mesures, Panel Meeting: Discussion of Four International Comparisons of Radionuclide Solutions Organized by the BIPM, October 15, 1966, Report by BIPM, dated Apr. 24, 1967.
96. V. Naggiar, Comparison Internationale des Mesures de Taux d'Émission de la Source de Neutrons Ra–Be (α,n) n° 200-1 du Conseil National de Richerches, *Metrologia*, 3: 51-52 (1967).
97. A. Capgras, Étalonnage de Sources de Neutrons (α,n), in *Neutron Monitoring for Radiological Protection*, Symposium Proceedings, Vienna, 1966, International Atomic Energy Agency, Vienna, 1967 (STI/PUB/136).
98. G. J. Safford and W. W. Havens, Jr., Fission Parameters for ^{235}U, *Nucleonics*, 17(11): 134-138, 205-206 (November 1959).
99. J. R. Smith and E. Fast, Techniques for Determining Eta for the Thermally Fissionable Isotopes, USAEC Report IDO-17173, Phillips Petroleum Company, April 1966.
100. A. Okazaki, M. Lousbury, and R. W. Durham, A Determination of the Ratio of Capture to Fission Cross Section of ^{233}U, Canadian Report AECL-2148, December 1964.
101. G. J. Safford and E. Melkonian, Determination of the Absolute Neutron Fission Cross Section of ^{235}U, *Phys. Rev.*, 113: 1285 (1959).
102. S. J. Cocking, Measurement of the Ratio of Absorption Cross Section to Fission Cross Section for ^{233}U, ^{235}U, and ^{239}Pu with 0.0011-ev Neutrons, *J. Nucl. Energy*, 6: 285 (1958).
103. G. Fraysse and A. Prosdocimi, Fission Cross-Section Measurement of ^{235}U and ^{239}Pu for Low-Energy Neutrons, in *Physics and Chemistry of Fission*, Symposium Proceedings, Salzburg, 1965, International Atomic Energy Agency, Vienna, 1965 (STI/PUB/101); Paper SM-60/17.
104. A. J. Deruytter, The Fission Cross Section of ^{235}U from 0.01 ev to 0.1 ev and Its Absolute Value at 0.0253 ev, *J. Nucl. Energy, Parts A & B*, 15: 165-175 (1961).
105. J. F. Raffle, Thermal Neutron Fission Cross-Sections of Several Isotopes, British Report AERE-R-2998, July 1959.
106. G. Fraysse, A. Prosdocimi, F. Netter, and C. Samour, Measurement of the Fission Cross Section of ^{235}U and ^{239}Pu for Thermal Neutrons, French Report CEA-R-2775, April 1965.
107. P. A. Egelstaff and J. E. Sanders, Neutron Yields from Fissile Nuclei, in *Proceedings of the International Conference on the Peaceful Uses of Atomic Energy, Geneva, 1955*, Vol. 4, p. 307, United Nations, New York, 1956. See also J. E. Sanders, A Comparison of the Average Number of Neutrons Emitted in Fission of Some Uranium and Plutonium Isotopes, *J. Nucl. Energy*, 2: 247 (1956).
108. V. I. Kalishnikova, V. I. Lebedev, L. A. Mikaelyan, P. E. Spivak, and V. P. Zakharova, Measurements of the Average Number of Neutrons Emitted in the Fission of Some Uranium and Plutonium Isotopes. Part I. Relative Measurements of the Average Number of Neutrons Emitted in the Thermal Fission of ^{233}U, ^{235}U, ^{239}Pu, and ^{241}Pu, in Proceedings of the Conference of the Academy of Sciences of the USSR on Peaceful Uses of Atomic Energy (Physics and Mathematics Section), USAEC Report AEC-tr-2435 (Pt. 1), 1956.
109. D. W. Colvin and M. G. Sowerby, The Most Recent Values of $\bar{\nu}$ for a Number of Fissile Isotopes Measured Using the Boron Pile, British Report TNCC(UK)-43, August 1959.
110. A. Moat, M. H. Taggart, and D. S. Mather, Discrepancies in $\bar{\nu}$ Values, British Report NR/p-1/59, April 1959.
111. D. W. Colvin, personal communication quoted in Ref. 16.
112. W. W. Crane, G. H. Higgins, and S. G. Thompson, Average Number of Neutrons Emitted During the Spontaneous Fission of ^{252}Cf, *Phys. Rev.*, 97: 242 (1955). Errata: *Phys. Rev.*, 97: 1727 (1955).
113. A. Hicks et al., Probabilities of Prompt-Neutron Emission from Spontaneous Fission, *Phys. Rev.*, 101: 1016-1020 (1956).
114. W. W. Crane et al., Average Number of Neutrons per Fission for Several Heavy-Element Nuclides, *Phys. Rev.*, 101: 1804 (1956).
115. B. C. Diven, Los Alamos Scientific Laboratory, personal communication, 1961.
116. J. W. Meadows and J. F. Whalen, Energy Dependence of Prompt $\bar{\nu}$ for Neutron-Induced Fission of ^{235}U, *Phys. Rev.*, 126: 197 (1962).
117. D. W. Colvin, personal communication quoted in Ref. 61.
118. D. S. Mather et al., Measurement of Prompt $\bar{\nu}$ for the Neutron-Induced Fission of ^{232}Th, ^{233}U, ^{234}U, ^{238}U, and ^{239}Pu, *J. Nucl. Phys.*, 66: 149 (1965).

AEC Proposes Criteria for Pressure Vessels, Invites Comments

To help ensure that pressure vessels for reactor systems are built to the highest practicable quality standards, the U. S. Atomic Energy Commission issued on Aug. 23, 1967, a set of 34 criteria for the design, material, fabrication, inspection, and testing of such vessels. Entitled "Tentative Regulatory Supplementary Criteria for ASME Code-Constructed Nuclear Pressure Vessels," these new criteria are intended to be in accord with Criterion 1 of the Commission's previously* proposed "General Design Criteria for Nuclear Power Plant Construction Permits" in that the dependability of pressure vessels must reflect their importance in preventing accidents that could affect public safety. Thus the vessel criteria indicate what AEC expects of vessel designers, manufacturers, and potential operators.

Supplementary. The new criteria supplement the rules of the American Society of Mechanical Engineers (ASME) *Boiler and Pressure Vessel Code*, Section III, Rules for Construction of Nuclear Vessels, 1965 Edition, and its addenda. (Each criterion is referenced to the appropriate ASME Code paragraph; explanations give the reasons for each criterion.) Applicants for AEC construction permits usually specify the ASME Code for reactor-plant vessels. Some of the new criteria are derived from specifications of the American Society for Testing and Materials and from standards of the Society for Nondestructive Testing and other code groups; others of the new criteria go beyond the scope of existing codes. For instance, in addition to normal operating transient conditions, the criteria call for the designer to consider the loads and other effects of postulated accident situations. Criterion 1.37 requires that the vessel design include provisions to permit periodic inspections during the life of the vessel. In all cases the significant intention is to ensure the reliability and safe functioning of vessels over their service lifetimes.

Regulatory. The Commission has followed the practice, on a case-by-case basis, of requiring that nuclear pressure vessels be designed, fabricated, and inspected to quality standards beyond the rules in the existing engineering codes. In this connection, some of the tentative criteria have already been used by AEC in evaluating designs proposed in applications for plant construction permits. Thus the criteria issued August 23 formalize the current and intended regulatory practices of the AEC. Although the supplementary criteria to a considerable degree reflect experience with water-cooled power reactors, the Commission also considers them generally applicable to pressure vessels for other types of reactors as well. The new criteria were compiled by the Commission's regulatory staff in cooperation with the Reactor Development and Technology staff and national laboratories; the criteria also reflect review comments by the Advisory Committee on Reactor Safeguards.

Tentative. For guidance in evaluating the safety of vessels planned for proposed nuclear plants, the Commission intends to apply both existing basic codes and standards and the new supplementary criteria. All these will change as the various code groups and the Commission develop new standards that keep pace with advancing technology. In the meantime the AEC expects that these tentative regulatory criteria will be useful to code groups and that many of the principles may be incorporated into revised engineering codes.

To influence their further development and use, comments on the regulatory criteria are invited by the Director of Regulation, U. S. Atomic Energy Commission, Washington, D. C. 20545, by March 15.

The 34 criteria, organized in seven groups, follow.

General Requirements

1.10 *CLASSIFICATION OF NUCLEAR VESSELS*

Pressure vessels in the reactor coolant system of pressurized-water reactor (PWR) and boiling-

*The General Design Criteria were published in the *Federal Register* (32 FR 10213) on July 11, 1967, and in *Reactor and Fuel-Processing Technology*, 10(3): 220-225 (Summer 1967).

water reactor (BWR) plants shall be classifed as follows:

Component	Vessel class	
	PWR plants	BWR plants
Reactor vessel	A	A
Steam generators (shell and tube side)	A	
Pressurizer	A	
Pressurizer relief vessel (or quench tank)	C′	
Regenerative or excess letdown heat exchangers (chemical and volume control system) (primary system)	A	A
Letdown coolers (high pressure injection and purification system or chemical and volume control system)	A	
Shutdown-containment spray heat exchangers (reactor shutdown cooling system)		C′
Drain coolers (chemical and volume control system)	C′	
Reactor coolant purification demineralizers	C′	C′
Reactor residual-heat removal or shutdown cooling exchangers	C′	
Radioactive waste disposal or control system vessels (subject to pressures greater than would prevail if vented to atmosphere)	C′	C′

Class C′ requires compliance with rules of Subsection C of the Code for Class C vessels and the supplemental requirements of Code paragraph N-2113. Class C′ vessels may be optionally reclassified as Class A vessels.

These requirements supplement Code paragraph N-130.

Explanation. The quality of Code-constructed pressure vessels is dependent upon the classification selected (i.e., Class A or Class C′). Selection of appropriate vessel classification requires consideration of the operating conditions to which the vessel will be exposed and the nature of the safety functions which it will be required to perform to protect the public health and safety.

Code rules which would assure appropriate and consistent classifications of all vessels in nuclear power plants have not been developed. This criterion classifies the principal nuclear vessels whose performance during their service lifetime is essential to the protection of public health and safety.

1.11 *CONDITIONS FOR DESIGN*

For pressure vessels classified as Class A or Class C′ under Criterion 1.10, the Design Specification shall set forth the conditions for vessel design associated with:

(*a*) *Normal operating conditions.* Conditions to which the vessel will be exposed during normal operation of the facility (e.g., for a reactor vessel, the conditions include criticality, warm-up, cooldown, operation from partial power level up to and including the anticipated maximum overpower level, and the expected transients in changing from one normal condition to another).

(*b*) *Abnormal conditions.* Conditions not expected during normal service but to which the vessel will be exposed as a result of equipment failures, operating personnel errors, system load disturbance, or postulated malfunctions of components [e.g., for a reactor vessel, these conditions include (1) reactivity excursions due to inadvertent control-rod withdrawal, program error, or component malfunction, etc., (2) interruption or partial loss of core coolant flow, (3) depressurization by active elements (e.g., relief valves), (4) malfunctions or failures in the steam or power conversion system, (5) reactor-turbine load mismatch or turbine trip].

(*c*) *Fault conditions.* Conditions associated with extremely low probability events but which the vessel must be designed to withstand without loss of integrity because of their potentially serious consequences [e.g., for reactor vessels, the fault conditions include those postulated accidents which may transmit undue static or dynamic loadings and blowdown forces onto the vessel, such as a major rupture of a reactor coolant system component (or in associated systems) or ejection or drop of maximum-worth control rod].

(*d*) *Environmental conditions.* Natural or service environmental conditions that when considered in conjunction with (*a*), (*b*), and (*c*) above may influence vessel design [e.g., for reactor vessels, the environmental conditions include those associated with service environments and natural phenomena such as (1) instability of vessel materials that may develop during service such as strain aging, temper embrittlement, hydrogen embrittlement, etc., (2) anticipated changes in mechanical properties of the vessel material from irradiation exposures during service lifetime, (3) mechanical and hydraulic shock or vibratory forces transmitted to the vessel from postulated component malfunctions and faults originating in system components or from coolant flow-induced effects, and (4) seismic ground accelerations that have an expectancy of occurring in the vicinity of or at the plant site].

(*e*) *Cyclic conditions.* For each pressure, thermal, and mechanical transient that a vessel may be subjected to under the conditions of (*a*), (*b*), (*c*), and (*d*), the cyclic conditions and their expected number of occurrences over the design service life of the vessel shall be specified in the Design Specification. The transients considered shall include both preoperational and such other hydrostatic or pressure tests that the vessel may be subjected to during its design life, whether imposed on the vessel alone or on the system of which it is a part. Transients associated with safety actions as imposed by the operations of engineered safeguard systems shall be included.

The number of cycles specified for each transient shall be conservatively estimated and shall be considered as the limit of occurrences permitted during the vessel's service life. The design cycles shall be specified in sufficient detail to enable the plant op-

erator to identify and log the service cycles during plant operation over the vessel's service life.

The requirements supplement Code paragraph N-141.

Explanation. Because the safety functions associated with the reactor coolant systems must not only be reliably performed under normal operating conditions but also under abnormal situations, postulated design basis accidents, and environmental forces, the "conditions of design" for nuclear vessels must take into account all these conditions if safety requirements are to be met.

To meet this objective, Code-constructed nuclear vessels must be designed to withstand without impairment of their structural integrity the conditions identified in this criterion in addition to the conditions specified by Code rules.

1.12 *CERTIFICATION OF STRESS REPORT*

(*a*) In addition to Code-required certification, the registered Professional Engineer(s) certifying the Design Specification shall review, or cause to be reviewed by engineers responsible to him, the Stress Report prepared by the vessel manufacturer and shall certify that the conditions of design specified in the Design Specification have been correctly interpreted and applied in the Stress Report. This certification shall be appended to the Stress Report with the Code-required certification.

(*b*) In addition to certification of the Stress Report by the vessel manufacturer or its design agent, the vessel owner or its agent shall provide, or cause to be provided, an independent review of the Stress Report by a registered Professional Engineer(s) competent in the field of pressure-vessel stress analyses who shall certify with respect to:

(1) The applicability of the analytical methods employed as related to the conditions of design and design configurations.

(2) The acceptability of the assumptions, loading combinations, boundary conditions, and mechanical properties of materials as applied in the analyses for the service conditions specified in the Design Specification.

(3) The extent of design agreement with similar analyses for components of comparable vessels with similar service conditions.

The certification shall be appended to the Stress Report with the Code-required certification.

These requirements supplement Code paragraphs N-141 and N-142.

Explanation. To provide assurance that the design of a nuclear vessel satisfies the safety requirements applied to the nuclear power plant, the Code-required Stress Report which documents the vessel stress analyses must reliably reflect the correct application of the "conditions of design" as specified in the vessel's Design Specifications. It is incumbent upon the engineers responsible for preparation of the Design Specifications to verify the application and interpretation of the conditions of design as employed in the Stress Report.

In addition, to maintain the high quality standard in nuclear vessel design, the Stress Report must be subjected to an independent review if its adequacy in meeting the vessel's safety requirements is to be assured.

1.13 *CONDITIONS WITH UNSPECIFIED DESIGN RULES*

Stress analyses shall be made for conditions for which design rules are not specified in the Code (e.g., mechanical shock, vibration effects, and dynamic loads). These stress analyses, including the design criteria, shall be identified in the Stress Report together with the bases upon which the structural capability of the vessel to withstand these vessel loadings are established.

This requirement supplements Code paragraph N-142.

Explanation. Nuclear vessels are subject to unusual conditions which impose mechanical shock, vibrations, or dynamic loads for which Code design rules are not available. Since the long-term reliability and safety of nuclear vessels may be influenced by the loadings imposed under these conditions, the vessel designer must establish conservative design criteria and perform appropriate stress analyses.

1.14 *VESSEL OWNER'S RESPONSIBILITY FOR INSPECTION*

For Class A vessels, in addition to the Code-required inspections, it shall be the responsibility of the vessel owner or its agent to employ and maintain one or more qualified owner's representatives at the vessel manufacturer's plant on a continuing basis during the course of vessel manufacture, and in the field during installation, to make or witness those inspections and review and verify those reports which are essential to assure that vessel construction is in accord with the requirements of the Design Specifications, material specification, approved fabrication drawings, and inspection and testing procedures, as implemented by the vessel manufacturer's quality-assurance program.

The vessel manufacturer shall permit access for surveillance by the vessel owner's authorized representatives to any place where vessel design, material manufacture and storage, vessel fabrication, assembly, inspection, and testing are performed.

The vessel owner or its agent shall review the quality-assurance program of the vessel manufacturer, and shall, if necessary, impose specific additional requirements to assure itself that adequate quality in manufacture will be attained.

The inspections shall not be considered complete until the vessel is fully installed (or erected), including all internals and piping connections at the installation site, and subjected to the final pre-operational hydrostatic test of the reactor coolant system of which it is a part.

Such inspections shall not relieve the vessel manufacturer of the responsibility for the structural integrity of the vessel to the extent prescribed by the Code and with which it must certify compliance.

These requirements supplement Code paragraph N-143.

Explanation. The most important contribution to assurance of attainment of the quality standard of nuclear vessels is the establishment and continued enforcement of all rules and requirements of design, materials, fabrication, inspection, and testing prescribed to achieve the intended final quality of the finished vessel.

Since the ultimate responsibility for the safe and reliable operation of nuclear power plants rests with the vessel owner, it is incumbent upon the vessel owner to assure himself that all procedures and practices in the course of vessel manufacture are being completely performed without deviations from acceptance standards.

1.15 *MANUFACTURER'S RESPONSIBILITY FOR QUALITY ASSURANCE*

For Class A vessels the manufacturer shall have a quality-assurance program, including an adequate administrative and technical-support organization.

The quality-assurance program shall embrace all phases of manufacturing to assure a high level of quality throughout all areas of performance: design, development, materials, fabrication, processing, assembly, inspection, test, equipment maintenance, and handling for shipment. The program shall include the Code requirements specified in Appendix IX, Sec. IX, 200, Quality Control System Requirements.

The vessel manufacturer shall make readily available to the vessel owner or its agent the written procedures and records of its quality-assurance program as evidence of conformance with specified quality standards.

This requirement supplements Code paragraph N-144.

Explanation. Quality assurance in the manufacture of nuclear vessels must be extended to all facets of performance if the intended high level of quality is to be achieved in the finished vessel.

Such assurance must, of necessity, include the conduct by the vessel manufacturer of a program which verifies the appropriateness of the vessel design, the adequacy and approval of the stress analyses, the properties and soundness of the vessel's materials, the procedures for each fabrication operation, the monitoring of each fabrication step, the resolution of manufacturing deviations, and the competency of the performance of all inspection and testing practices.

Evidence of such conformance is a prerequisite in determining the acceptability of the fabricated vessel and provides the required measure of assurance of the quality and safety of nuclear vessels.

1.16 *VESSEL FABRICATION REPORT*

The vessel manufacturer shall prepare a Vessel Fabrication Report within 6 months of completion of fabrication of a Class A vessel. The report shall be certified by the vessel manufacturer with respect to the accuracy of the contained information after an audit performed by the vessel owner's representatives present during the course of vessel manufacture. The report shall be made available to the vessel owner who shall assume the responsibility of maintaining the report on file for the period of the vessel's service life. The Vessel Fabrication Report shall include, at least, the following:

(*a*) Mill test reports of all materials within the vessel's pressure boundary, including the heat-treatment data and the Charpy impact-test results of the material test coupons.

(*b*) The written weld-procedure qualifications, including the results of mechanical-properties tests, Charpy impact tests, and metallurgical examinations performed on test specimens and weld materials.

(*c*) The written nondestructive examination procedures, including any additional requirements and acceptance criteria beyond those specified in the Code.

(*d*) Material and weld-joint repairs and postweld heat-treatments performed in the course of manufacture accompanied by identification and location of such repairs on the vessel drawings.

(*e*) All manufacturing deviations, which occurred during any phase of fabrication, and the corrective actions or dispositions taken, as approved by the vessel owner or its agent.

(*f*) A detailed record of findings from all final nondestructive examinations (radiographic, magnetic particle, liquid penetrant, and ultrasonics) performed on the vessel or vessel components. For vessel components not accessible during the final vessel examination, the record of the last examination performed at an earlier stage shall be included. The records shall be adequate to serve as a reference examination for comparison with future examinations as may be required during the service life of the vessel.

(*g*) Vessel-flange bolt-tightening procedures and preloads and bolt elongation measurements taken during assembly at the manufacturer's plant, which are required for bolting operations during the service life of the vessel.

This requirement supplements Code paragraph N-144.

Explanation. In recognition of the long-term reliability and safety expected of nuclear vessels, examinations of these vessels at periodic intervals during service life may be required. To enable a meaningful assessment of the structural integrity of the vessel following such examinations, a fabrication history of the vessel is essential to evaluate any unexpected structural deterioration or damage sustained in service.

The Vessel Fabrication Report serves as a reference upon which the adequacy of the vessel for continued service may be assessed by comparison with the records of the examinations performed during the vessel manufacture.

1.17 *BOUNDARY BETWEEN VESSEL AND PIPING*

The control-rod housings of a reactor vessel shall be considered as extensions of the vessel's pressure-retaining boundary, and the rules of Subsection A of the Code shall apply to that portion of control-rod

housings which are exposed or may be exposed to the reactor coolant pressure.

This requirement supplements Code paragraph N-150.

Explanation. Control rod systems of reactor vessels constitute a group of appurtenances directly connected to the reactor vessel. The safety and reliability of the control rod housing in service are of paramount importance to the safe operation of the reactor vessel. It is, therefore, essential that the standard of quality of the reactor vessel be extended to the control rod housings.

Materials

1.20 *VESSEL MATERIAL-PROPERTY IMPROVEMENTS*

For Class A vessels the material specifications of ferritic materials of any product form (wrought or cast) to be used in the pressure-retaining boundary shall require aluminum killing and vacuum degassing treatment in manufacture or other treatments producing comparable material-property improvement.

For reactor-vessel ferritic materials that are intended to directly surround the reactor core where the neutron fluence is above 10^{17} neutrons/cm^2 (E_n of 1 Mev or above), the material specification shall limit the phosphorus content to 0.012% maximum and the sulfur content of 0.015% maximum for both ladle and check analysis.

This requirement supplements Code paragraph N-310.

Explanation. The reliance placed upon the materials of construction of nuclear vessels to retain their physical and mechanical properties over long intervals of service without jeopardy to the vessel's structural integrity demands the selection of high quality materials in vessel manufacture.

To attain the level of quality expected of nuclear vessels, it is essential to require manufacturing practices which produce cleaner steels with improved metal fatigue properties and less susceptibility to the detrimental effects of strain-aging and material embrittlement under service conditions. Improvements in material quality are achieved by the application of vacuum degassing processes employed during material manufacture as well as by more rigid controls of the chemical composition than applied to materials for nonnuclear applications.

1.21 *MATERIAL TEST COUPONS*

Material test specimens shall be taken from the end of each mill-rolled plate that represents the top end of the ingot.

This requirement supplements Code paragraph N-313.4(*a*).

Explanation. In large ingots intended for components of nuclear vessels, material properties vary substantially. To assure the selection of vessel materials throughout the vessel plates which meet the minimum material specification properties, it is essential to remove specimens from those areas of steel plates representative of the poorest quality of the ingot for the purpose of verifying their physical and mechanical properties.

1.22 *NONDESTRUCTIVE EXAMINATION OF REACTOR VESSEL PLATES*

(1) *Ultrasonic examination.* In addition to the inspection employing the straight-beam technique, all plates for reactor vessels shall be ultrasonically inspected over 100% of the plate surfaces using a 45° angle beam or shear-wave technique, both longitudinally and transversely to the major plate-rolling direction.

The examination shall be performed on the shell courses and head segments of the vessel after final forming operations and any heat-treatment employed directly upon completion of forming but prior to welding of the shell courses or head segments. Vessel plates subject to an accelerated cooling phase of the heat-treatment to enhance properties shall be ultrasonically examined after accelerated cooling.

(2) *Test surface for angle-beam test.* The test surface shall contain a machined calibration notch with a 60° included angle whose depth is equal to 2% of the plate thickness and whose length is between $\frac{1}{2}$ and $\frac{3}{4}$ in. The test surface shall not be part of the vessel pressure boundary nor closer than 2 in. to any edge.

(3) *Acceptance standard for angle-beam test.* Any ultrasonic indication equal to or exceeding that obtained from the calibration notch shall be cause for rejection or repair in accordance with requirements of the Code and Criterion 1.23.

These requirements supplement Code paragraph N-321.1.

Explanation. The manufacturing difficulties in maintaining steel quality generally increase with the plate thicknesses. The use of heavy steel plate thicknesses in nuclear reactor vessels introduces the need to verify the quality of these plates prior to vessel fabrication. The technique of nondestructive examination of the materials provides the means for locating significant and unacceptable manufacturing defects.

Because of the importance of the safety functions associated with the reactor vessels in nuclear power plants, it is essential to adopt examination techniques for vessel materials which will assure elimination of defective materials.

Defects can be introduced in vessel steel plates both during their manufacture and during vessel fabrication processes such as forming and heat-treatment. Examinations which follow these processes are more likely to reveal unacceptable flaws.

1.23 *NONDESTRUCTIVE EXAMINATION AND REPAIRS OF MATERIALS*

Areas repaired by welding in materials intended for Class A vessels shall be radiographically examined following the postweld heat-treatment. Such welds shall meet the acceptance standard applied to vessel welds in accordance with Code rules and as supplemented by Criterion 1.51.

The welding procedure and the welders or welding operators employed by the manufacturer of materials (in any product form) in making weld repairs shall be qualified in accordance with Section IX of

the Code and meet the following applicable requirements of Section III of the Code with respect to:

(1) N-320, Nondestructive Examination and Repairs of Material

(2) N-520, Welding Processes, Weld Qualifications and Records, and Precautions for Welding

(3) N-530, Preheating and Postweld Heat-Treatment

(4) N-620, Inspection of Welding and Acceptance Standards

(5) Appendix IX, Quality Control and Nondestructive Examination Methods

The material manufacturer shall make available to the vessel owner or its agent, upon request, records of the written welding qualification procedures used in making repairs, repair procedures, extent of repairs, results of nondestructive examinations, and certification of compliance with the applicable rules of Section III of the Code.

These requirements supplement Code paragraphs N-321.2, N-322.4, N-323.5, and N-324.9.

Explanation. In order not to degrade the high quality of the finished vessel, it is essential that nondestructive examination requirements and acceptance standards for material repairs be equal to those required for welding of the fabricated vessel.

1.24 *EXAMINATION OF REACTOR VESSEL BOLTS*

Nondestructive examinations of the bolts for reactor vessel flange closure shall be performed on the finished component after completion of threading operation and heat-treatments.

The liquid-penetrant examination shall be in accord with Code paragraph N-627, except that a high-sensitivity postemulsifiable fluorescent penetrant shall be used, and shall meet the acceptance standard of N-325.2.

The ultrasonic examination shall be performed in accordance with N-625.3 and meet the acceptance standards of N-325.3.

Where threads are subject to surface treatment or plating processes, the examination shall be performed both prior to and after surface treatment.

These requirements supplement Code paragraph N-325.

Explanation. Closure studs and bolts of reactor vessels constitute critical components whose structural integrity is relied upon during the entire service life of the vessel to the same extent as the materials that form the pressure-retaining boundary of the vessel.

Nondestructive examinations of these components upon the completion of all manufacturing operations and heat-treatment are essential to reveal defects which could potentially contribute to loss of integrity or failure under service loading conditions.

1.25 *DUCTILE–BRITTLE TRANSITION PROPERTIES*

For reactor vessels, the ductile–brittle transition properties of ferritic materials shall conform with the following requirements:

(*a*) Impact-absorbed energy values of all carbon and low-alloy steel intended for the main closure flanges, and the shell and head materials connecting thereto, shall meet the impact test values specified in Code Table N-421 at a temperature no higher than 10°F.

(*b*) The properties of carbon and low-alloy steel intended for the shell materials directly surrounding the reactor core shall satisfy the following requirements:

(1) A ductile-to-brittle transition (NDT) temperature no higher than 10°F as determined by drop-weight tests conducted in accordance with Code paragraph N-331.1.

(2) The impact test value specified in the Code Table N-421 at a test temperature no higher than 10°F as determined by Charpy V-notch tests conducted in accordance with Code paragraph N-331.3.

(*c*) Impact-absorbed energy value of carbon and low-alloy steel pressure-retaining material not specified in (*a*) or (*b*) above, and of the material for the vessel support skirt shall meet the requirements specified in Code Table N-421 at a temperature no higher than 40°F.

Where Charpy V-notch specimens are used for the impact tests of (*a*), (*b*), and (*c*) above, impact-absorbed-energy values shall be determined from specimens taken in a plane parallel to the material surface with the long axis of the specimen parallel to the direction of the major rolling or forging operation and at a location with respect to material thickness and heat-treated edge as specified in Code paragraph N-313.4.

In addition to the test specimens required for (*a*), (*b*), and (*c*) above, at least nine additional Charpy V-notch specimens from each heat of the materials shall be used to determine the temperature region of transition from ductile to brittle fracture and the energy absorbed in the region of 100% shear fracture. The upper-shelf absorbed energy shall, as a minimum, meet the following requirements:

(*d*) For materials directly surrounding the reactor core, including welds and weld heat-affected zones, the upper-shelf absorbed-energy test value of any longitudinal specimen of carbon and low-alloy steels shall be no less than 60 ft-lb at a temperature no higher than 160°F.

(*e*) For materials of formed heads, including welds and weld heat-affected zones, the upper-shelf absorbed-energy test value of any transverse specimen of carbon and low-alloy steels shall be no less than 40 ft-lb at a temperature no higher than 160°F.

(*f*) For bolting materials, the upper-shelf absorbed-energy test value of any longitudinal specimen shall be no less than 40 ft-lb at a temperature no higher than 160°F.

All impact-absorbed-energy values of (*d*), (*e*), and (*f*) shall be determined from Charpy V-notch specimens taken in a plane parallel to the material surface, with the long axis of the specimen parallel to the direction of the maximum principal stress that the material will be subjected to in service and at a location with respect to thickness and heat-treated edge as specified in Code paragraph N-313.4. For plates used in formed heads, the direction of the maximum principal stress shall be considered to coincide with the direction of the minor rolling operation.

These requirements supplement Code paragraph N-331.

Explanation. The major irradiation-induced changes in the mechanical properties which occur in ferritic steels require that the reactor vessel materials possess properties (ductile–brittle transition) which provide a safe margin for operation from the range of conditions where the potential for a brittle mode of vessel failure exists.

To provide this margin, it is essential to select materials whose initial ductile–brittle transition characteristics are sufficiently conservative to accommodate the expected irradiation-induced embrittlement in service without imposing unacceptable operating limitations and without jeopardizing the safety of the reactor vessel during service.

1.26 *EXCLUSION OF REPAIRS IN BOLTING MATERIALS*

Bolting materials with defects requiring repairs by welding shall be unacceptable for vessel-flange closure studs, bolts, and nuts.

This requirement supplements Code paragraph N-322.4.

Explanation. Bolting materials for reactor vessel closure flanges are subject to cyclic loading conditions in service which may adversely influence the metal fatigue life of the material. The presence of defects or weld repairs in the materials of these critical vessel components reduces their long-term reliability. To obtain the high level of bolting integrity for safe operation of the reactor vessel, it is essential to select bolting materials free of defects or weld repaired areas.

Design

1.30 *FRACTURE MECHANICS ANALYSES*

For reactor vessels that may be exposed to a neutron fluence in excess of 10^{17} neutrons/cm^2 (E_n of 1 Mev and above), an analysis shall be performed to estimate the margin between the crack size as a result of growth under design cyclic loads and the critical crack size for brittle fracture in the welds of the vessel shell material which directly surrounds the reactor core region. The analysis shall be based on the growth rate of anticipated flaws under design cyclic loads and on material properties at a temperature 60°F above the nil-ductility transition temperature. The critical crack size shall be calculated for each period during which the material properties may significantly change to affect the results.

The analysis shall demonstrate that the estimated fatigue-crack size at any time in the vessel service life will be significantly less than the critical crack size for brittle failure.

This requirement supplements Code paragraph N-415.

Explanation. Nuclear vessels are subject to transient loads of cyclic character which may cause flaws in critical weld zones to grow.

In evaluating the severity of fatigue crack growth in zones of the reactor vessel where irradiation tends to embrittle the material, it is in the interest of safety to estimate the margin between the ultimate size of the fatigue crack under repeated load variations and the critical size for fracture. Fracture mechanics provides the principles upon which this brittle fracture potential may be assessed.

1.31 *DESIGN FOR CYCLIC LOADING*

The Code design fatigue curve of Fig. 415(*a*) for reactor vessel components subject to a neutron fluence in excess of 10^{17} neutrons/cm^2 (E_n of 1 Mev and above) in service shall be modified by reducing the allowable amplitude of alternating stress intensity, Sa, by 25%.

This requirement supplements Code paragraph N-415.2(*c*).

Explanation. Neutron irradiation of ferritic steels in reactor vessels causes changes in ductility of the material during service which introduces uncertainties, as yet undefined, with respect to the low cycle fatigue resistance of the steels.

Nuclear vessels may contain cracks or flaws of a size below the threshold of detection by the nondestructive examination techniques employed during fabrication. It is essential to provide an increased safety margin for materials in an irradiation environment beyond the margin required for nonirradiated materials.

1.32 *BOLTING DESIGN REQUIREMENTS*

The design of bolted connections for Class A vessels shall take into account the provisions necessary to facilitate periodic examinations of the bolting or studs during service lifetime, and bolting or stud replacement if required.

Thread roots shall be appropriately radiused and machined or rolled to a fine finish to reduce stress concentrations.

Closure studs 2 in. and larger in diameter shall be designed to accommodate any anticipated rotation of flange faces during initial bolt-tightening operations to limit stud bending within the Code allowable design stress intensities (e.g., spherical washers).

Bolting design shall provide for the use of bolt tighteners that axially elongate the bolts under controlled preload conditions and enable precise measurement of both the applied preload and the actual bolt elongation. The bolt-tightening procedures, preloads, and bolt elongation measurements shall be recorded in sufficient detail to enable all subsequent bolting operations during the service life of the

vessel to be performed within the prescribed limits. Such information shall be contained in the appropriate section of the Vessel Fabrication Report (Criterion 1.17).

These requirements supplement Code paragraph N-416.

Explanation. The bolts for flanged closures of nuclear vessels are components which, by design, have areas of high stress concentrations. The load carrying capability of the bolting is vital to the safety of the vessel.

Unless design provisions enable both in-service inspection and replacement of bolts or studs, the development of cracks in bolting under cyclic loading may jeopardize the structural integrity and the continued safe operation of nuclear vessels.

1.33 *EARTHQUAKE LOADING*

Where earthquake loadings are specified in the Design Specifications, the determination of the seismic-induced stresses shall be based upon the application of acceptable methods of dynamic analysis for the calculation of the structural response of the vessel to earthquake motions. The analysis shall take into account the response spectra of the ground motions, the degree of structural damping, and the amplification of ground motions as directed by specific site conditions.

In determining the maximum stresses, the effects of vertical components of seismic motion shall be combined directly and linearly with the effect of horizontal components of earthquake motion, and both vertical and horizontal components shall be combined directly and linearly with other loadings specified under Criterion 1.34.

The cyclic loading associated with design seismic-induced vibrations shall be included in the fatigue analysis.

Consideration shall be given to out-of-phase displacements of the vessel supports, or components of vessels (e.g., control-rod assemblies on reactor vessels, connected piping, etc.) resulting from differences in seismic-induced motions of vessels, components, and appurtenances connected thereto, and to the possibility of tilting or rotation of structural foundations upon which the reactor vessel rests.

This requirement supplements Code paragraph N-447.

Explanation. A principal safety requirement for a nuclear power plant is the assurance of the capability for a safe and secure shutdown of the facility in the event of an earthquake occurring at the plant site. Such a capability must be provided for by designing nuclear power plant components (i.e., vessels) to resist the design basis earthquake without impairment of their structural integrity.

Because of the uncertainties associated with the effects of earthquake loadings on nuclear power plant components, it is imperative that safe shutdown be reliably achieved in order to render the plant secure for the protection of public health and safety. This shutdown capability is also essential to reverify the functional operability of the protective systems and engineered safeguards for the reactor coolant system prior to resumption of plant operation.

1.34 *DESIGN CONDITIONS—COMBINATION OF LOADINGS*

Class A vessels and their supports shall be designed on the basis of the loadings imposed by (*a*) normal operating conditions, (*b*) abnormal conditions, (*c*) fault conditions, and (*d*) environmental conditions. These conditions are identified under Criterion 1.11.

The vessel and its supports shall be designed to accommodate the most severe loading combinations that may act simultaneously. The combinations of loading shall include but not necessarily be limited to those imposed by the following combination of conditions:

(1) Normal operating conditions plus any system transients in changing from one normal condition to another.

(2) Normal operating conditions plus any system transient imposed by the development of abnormal conditions (emergency or upset system condition).

(3) Normal operating conditions plus any system transient resulting from the occurrence of postulated system fault conditions (system component failure).

(4) Normal operating conditions plus environmental forces (earthquake where specified).

(5) In addition to the vessel loading combinations specified in (1), (2), (3), and (4), a reactor vessel, its external supports, and the internal reactor core and structure supports shall be designed to accommodate the most severe coincident loadings associated with:

a. The dynamic loads imposed on the vessel by the design basis earthquake at a time when the reactor is operating at full-rated power, and

b. The system transient loads transmitted to the vessel upon a postulated severance of any connected piping or upon a failure of a reactor coolant system component assumed to occur in consequence of the design basis earthquake of *a*, and

c. The transient forces transmitted to the vessel via the supports of the reactor core and other vessel internal structures as a result of the sudden depressurization caused by the system transient of *b*.

For loading combinations (1) and (2), the design stress intensities shall be in accord with the values specified in the Code.

For loading combinations (3) and (4), the design stress intensities for general primary stress shall not exceed 90% of the specified minimum yield strength of the vessel steel at maximum operating temperature (Sy value from Code Table N-424).

For loading combination (5) the principles of limit analysis may be applied, in which case the combined loadings shall be limited to 90% of the lower bound limit for yield collapse load (based on the maximum-shear-stress failure criterion and the Sy value

specified in Code Table N-424 corresponding to the maximum vessel operating temperature). If the yield collapse load is not determinate, tests may be performed to define its value for the specified loading combination. In such tests the collapse load shall be taken as that combination of loading when the measured strain is two times the strain value at the point of the initial deviation from the elastic stress–strain linearity.

These requirements supplement Code paragraph N-447.

Explanation. The safety functions assigned to nuclear vessels are essential not only under normal operating conditions, but also under the combination of conditions or a simultaneity of forces which may prevail in the event of anticipated system malfunctions, postulated failures in reactor coolant system components, and the multiple effects of earthquake shocks and system ruptures.

Nuclear vessels constitute those components of nuclear power plant which contain the major portion of the system energy with the greatest potential for destructive forces upon failure. To protect the public health and safety, they must be designed to accommodate the most severe combination of loadings without failure.

1.35 *COMPUTER PROGRAMS*

Analytical design techniques may employ computer programs provided their applicability is appropriately established in the Stress Report, and the results are validated by comparison with proven analytical methods of stress analyses, other verified computer programs, or experimental procedures. Experimental stress analysis in compliance with Code Article 1-10 is an acceptable method in validating the use of new computer programs.

The information presented in the Stress Report with respect to computer programs employed in the vessel stress analyses shall be sufficient to enable independent verification of the input data, the analytical model adopted, the assumptions, and boundary conditions as they relate to the conditions for vessel design.

This requirement supplements Code paragraph N-432(*b*)

Explanation. Within the present state of the pressure vessel design technology, many analytical solutions to design problems have been computerized to reduce the work of stress analyses. However, the mathematical complexity associated with the commonly applied linear theory of elasticity has proven formidable in providing exact solutions to all pressure vessel design problems of interest. The analytical solutions derived from approximate theories with simplified assumptions based on gross structural behavior and empiricism can only be verified by comparison with proven analyses or experimental investigations.

The validity of the analytical solutions cannot readily be verified by measurements of stresses and strain on the completed nuclear vessels. Neither can such measurements be taken in a practical manner after the vessel is placed in service. In consequence, limited data of vessel structural response are available. Design predictions must therefore depend heavily upon the adequacy and accuracy of the analytical methods employed by the vessel stress analyst.

1.36 *ENVIRONMENTAL EFFECTS*

(*a*) *Irradiation-induced effects.* For reactor vessels of ferritic materials, where the expected neutron fluence over the specified life exceeds 1×10^{17} neutrons/cm^2 (E_n of 1 Mev and above), the design shall make provisions for the placement of material surveillance specimens in the vessel for the purpose of monitoring and evaluating, at periodic intervals, the radiation-induced material property changes and to establish, as required, limitations on operating conditions. The design shall accommodate sufficient material surveillance specimens conforming with ASTM Standard E 185-66T, and enable surveillance tests to be performed at intervals of $\frac{1}{4}$, $\frac{1}{2}$, and $\frac{3}{4}$ of the vessel's service lifetime.

(*b*) *Time-dependent effects.* For reactor vessels the design shall take into account the time-dependent effects of deteriorative factors (i.e., corrosion fatigue, creep instability, strain aging, etc.) under operating conditions for the specified vessel life. Whenever anticipated changes of the initial mechanical or physical properties of the materials toward the end of vessel life may adversely influence their serviceability, the design shall accommodate material surveillance specimens to monitor the progress of these deteriorative factors.

This requirement supplements Code paragraph N-446.

Explanation. Based on currently available data and experience, accurate predictions of the environmental effects such as irradiations and service conditions on nuclear reactor vessel materials are either uncertain or subject to significant error. To assure that the mechanical properties remain within the acceptable range for safe operation of the nuclear vessel, it is necessary to employ means of monitoring changes which may occur in service.

1.37 *DESIGN FOR INSPECTABILITY*

The design of the reactor vessel shall provide accessibility for visual inspection at appropriate intervals during its service lifetime of all critical areas and the interior surfaces of the vessel, including the bottom head. Critical areas include structural discontinuities and the principal weld joints of the vessel. The attachments to the inside of the reactor vessel shall be designed to enable removal of all internal components necessary to permit visual inspection of the interior surfaces of the vessel aided by remotely operated optical equipment where necessary.

The provisions of accessibility for inspection shall further enable examination of essentially 100% of the volume of the reactor vessel material, either from the inside or outside surfaces of the vessel or a combination thereof, by ultrasonic or other methods. The extent of the vessel subject to examination shall include all welds within the vessel boundary up to and including the welds of transition sections between the vessel nozzles and the connected piping,

and the welds of the reactor control-rod housings to the vessel head.

The design of Class A vessels, other than the reactor vessel, shall provide accessibility for inspection and examination of all critical areas either from the inside or outside surfaces of the vessel or a combination thereof.

These requirements supplement Code paragraph N-440.

Explanation. In recognition of the critical safety functions associated with the nuclear reactor vessel, the preservation of its structural integrity throughout its operating history is of primary importance to the safety of nuclear power plants. To demonstrate that continued operation of the reactor vessel at any time does not incur a risk of a rupture of the vessel, a program of periodic examination and inspection is necessary.

Because of the attendant difficulties associated with the inspection of reactor vessels in the presence of a radioactive environment, implementation of postoperational inspections requires consideration on the part of both the plant and vessel designers in developing designs which enable and facilitate these inspections.

1.38 *ATTACHMENTS TO REACTOR VESSELS*

(*a*) For reactor vessels of ferritic materials, vessel nozzles shall not be located in any shell sections which directly surround the reactor core region and which is calculated to receive integrated neutron doses in excess of 1×10^{17} neutrons/cm^2 (E_n of 1 Mev and above).

(*b*) Partial-penetration welds, shown in Code Figure N-462.4(*d*) as applied to control-rod housings of reactor vessels shall be limited to the inside of the vessel.

(*c*) Supports and supporting members attached to the reactor vessel wall by welding shall be located in areas other than the shell sections that directly surround the reactor core.

These requirements supplement Code paragraphs N-457(*a*), N-457(*c*), and N-473, respectively.

Explanation. The attachment of appurtenances to nuclear vessels superimposes structural discontinuities which significantly alter the normal stress patterns in the walls of the vessel under load or which introduce undesirable stress intensifications.

These areas of stress intensifications at the attachments introduce conditions susceptible to the crack development in service. In turn, these cracks may initiate either ductile or brittle fractures through the pressure-retaining wall of the vessel.

Avoidance of attachments in the zones of the reactor vessel where the mechanical properties change during service is essential to eliminate these adverse stress conditions.

1.39 *REACTOR VESSEL CORE SUPPORT*

(*a*) Attachments to the inside of a reactor vessel for support of reactor fuel-core structure shall be designed to withstand the loadings under normal operating cycles, abnormal conditions, postulated fault conditions, and combination thereof as stated in Criterion 1.34.

The attachments shall be designed to sustain the most severe of the loading combinations within the design stress intensities specified by the Code and within deflection limits that allow unimpaired control-rod motion under such loadings as well as preclude mechanical damage to fuel assemblies.

Load-carrying attachments welded to the inside of the reactor vessel shall be designed to provide full-penetration welds that enable either radiographic examination for their entire length or examination by means of ultrasonic techniques, magnetic particle, or dye penetrant methods specified in the Code. If the examination is performed by magnetic particle or dye penetrant methods, each weld layer shall be progressively examined.

(*b*) Where the internal supports of the reactor core structure are welded directly to the weld overlay cladding of the reactor vessel, the area of attachment shall be examined 100% by the ultrasonic technique prior to welding of the structural support. The ultrasonic examination shall be performed in accord with Code paragraph N-625.2, weld repairs in accord with Code paragraph N-625.4, and the acceptance standards of Code paragraph N-625.3 shall be met.

Requirements (*a*) and (*b*) supplement Code paragraphs N-474 and N-518.5, respectively.

Explanation. The design of the structural attachments to a reactor vessel which provide the principal support for the reactor's nuclear fuel core must provide a reliable means of holding the core in position under any condition of loading, either anticipated or postulated which the reactor vessel may sustain.

The loss of the reactor core supports could allow a disarrangement of the nuclear fuel assemblies, or the disengagement of the reactor core structure from the system of the control rods with a concomitant uncontrollable reactivity change. The consequences would carry the risk of overpressurization of the reactor vessel and crack development. To protect the public health and safety, this requires a design and fabrication of reactor core supports which provide the highest integrity in service.

Fabrication

1.40 *CHEMICAL ANALYSIS OF WELD WIRE*

A chemical analysis of solid and stranded wire filler metal shall be performed on each section of wire which may be spliced together in one coil. The wire coil shall be obtained from the manufacturer with not more than one splice to enable sampling for chemical analysis of the accessible ends as a practical means to verify that the entire wire coil meets specifications.

This requirement supplements Code paragraph N-511.5.

Explanation. Within the limits of the present day pressure vessel technology, the structural integrity achieved in the fabrication of the vessels depends substantially upon the welding processes employed to join and assemble the vessel components, and the properties of the welded joints.

Although many tests are conducted on weld materials prior to their welding application to verify their compliance with specifications, it is not practical to reverify the properties of completed welds on nuclear vessels. Because misapplication or the improper use of weld materials cannot be discovered, it is essential that all weld materials be tested in a manner which will preclude weld materials in nuclear vessels not in conformance with specifications.

1.41 *CUTTING PLATES AND OTHER PRODUCTS*

Plates and other products cut to shape by thermal cutting in preparation for welding shall have the edge surfaces cleaned by mechanical means (machining, shearing, chipping, or grinding) before examination in accord with the requirements of Code paragraph N-513.2 and prior to welding.

At least $\frac{1}{32}$ in. of metal shall be removed from all surfaces thermally cut by air arc, inert gas arc, or carbon arc. Not less than $\frac{1}{8}$ in. shall be removed where oxygen arc or oxygen cutting (including both powder and flux cutting) is used.

The weld preparation and adjacent base-metal surfaces for a minimum of 1 in. on each side of the weld preparation shall be smooth, clean, and free of any foreign matter. The weld preparation shall be protected from contamination until welding is started and fully completed.

This requirement supplements Code paragraph N-519.

Explanation. Despite the practice of nondestructive examinations of materials for the purpose of detecting flaws prior to their acceptance, experiences have demonstrated that small flaws may escape detection, particularly at the edges of vessel materials which are to be joined by welding.

The existence of any flaw in the welds of a nuclear vessel where unavoidable residual weld stresses and operating stresses coexist may pose a threat to the continued safety of the vessel in service. Adherence to practices which enable the elimination of unsound materials in the metal regions subject to welding is recognized as a prerequisite for sound welds.

1.42 *WELDING QUALIFICATION PROCEDURE REQUIREMENTS*

(*a*) *Test material requirements.* In lieu of test-material thickness requirements of *ASME Boiler and Pressure Vessel Code*, Section IX-(1965), Tables Q-13.1 and Q-13.2, the requirements of the weld procedure qualification test of Code paragraph N-541.2, and of the impact tests of Code paragraph N-541.3(e) as applied to Class A vessels shall be met by welding test material obtained from one or more heats of the vessel and whose thickness is equal to the major thickness of any joint in the vessel.

Alternatively, if the test-material thickness requirements as specified in *ASME Boiler and Pressure Vessel Code*, Section IX-(1965), Tables Q-13.1 and Q-13.2, are used for the requirements of the weld-procedure qualification test of Code paragraph N-541.2, only the requirements of impact test of Code paragraph N-541.3(e) need be met by welding test material obtained from one or more heats of the vessel and whose thickness is equal to the major thickness of any joint in the vessel.

(*b*) *Base material.* Weld-procedure qualifications for reactor vessels of ferritic materials shall require the use of base-material test plates meeting the impact test values in Code Table N-421 at a temperature no higher than 10°F. The procedure qualification test plate for weldments that are to be subject to an austenitizing heat-treatment shall be at least 3 by 3*t* in size with the weld test coupons taken at least *t* from any edge of the plate.

(*c*) *Metallurgical examination.* The weld-procedure qualification report shall be accompanied by a report of a metallurgical examination, including photographs of the bend test specimens, of the tensile test coupons, and a photomacrograph of the etched cross section of the welds in the area where the tensile coupons have been removed.

The photomacrograph shall show weld bead sequence and groove design substantially similar to that specified in the procedure qualification. The photomacrograph specimens shall be subjected to a magnetic-particle examination in accord with Code paragraph N-626, a liquid-penetrant examination in accord with Code paragraph N-627 and meet the acceptance standards of Code paragraph N-320.

(*d*) *Impact test of procedure qualification welding.* For welding-procedure qualifications intended for the welding of reactor vessel components, impact testing of the procedure qualification weld deposit and heat-affected zone shall meet the impact test values assigned the base material in Code Table N-421 at a temperature no higher than 10°F.

Requirements (*a*) and (*d*) supplement Code paragraphs N-541.1 and N-541.3(*e*), respectively. Requirements (*b*) and (*c*) supplement Code paragraphs N-541.2(*a*) and N-541.2(*d*), respectively.

Explanation. Prior to the performance of production welding on nuclear vessels, the practice is to qualify the weld procedure in accord with prescribed rules and tests to ensure that the mechanical and metallurgical properties of vessel weld joints will be comparable to those of the vessel materials.

The safety of nuclear vessels is directly and adversely influenced by any disparity between the properties of weld joints and the vessel material. Normal variations in the chemistry, mechanical and physical properties are experienced in both the vessel materials and weld metal. It is imperative to verify the quality of welds for each vessel as may be produced by combinations of different lots of the actual vessel materials and weld metals used if a consistent quality is to be assured in manufacture.

1.43 *PRECAUTIONS FOR WELDING*

All low-alloy, low-hydrogen electrodes, and fluxes used in welding shall be stored in a dry place.

The coated electrodes shall be baked for 1 hr in an oven at 800°F before use. After the baking cycle the electrodes shall be stored in holding ovens

maintained at 300 ± 50°F. Welders shall be permitted to remove only that amount of electrodes that can be used during a 2-hr period.

Welding fluxes shall be stored in holding ovens maintained at 300 ± 50°F. Fluxes transferred to welding machines from the holding oven shall be maintained continuously at a temperature sufficient to preclude moisture absorption or shall be returned to holding oven, if unused.

This requirement supplements Code paragraph N-523(*b*).

Explanation. The storage conditions for weld materials are recognized as contributory to the resulting quality of weld joint in nuclear vessels. The importance of adopting acceptable practices as part of the quality control program for weld materials is emphasized by the experiences of poor quality of welds resulting from improperly maintained weld materials.

Since weld analyses are not practical after weld metal deposition in the nuclear vessel, precautionary controls of weld material must be relied upon to preclude degrading the quality of the completed vessel.

1.44 *WELDING REQUIREMENTS*

(*a*) *Weld root examination.* In addition to the preparation requirements specified by the Code for the root of the second side of double-grooved joints welded from both sides, a magnetic-particle inspection of ferritic materials in accord with Code paragraph N-626, or a liquid-penetrant test for nonferritic materials in accord with Code paragraph N-627, shall be performed prior to the application of weld metal. The tests shall be followed by an appropriate cleaning procedure to remove all traces of materials used in conducting the tests.

(*b*) *Preheating requirements.* The minimum preheating temperature to be maintained prior to any flame-cutting operations and during the performance of category A, B, C, and D welds, including weld repairs, shall meet the following requirements:

	°F
P3 materials: 1 in. or less thick	200
Over 1 in. thick	300
P4 materials: ¾ in. or less thick	300
Over ¾ in. thick	400
P5 materials: ¾ in. or less thick	400
Over ¾ in. thick	500

The preheating temperature shall extend at least 2t on both sides of the weld where t is the weld-section thickness. The preheat shall be maintained until the vessel or component of the vessel is subjected to the postweld heat-treatment. Any loss of preheat before completion of the weld shall require a weld-surface magnetic-particle inspection and a radiographic examination before resumption of welding.

(*c*) *Requirements for postweld heat-treatment.*

(1) The postweld heat-treatment temperatures existing throughout a vessel or component shall not differ from that employed in the weld-procedure qualification test plate by more than −25° F or +50° F, taking into consideration the temperature tolerance measured in the test plate with respect to the minimum holding temperature specified in Code Table N-532.

(2) A written heat-treatment procedure shall be prepared detailing temperature, times, heating and cooling rates, thermocouple location, number of recordings, and chart speed.

(3) Temperatures shall be measured by the use of sufficient number of thermocouples attached to the vessel to assure that the temperature gradients do not exceed the limit of subparagraph (1) above. Such temperature measurements shall be autographically recorded and made available to the vessel owner or its agent upon request.

(4) The temperature-measuring equipment shall be calibrated at least once each month. Records of calibration shall be made available to the vessel owner or its agent upon request.

Requirement (*a*) supplements Code paragraph N-527.1, requirement (*b*) supplements Code paragraph N-531, and requirements (*c*) supplement Code paragraphs N-532.3 (3), (6), (7), and (8), respectively.

Explanation. The design of the major strength welds in a nuclear vessel requires the application of weld metal from both the inside and outside of the vessel, principally because of the heavy wall thickness which must be joined.

Experiences have demonstrated the need to examine by nondestructive techniques the weld deposit at the root of the joint to preclude weld defects from lack of fusion or penetration.

Additionally, nuclear vessel materials require not only preheating to establish temperatures to lessen their susceptibility to cracking or microfissuring as the weld joints are completed, but also closely controlled postweld heat treatment to enhance their mechanical and metallurgical properties after welding.

To achieve the high quality expected of nuclear vessels, closely controlled weld preheating and postheating is a necessary practice to preclude weld defects detrimental to the vessel's safety.

Inspection

1.50 *FINAL INSPECTION AND EXAMINATION*

In addition to the nondestructive examinations required by Code paragraph N-618.2, the vessel shall be subjected, after completion of the hydrostatic test, to an ultrasonic examination of all accessible weld surfaces of the pressure boundary including the weld cladding surfaces. The examination shall be performed to provide for 100% volumetric inspection of the metal bounded by a 1t dimension on each side of the center line of the weld where t is the thickness of the weld joint. The examination shall be in accord with Code paragraph N-625.

The examination method employed shall provide a means for producing a permanent record, properly identified with respect to the location and extent of the areas of the vessel examined, including annotated interpretations of all significant indications observed. The records shall be appropriate to serve as a reference examination for comparison with future inspection that may be required during the vessel's service life.

In areas where either the interpretations of the reflections observed are in doubt, or the recorded indications appear to exceed the acceptance standards of Code paragraph N-625.3, a supplemental examination shall be performed by means of a radiographic examination in accord with Code paragraph N-624.

The radiographic examination shall employ special techniques of exposure orientation necessary to fully define and interpret the reflectors observed by the ultrasonic examination.

Any indications revealed by the radiographic examination which exceed the acceptance standard of N-625.3 shall be subject to review and evaluation by the vessel manufacturer, the professional engineers who certified the vessel Design Specification and the Stress Report, and the vessel owner or its agent, before the need for repairs and retests is established.

Any weld repairs shall be performed in accord with Code paragraph N-625.4. All areas of the vessel of questionable interpretation, weld repaired areas, and the result of nondestructive reexaminations shall be recorded as part of the Vessel Fabrication Report and accompanied by appropriate identification and location of these areas on vessel drawings. These records shall be made available to the vessel owner or its agent upon request.

This requirement supplements Code paragraph N-618.

Explanation. In recognition of the numerous fabrication processes through which a nuclear vessel must pass, each of which may cumulatively contribute to the development of flaws during the course of fabrication, a program of final inspection and examination is necessary to verify the "as built" structural integrity, prior to its acceptance for service. To obtain meaningful results, such examinations must be performed following completion of fabrication, heat treatment and testing.

The examination results assume additional values in that they provide a reference for reexamination of the vessel as may be required periodically to reverify its structural integrity for continued service. The maximum advantage of nondestructive techniques employed in the vessel inspection can be obtained by comparing results between the vessel's preoperational and postoperational examinations.

1.51 *NONDESTRUCTIVE EXAMINATION AND RESPONSIBILITIES*

(*a*) *Radiograph Examination of Welded Joints.* Radiograph examination employed for the examination of welding to meet Code requirements shall conform, as a minimum, with the applicable requirements of Code, Appendix IX, Section IX, 200, Quality Control System Requirements, and Section IX, 300, Nondestructive Methods of Examination, and the requirements contained herein.

(*b*) *Nondestructive examinations.* Nondestructive examinations employed for the examination of materials and welding to meet Code requirements shall conform as a minimum with the requirements of Code Appendix IX, Section IX, 200, Quality Control System Requirements, and Section IX, 300, Nondestructive Methods of Examination.

Each written procedure of (*a*) and (*b*) shall be qualified by the vessel manufacturer and made part of the quality assurance program and shall be made available for review and approval by the vessel owner or its agent. Such approval shall not relieve the vessel manufacturer of its responsibilities for compliance with Code rules.

This requirement supplements Code paragraph N-611.1.

Explanation. The structural integrity built into nuclear vessels is dependent upon the meaningful performance of the nondestructive examinations of the vessel as a means to achieve and control the quality standards during the course of vessel manufacture.

Equally important to the attainment of high quality standards in nuclear vessel manufacture is the quality assurance effort invested in establishing the adequacy of nondestructive examination methods. The vessel owner who ultimately assumes the responsibility for the safety of nuclear power plant, in which nuclear vessels represent major components, must assure himself of the adequacy of the vessel manufacturer's methods of nondestructive examination by a review of the quality assurance program.

Testing

1.60 *HYDROSTATIC TESTING REQUIREMENTS*

(*a*) *Examination for leakage during hydrostatic test.* Any indication of leakage in the pressure boundary of a vessel at other than a flanged connection shall be reported to the vessel owner or its agent before corrective action is taken. Both the location and extent of the leak indication and the corrective action taken shall be reported in the Vessel Fabrication Report.

(*b*) *Testing temperature.* Prior to and during the performance of the hydrostatic test, the vessel material temperature shall be not less than 60°F above the highest of the impact-test temperatures required to meet the impact-test values of Code Table N-421, taking into account materials and welds of the vessel's pressure boundary and the materials of nonpressure parts directly welded to either the inside or outside surfaces of the vessel. The test temperature shall be reported in the Vessel Fabrication Report.

(*c*) *Water and cleaning requirements for testing.* Prior to hydrostatic testing, the vessel interior surfaces shall be cleaned with compounds free of halogen

or other deleterious material, as approved by the vessel owner or its agent.

For vessels constructed or clad with austenitic or Ni–Cr–Fe alloy, the water used for a hydrostatic test conducted below 150°F shall be demineralized water with a maximum chloride plus fluoride ion content of 25 ppm. For vessels constructed or clad with austenitic alloy, tests conducted above 150°F, but not exceeding 200°F, demineralized water with maximum chloride plus fluoride content not in excess of 1 ppm shall be employed. For vessels constructed or clad with Ni–Cr–Fe alloy, water with an initial halogen ion content not in excess of 25 ppm may be used for tests conducted above 150°F but not exceeding 200°F provided a flush or rinse with 1 ppm demineralized water is performed. The measurements of water chemistry during the test shall be recorded in the Vessel Fabrication Report.

Following the hydrostatic test, the vessel surfaces shall be completely dried and protected from contamination by sealing all openings and using desiccants or heated dry air when practical to preclude moisture accumulation within the vessel. Such protection shall be effective until final installation of vessel in a closed system.

Requirements (*a*), (*b*), and (*c*) supplement Code paragraphs N-714.3, N-714.4, and N-714.5, respectively.

Explanation. The performance of a hydrostatic pressure test upon completion of vessel fabrication serves to detect manufacturing flaws as indicated by water leaks, to locate inadequate design as evidenced by excessive distortions under pressure, and to verify the adequacy of the ductile–brittle transition properties of all materials used in the construction of the vessel.

Hydrostatic testing under improperly controlled conditions may potentially injure the vessel or may expose the vessel material to deleterious effects of halogens in the test water. These effects may not be readily detected until after a significant service period.

Appropriate test conditions are essential to preclude effects detrimental to the vessel's safety in service.

New Materials—Special Requirements

1.70 *APPROVAL OF NEW MATERIALS FOR ASME CODE-CONSTRUCTED NUCLEAR VESSELS*

(*a*) *Crack-susceptibility test for ferritic materials.* In addition to Code requirements, new materials intended for reactor vessels shall be subjected to crack-susceptibility tests meeting with the following requirements:

For each product form used in reactor vessels, the base metal, weld metal, and heat-affected zone shall be subjected to comparative tests to determine its crack susceptibility from embrittlement by strain aging, hydrogen embrittlement, or temper embrittlement.

(1) The strain-aging test shall consist of a reverse bend test, using a specimen 0.75 × 10 in. long, prestrained by an initial 180° bend, aging at 300°F (or 550°F) for 1.5 hr, and finally opening the bend specimen at room temperature. The results, in terms of observed cracking, shall be compared with that of Code-approved materials of known low susceptibility to strain aging.

(2) A test to detect susceptibility to hydrogen embrittlement shall consist of immersing a precracked specimen (cantilever bar) in an electrolytic solution conducive to hydrogen release or exchange for a specified period. The results in terms of increased crack growth or development shall be compared with that of Code-approved materials having low susceptibility to hydrogen embrittlement.

(3) A test to detect susceptibility to temper embrittlement in consequence of heat-treatments shall be conducted by subjecting two test plates—one plate to the postweld heat-treating temperature and time as specified in the Code and a second plate to a temperature of 900°F for 24 hr, followed by furnace cooling. Charpy V-notch tests shall then be performed with at least 12 specimens to develop the transition curve for each test plate and to determine the difference in transition-temperature shift caused by the heat-treatments.

(*b*) *Fracture-toughness properties.* For ferritic materials intended to be used in reactor vessel region directly surrounding the core, appropriate tests shall be made to compare the fracture-toughness properties with steels of acceptable toughness.

Information on the fracture-toughness properties of the material shall be developed by an acceptable test procedure. In addition, a crack growth-rate test under cyclic loading conditions shall be conducted on specimens to obtain information in the temperature range of interest.

Similar information shall also be furnished for the welded specimens of these materials to demonstrate that comparable properties are attainable in the heat-affected weld zone and weld metal as in the base metal.

Requirements (*a*) and (*b*) supplement Code Appendix VIII-100(*c*) and (*d*), respectively.

Explanation. The application of new steels in reactor vessels with physical and mechanical properties substantially different from those currently in use is beset with some uncertainties in regard to their suitability under the long-term service effects of an irradiation environment and exposure to reactor coolant conditions.

Unless appropriate tests are performed to compare the crack-susceptibility and fracture-toughness properties of new steels with those of proven and acceptable properties, the assurance of reactor vessels meeting safety requirements for extended service periods cannot be established.

Research and Development on Aqueous Processing

By C. E. Stevenson and D. M. Paige

Basic studies of the kinetics of acid dissolution of uranium and thorium are reported, and methods for the preparation of graphite-matrix pyrolytic carbon (PyC)-coated particle fuels are reviewed. Operations for the recovery of enriched uranium and of plutonium from Pu–Al targets are described. Operating experience for the Windscale plant is reported.

Preparation of Fuel for Processing

The Karlsruhe processing plant will use a single-rod fuel chopper. Kinetic studies of the dissolution of uranium and thorium in HNO_3 and H_2SO_4 indicate that active–passive behavior is encountered and that acid concentration, temperature, and oxidant concentration significantly affect observed rates of attack.

Review of the development of fluidized-bed combustion, pressurized aqueous combustion, and grinding and leaching for the preparation of PyC-coated carbide fuels in a graphite matrix indicates that the fluidized-bed process possesses significant advantages.

MECHANICAL PROCESSING METHODS

Dluzniewski and Walther report[1] (in German) on the development and testing of a fuel-rod chopper for the Karlsruhe reprocessing plant, a device (Fig. 1) that is somewhat different from the Oak Ridge shear.[2]

The fuel elements must be disassembled into rods and fed vertically into the cutter. The cut is made by moving the blade forward by hydraulic cylinder, and the cut piece can drop directly into a dissolver. The unit tested takes rods up to 14 mm in diameter and 4000 mm long. Several types of cold fuel were tested, such as ceramic-filled stainless steel, ceramic-filled Zircaloy-2, UO_2-filled Zircaloy-2, and solid bar stock (St-37). Life tests on the blade were reported for several fuels, e.g., 6000 cuts on the UO_2-filled Zircaloy-2. The authors report that, in general, the device works very well.

DISSOLUTION OF URANIUM AND THORIUM

The dissolution of metallic uranium and thorium is an important step in the preparation of pure and alloyed nuclear fuel and blanket materials for processing. A good understanding of the mechanism of the processes involved is needed to devise efficient processes. Kindlimann and Greene[3] have recently presented the results of studies of the dissolution kinetics of uranium and thorium in HNO_3 and H_2SO_4; these studies were aimed to facilitate process optimization.

The studies were conducted by making anodic polarization measurements by both potentiostatic and galvanostatic techniques on metal specimens immersed in the acid solutions, with and without various salt additions. Cubic specimens 2 to 7 cm^2 in area and initially etched in HNO_3 were used. The uranium metal was relatively pure (331 ppm C and 10 to 92 ppm Ca, Be, Cr, Cu, Mg, Na, Zn, Si, Mg, Ni, Fe, and N), whereas the thorium contained 4.5% ThO_2 and 28 to 586 ppm Ni, Al, Cu, Cl, Zn, U, C, F, Fe, and N. Dissolution rate was evaluated in terms of anodic current density as a function of applied potential. A typical relation for uranium (in 1*N* H_2SO_4) is shown in Fig. 2, which indicates the typical active–passive transition with a maximum in the current curve at an intermediate potential.

The rate of dissolution of uranium in H_2SO_4 increases with temperature at all potentials but decreases with increases in acid concentration over the range 1*N* to 10*N*. Studies of the effect of *p*H in Na_2SO_4 solutions indicated that the retarding effect of acid concentration is primarily due to hydrogen-ion concentration, with a lesser effect due to sulfate concentration. The presence of 0.1*N* Cl^- markedly accelerates dissolution, and pitting is observed.

In HNO_3, similar effects of the concentration of H^+ and NO_3^- are observed, but uranium spontaneously passivates in HNO_3 at concentrations up to 3*M* and corrodes slowly. Above 3*M* the corrosion potential

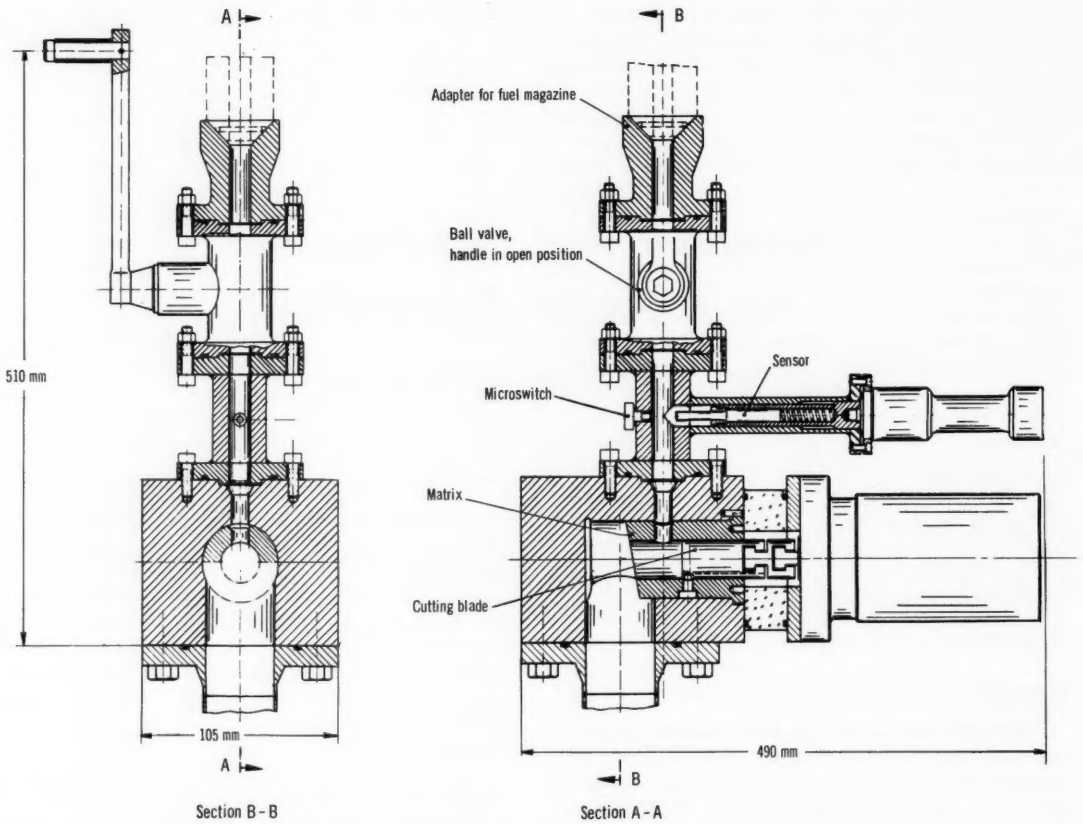

Fig. 1 Chopper.[1] [Reprinted, by permission, from Kerntechnik, *9(6): 246 (1967).]*

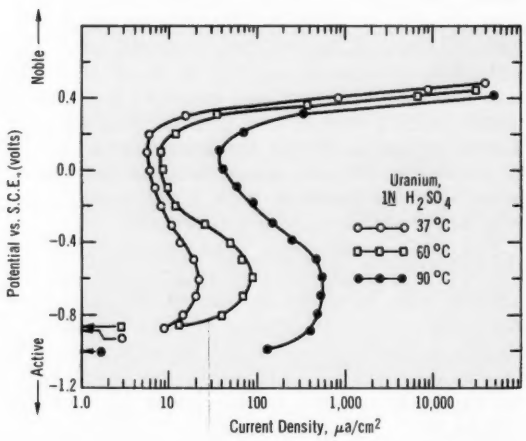

Fig. 2 Effect of temperature on potentiostatic anodic polarization curves of uranium in 1N H_2SO_4 (Ref. 3). [Potential was measured relative to a saturated calomel electrode (S.C.E.).] [Reprinted, by permission, from Corrosion, *23(2): 30 (1967).]*

is in the transpassive region, and rapid attack occurs. This is a direct result of the oxidizing characteristic of NO_3^-. In the transpassive state, uranium dissolves in the hexavalent state without gas evolution and at virtually 100% current efficiency.

The anodic dissolution of uranium in 1*N* NaOH was also observed. Active–passive behavior was also noted, but indicated dissolution rates were relatively low.

It was concluded that most efficient dissolution of uranium could be accomplished in hot, dilute HNO_3 or H_2SO_4 with soluble oxidizing agents and that electrolytic dissolution would permit ideal control at high efficiency for potentials of 0.25 to 0.9 volt.

In similar studies of washed but unetched thorium samples, relatively low dissolution rates were observed in HNO_3, H_2SO_4, and NaOH, i.e., currents of less than 0.1 ma/cm^2 for thorium compared with currents approaching 1 amp/cm^2 for uranium at potentials less than a volt. Gas evolution, indicating low current efficiency, was also observed with thorium. Inertness was ascribed to the presence of a

stable passive surface-barrier film. The presence of $0.1N$ Cl^- in $1N$ H_2SO_4 was found to accelerate thorium dissolution markedly, but dissolution becomes highly localized and is accompanied by the formation of insoluble products.

The wide differences in dissolution rates of uranium and thorium led to the suggestion that a separation of these metals, in the form of a uranium-rich alloy, could be accomplished by controlled dissolution in H_2SO_4 or HNO_3.

PREPARATION OF GRAPHITE FUELS

Methods proposed for the preparation of graphite-matrix reactor fuels for processing are generally based on mechanical or chemical disintegration of the matrix and of any refractory coating on the fuel particles, accompanied or followed by dissolution of the fuel material in HNO_3.

Mechanical disintegration is accomplished by crushing and grinding, and chemical disintegration is effected by combustion in a fluidized bed, attack by $HNO_3-H_2SO_4$ mixtures, HNO_3 in a pressurized system, or electrolysis. Work on the grind–leach, mixed-acid, and electrolytic-dissolution processes at the Idaho Chemical Processing Plant (ICPP) was recently reviewed,[4] and Ferris has summarized ORNL laboratory studies on grinding and leaching graphite-base PyC-coated fuel particles.[5]

ORNL Grind–Leach Studies. The bulk of the Oak Ridge work was accomplished on Peach Bottom High-Temperature Gas-Cooled Reactor (HTGR) prototype fuel, consisting of compacts containing PyC-coated ThC_2-UC_2 particles (150 to 420 μ in diameter) coated with a 45- to 65-μ layer of laminar pyrocarbon, which was roll-crushed to maximum sizes of 100 to 140 mesh to ensure coating rupture. Since inadequate recovery of uranium and thorium was obtained by a single 5- to 24-hr leach with sufficient cold or boiling $2M$ to $21.5M$ HNO_3 [with or without $0.05M$ HF and $0.05M$ $Al(NO_3)_3$] to produce a $0.2M$ (U + Th) solution, the effect of repeated leaching after washing the residue was examined. A recovery of 99.9% of the uranium and thorium was attained by leaching twice with boiling $5M$ to $16M$ HNO_3. However, a similar treatment of crushed reactor fuel for the Ultrahigh-Temperature Reactor Experiment (UC_2 particles coated with successive layers of porous carbon, isotropic carbon, and granular pyrolytic carbon) resulted in uranium losses approaching 1%, which were attributed to absorption of uranium by the porous-carbon layer. In the leaching process an appreciable amount of the carbon present is oxidized to soluble carbon compounds of a surfactant character, which interfere with solvent extraction. Although it is possible to remove these compounds by $KMnO_4$ oxidation, in the course of which MnO_2 is produced, a more attractive method for their elimination consists of extracting the uranium and thorium from the solution at $2M$ to $5M$ acid concentration and then repeating the solvent extraction process under acid-deficient conditions to effect adequate decontamination.

Although adequate recoveries appear possible, the author concludes that the grind–leach process is unattractive relative to the burn–leach technique because of indications of increased losses with irradiated fuels, graphite-washing and filtration problems, extra processing involved in the removal of soluble carbon compounds, and the need for disposal of the highly active graphite waste.

ICPP Work. Development of the fluidized-bed combustion process was continued at ICPP as previously noted.[4]

A two-stage fluidized bed of alumina particles has been operated satisfactorily in which the primary combustion of the uncrushed Rover-type fuel element is effected in the lower section and combustion is completed in the upper and expanded section with the addition of more oxygen to the gases.[6] Over 97.5% of the graphite is burned in the two stages. The U_3O_8 and Nb_2O_5 solid particles are elutriated by the fluidizing gas and are scrubbed from the gas by HNO_3, which dissolves U_3O_8 but not Nb_2O_5. The scrub solution, after filtration, is fed to solvent extraction for uranium recovery and decontamination. Some of the uranium is retained in a coating on the Al_2O_3 particles, but continued fluidization of the bed removes the uranium. A variety of additives were tested thermogravimetrically in attempts to accelerate combustion of the graphite; HNO_3, H_2O_2, and H_2O were ineffective.

Pressurized Aqueous Combustion. The pressurized aqueous combustion process, using HNO_3 and air at 1500 to 2000 psi and 300°C, has been reported previously in application to HTGR fuel particles.[7] Farrell and Haas[8] have extended the earlier work by evaluating the kinetics of graphite oxidation under these conditions. Reaction rates of the order of 0.1 to 1.0 hr^{-1} were observed, the increases occurring with temperature in the range 275 to 300°C, with acid concentration ($1.0M$ to $4.0M$ HNO_3), and with time up to a consumption of 0.3 to 0.5 of the charge. Optimum conditions appeared to be at 300°C with $2M$ acid under 1600-psi pressure. Corrosion of the 347 stainless-steel vessel was excessive at higher acidity.

Separation Processes

The uranium in a partially melted-down U–Zr alloy core from the Experimental Breeder Reactor No. 1 (EBR-I) was recovered satisfactorily by hot-cell dissolution in HNO_3–HF and plant-scale solvent extraction with hexone at the ICPP. The Savannah River Plant has accomplished the recovery of 89 kg of plutonium from irradiated Pu–Al alloy over a

5-year period through the use of adapted plant-scale equipment and facilities.

EBR-I FUEL RECOVERY

A recent report[9] from ICPP amplifies a note[10] in a previous issue of this journal concerning the recovery of the highly enriched uranium contained in the second core of EBR-I, which suffered a partial meltdown some years ago.

The original fuel consisted of rods of 98% U–2% Zr alloy contained in stainless-steel tubes with a NaK bond. Unenriched-uranium blanket material was located at both ends of the fuel tubes. Significant portions of the core melted in the course of a transient nuclear excursion, and the result was a melted fuel–cladding mixture with an estimated average composition of 82% U (of 69% enrichment), 1.6% Zr, 11.1% stainless steel, 1% NaK, 4.3% O, and 0.1% Pu. Following removal from the reactor, the fuel–cladding mixture, containing about 66 kg of uranium, was placed in small food cans and held for processing.

Because of the inhomogeneous and flammable nature of the reclaimed material, it was chosen to effect dissolution in 1-kg batches in a manipulator-equipped hot cell by perforating the can lids and charging the cans one at a time to a Carpenter-20 dissolver containing sufficient 12.6*M* HNO_3–0.6*M* HF to yield a dissolver product of about 1*M* $UO_2(NO_3)_2$. Fuming and small flames had been observed when the cans were opened to air, but no problems were encountered in charging the perforated cans, and the fuel dissolved so rapidly that heating was unnecessary. A total of 87 batches was dissolved in this way.

The dissolver product was neutralized to 0.5*M* H^+ with NH_4OH and adjusted to contain 1*M* $Al(NO_3)_3$ prior to solvent extraction of uranium with hexone as shown in Fig. 3. The first-cycle product was concentrated by evaporation, and the yield after a second hexone extraction cycle and evaporation was a product containing 1.5*M* $UO_2(NO_3)_2$ with losses of about 0.001%. As indicated by dispersion–coalescence tests of the feed, no difficulty was encountered in extraction.

RECOVERY OF HIGHLY IRRADIATED PLUTONIUM

In connection with the overall U. S. program for the production and separation of transplutonium isotopes,[11] the recovery of plutonium from irradiated Pu–Al alloy target material has been undertaken at Savannah River over a period of years. Some results

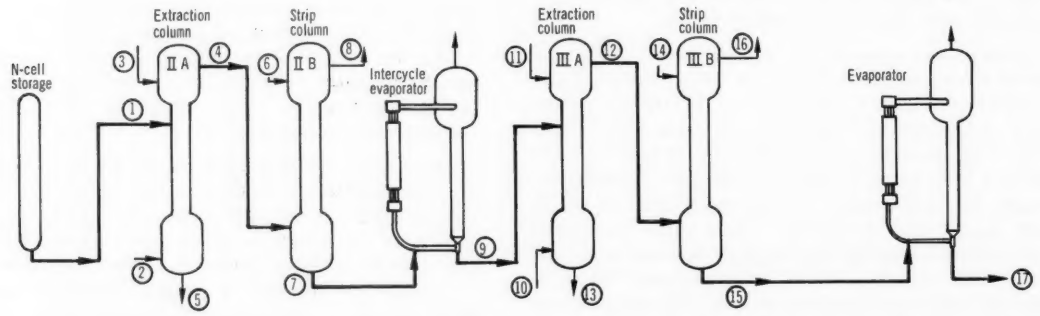

Stream	1	2	3	4	5	6	7	8	9	10	11	12	13	14	15	16	17
Description	I AF	I AX	I AS	I AP	I AR	I BX	I BP	I BR	Cycle I product	II AX	II AS	II AP	II AR	II BX	II BP	II BR	Product
Flow, liters/batch																	
Flow, liters/hr	18	0.45	30	45	48	20	20	40	4.6	17	12	17	16.6	10	10	17	4.6
Sp. gravity	1.36	0.80	1.31	0.87	1.26	1.00	1.11	0.80	1.48	0.80	1.31	0.94	1.23	1.00	1.22	0.80	1.48
Extractant		Hexone		Hexone				Hexone		Hexone		Hexone				Hexone	
$Al(NO_3)_3$, M	0.97		2.00		1.61						2.00		1.45				
HNO_3, M	0.52					0.04	0.04		0.17					0.04	0.04		0.09
NH_4OH, M			0.5		0.12						0.32		0.18				
NH_4NO_3, M	1.78				0.86								0.05				
$Fe(NH_2SO_3)_2$, M			0.05		0.04												
F, M	0.16				0.06												
U, g/liter	90			36	0.001		81	0.001	350			95	0.001		162	0.001	350

Fig. 3 Extraction flow sheet for EBR-I Core 2 fuel.[9]

of this program have recently been described by Eargle, Swindell, and Martens.[12] Americium and curium were also recovered and separated from plutonium in part of these operations.

The typical feed material consisted of aluminum-clad elements of Pu–Al alloy in the form of rods, tubes, or boxed plates. Dissolution was effected in a plant-scale dissolver (8 ft in diameter and 8 ft high) containing a basket insert to contain the fuel. Targets with low irradiation levels were dissolved in a single step in boiling HNO_3 containing $Hg(NO_3)_2$ and KF catalysts; from the more highly irradiated materials, aluminum was first dissolved with NaOH–$NaNO_3$, and then plutonium was dissolved by acidifying with HNO_3 and boiling with KF. The compositions of the dissolver solutions are given in Fig. 4.

The dissolver products were concentrated by evaporation and clarified by centrifugation after addition of 0.01% gelatin and heating to 60°C to yield a product containing $1M$ to $1.4M$ $Al(NO_3)_3$, $2.2M$ to $3.3M$ HNO_3, $2.8M$ to $0M$ $NaNO_3$, and 0.05 to 0.5 g of plutonium per liter. This solution was further processed by either ion exchange or solvent extraction. Because of the scale of the equipment available, ion exchange was more appropriate for recovering 10 kg or less of plutonium, whereas solvent extraction was used for larger batches. The ion-exchange process and equipment have been discussed previously;[11] sorption of Pu^{4+} was effected from $8M$ nitrate solutions onto Dowex 1-3X resin, and elution was accomplished with $0.35M$ HNO_3 after washing the resin with $8M$ HNO_3.

Two cycles of solvent extraction were carried out in 12- or 16-stage mixer–settlers using TBP diluted with kerosene. Prior to extraction the solution was adjusted by ferrous sulfamate reduction and $NaNO_2$ oxidation to provide Pu^{4+}, and acidity was adjusted to yield good decontamination. The first-cycle flow sheet is shown in Fig. 5. For the second extraction cycle, the feed was treated again with $NaNO_2$ ($0.03M$), adjusted to $4.2M$ HNO_3 to provide adequate salting strength, and extracted with an equal volume of 30% TBP–kerosene. After the product was stripped with $0.05M$ HNO_3–$0.04M$ ferrous sulfamate, plutonium was concentrated by ion exchange.

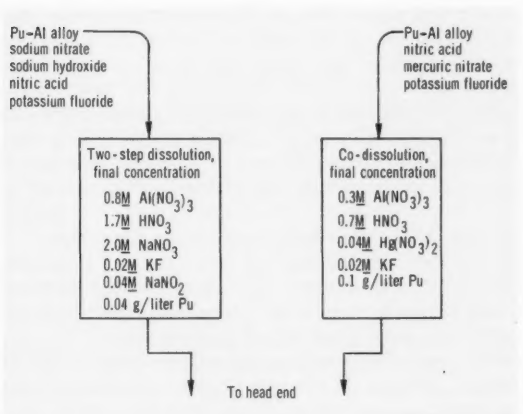

Fig. 4 Compositions of dissolver solutions.[12] [Reprinted, by permission, from Industrial & Engineering Chemistry, Process Design and Development, *6(3): 349 (July 1967).]*

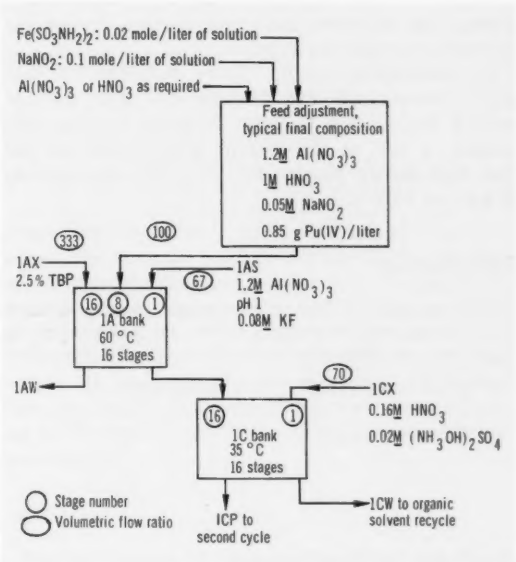

Fig. 5 First cycle for solvent extraction of plutonium.[12] [Reprinted, by permission, from Industrial & Engineering Chemistry, Process Design and Development, *6(3): 351 (July 1967).]*

Americium–curium recovery was effected in two campaigns by precipitation of the lanthanum double sulfate salts from the raffinate left after ion-exchange sorption of plutonium. The precipitate was metathesized to the hydroxides by treatment with hot NaOH.

In five campaigns a total of 91 kg of plutonium was processed with a recovery of at least 96% in each case, and fission-product decontamination factors of 0.9×10^6 to 3.0×10^6 were obtained for the plutonium.

Plant and Equipment Design and Operation

A recently published journal article[13] describes the new Windscale separations plant. The design of this plant was reported previously in *Reactor Fuel Processing.*[14] The design capacity of the plant was chosen as 1500 metric tons/year and 3000 Mwd/ton. Mechanical declad ding, a continuous dissolving scheme, and a three-cycle TBP solvent extraction process are the main features of the reprocessing flow sheet.

The article[13] briefly reviews operating experience. The plant achieved a throughput in excess of design within just a few weeks, and there has been no lost time since. The mechanical decanner has been modified to improve performance and to process fuels of new design. The centralized instrumentation system has worked so well that the analytical load was reduced considerably. Warner also reports that, owing to a better evaporation factor for highly active wastes, the stainless-steel-tank storage system has proved to be highly economical.

In commenting on the future foreseen for this plant, Warner indicates that the fuel from the Advanced Gas-Cooled Reactor Program can be processed as well as the present Magnox-clad fuel and that this should provide for all U. K. programs up to the late 1970's.

References

1. E. Dluzniewski and H. J. Walther, Development and Testing of a Fuel-Rod Chopper for a Reprocessing Plant (in German), *Kerntechnik*, 9(6): 246-248 (June 1967).
2. *Reactor Fuel Process.*, 5(3): 4 (July 1962).
3. L. E. Kindlimann and N. D. Greene, Dissolution Kinetics of Nuclear Fuels: I. Uranium, *Corrosion*, 23(2): 29-34 (1967); *ibid.*, II. Thorium, pp. 35-38.
4. *Reactor Fuel-Process. Technol.*, 10(3): 241 (Summer 1967).
5. L. M. Ferris, Grind-Leach Process for Graphite-Base Reactor Fuels That Contain Coated Particles: Laboratory Development, USAEC Report ORNL-4110, Oak Ridge National Laboratory, June 1967.
6. J. A. Buckham, Idaho Chemical Processing Plant, private communication, June 1967.
7. *Reactor Fuel Process.*, 9(2): 69 (Spring 1966).
8. J. B. Farrell and P. A. Haas, Oxidation of Nuclear-Grade Graphite by Nitric Acid and Oxygen, *Ind. Eng. Chem., Process Design Develop.*, 6(3): 277-281 (July 1967).
9. M. E. Jacobson, R. R. Mascarenas, G. F. Offutt, and K. L. Rohde, Recovery of Uranium from EBR-I Core 2 Melted Fuel, USAEC Report IN-1088, Idaho Nuclear Corporation, May 1967.
10. *Power Reactor Technol. Reactor Fuel Process.*, 10(2): 158 (Spring 1967).
11. *Reactor Fuel Process.*, 7(2): 94 (Spring 1964).
12. J. C. Eargle, C. W. Swindell, and R. I. Martens, Large Scale Processing of Highly Irradiated Plutonium by Solvent Extraction and Ion Exchange, *Ind. Eng. Chem., Process Design Develop.*, 6(3): 348-353 (July 1967).
13. B. F. Warner, The New Windscale Separation Plant, Design and Operating Experience (in English), *Kerntechnik*, 9(6): 249-252 (June 1967).
14. *Reactor Fuel Process.*, 8(2): 84 (Spring 1965).

Volatility Processes

By J. J. Barghusen

Fluorination of Oxide Fuels with ClF_3 and ClF

The reaction of fluorinating agents with nuclear fuel materials in fluid-bed systems to produce volatile uranium hexafluoride and plutonium hexafluoride is the basis of fluid-bed fluoride-volatility processing. Workers at Centre d'Étude de l'Énergie Nucléaire (CEN) at Mol, Belgium, are developing a fluid-bed process for the recovery of uranium and plutonium from UO_2 fuel based on the selective fluorination of uranium to UF_6 by the use of ClF_3 or ClF. Plutonium is recovered as PuF_6 in a subsequent step by the action of fluorine at temperatures up to 550°C. A general review of the work at CEN is presented in a recent paper by Schmets et al.[1]

Several laboratory experiments have been performed[2] to evaluate the use of ClF–oxygen mixtures for the decladding of UO_2 fuels clad in 304L stainless steel. At 450°C, with a gas mixture containing 20 vol.% ClF–30 vol.% O_2–50 vol.% Ar, only a slight reaction was observed. Significant attack of the stainless steel occurred at 550°C with a gas mixture of 40 vol.% ClF–60 vol.% oxygen. During the decladding operation the stainless steel was converted to a powder that was principally FeF_3. Some alpha Fe_2O_3 was observed in the powder layer immediately adjacent to the metal surface. Other experiments have shown that uranium is readily volatilized at 550°C by the decladding agents and plutonium is not volatilized.

A series of experiments has been performed to determine the nature of the gaseous products of the reaction between ClF_3 and various uranium compounds.[2] The experiments were carried out at temperature levels between 20 and 300°C with pure ClF_3 at 800 to 1000 mm Hg absolute pressure using powdered samples of UO_2, U_3O_8, UO_2F_2, and UF_4. In the case of UO_2 and U_3O_8, the principal gaseous reaction products other than UF_6 at temperatures less than 150°C are ClO_2F, ClO_3F, and ClF. As the temperature is increased to 150°C, the concentration of these gases decreases, and, above 150°C, chlorine and oxygen are the only products. With UO_2F_2, chlorine and oxygen are the only products at temperatures above 200°C; at lower temperatures ClF and ClO_2F are also produced. The reaction between UF_4 and ClF_3 yields chlorine and ClF in addition to UF_6. The reaction is complicated by the formation of intermediate uranium fluorides, which react slowly with ClF_3, and by the reaction of ClF_3 with the evolved chlorine to produce ClF.

ENGINEERING-SCALE STUDIES

Process studies in fluid-bed equipment are being carried out to demonstrate each of the steps in the ClF_3 process.[2] These studies have included the oxidation of 4 kg of UO_2 pellets to U_3O_8 fines in a fluid bed of alumina particles followed by reaction of the fines with HF. Studies were also carried out in a 100-mm-diameter Inconel fluid-bed reactor to evaluate the reaction between sintered UO_2 pellets and ClF_3. Although it was not possible in these studies to provide satisfactory temperature control within the fluid-bed reactor owing to inadequate reactor cooling facilities, there was no agglomeration of particles or formation of fines during the fluorination. Satisfactory cooling of the reactor walls to provide nearly isothermal fluorination conditions can be achieved by circulating cooling water in a coil about the reactor.

Previous studies[3] indicated that, since ClF does not react readily with sintered UO_2 bodies at temperatures up to 450°C, it is necessary to pulverize the oxide prior to fluorination with ClF. An experiment was performed[2] to determine if the addition of oxygen to ClF would enhance reaction between sintered UO_2 pellets and ClF. A gaseous mixture of ClF and oxygen diluted with nitrogen was contacted with sintered UO_2 for 2 hr at temperatures ranging from 350 to 450°C. Only slight volatilization of uranium and no pulverization of the pellets was observed. Evidently, the addition of oxygen to ClF does not enhance the fluorination of sintered UO_2 pellets.

BEHAVIOR OF VOLATILE FISSION-PRODUCT FLUORIDES AND NEPTUNIUM

A series of experiments was performed[2] to determine the sorption behavior of technetium and molybdenum fluorides on MgF_2 and NaF. Irradiated MoO_3 containing ^{99m}Tc in equilibrium with ^{99}Mo was treated with 20 vol.% ClF_3 in nitrogen for 2 hr at 200°C, and the resulting volatile fluorides were passed through a bed of NaF pellets and then through a bed of MgF_2 granules. More than 99% of the technetium was sorbed on NaF at 300°C. Sorption of molybdenum on NaF was greater than 99% at 100°C and slightly less at 200 and 300°C. This result was at variance with data on the dissociation pressure of the MoF_6–NaF complex; however the volatile molybdenum fluoride prepared in this experiment may have been an oxyfluoride and not MoF_6.

In experiments in which the sorption of molybdenum and technetium on NaF was high, no sorption of these elements on MgF_2 was detected. Some sorption of these elements on MgF_2 was observed (approximately 20%) in a test in which the MgF trap at 400°C was preceded by a NaF trap also maintained at 400°C. The sorption on the NaF trap was 81% of the molybdenum and 63% of the technetium.

The sorption behavior of neptunium hexafluoride was observed in an experiment in which UO_2 containing NpO_2 was contacted with ClF_3 for 2 hr at 200°C and the effluent gases passed through a MgF_2 trap, a NaF trap, and finally an activated alumina trap. Sorption of NpF_6 on MgF_2 at 100 or 200°C was slight (between 10 and 20%), whereas sorption on NaF at the same temperatures was essentially complete; no neptunium was found in the activated alumina. At 300°C, only partial sorption (62%) of NpF_6 on NaF was observed.

During fluorination of fuel with ClF, a previously irradiated sample containing UF_4, UO_2F_2, UO_2, and alumina was contacted[2] with ClF at 400 and 500°C to determine the fate of neptunium and certain fission products. Approximately 25% of the neptunium was volatilized after 4 hr of reaction at 500°C, which is less than that resulting from the use of ClF_3 as the fluorinating agent. Molybdenum and ruthenium both formed volatile fluorides at 400 and 500°C with ClF.

Fluid-Bed Fluorination of UO_2–PuO_2 Fuel with Bromine Pentafluoride

Work on the development of a fluid-bed fluoride-volatility process at Argonne National Laboratory (ANL) has concerned the application of BrF_5 as a fluorinating agent to selectively convert uranium in the fuel to volatile UF_6 while plutonium is converted to nonvolatile PuF_4.

The process flow sheet[4] for the recovery of uranium and plutonium from low-enrichment UO_2–PuO_2 fuel clad in Zircaloy is shown in Fig. 1. The process involves four principal steps:

1. Decladding: the fuel elements are immersed in a fluidized bed of inert alumina particles and contacted with HCl gas whereby the cladding is converted to volatile $ZrCl_4$, which is removed from the reactor and subsequently converted to solid ZrO_2 by pyrohydrolysis with steam.

2. Oxidation: the oxide fuel, which is unaffected by the decladding step and accumulates in the lower portion of the fluid-bed reactor, is contacted with 15 to 25 vol.% oxygen in nitrogen at 450°C to form a mixture of U_3O_8 and PuO_2 fines (approximately 20 μ in diameter).

3. Uranium fluorination: uranium is recovered from the oxide fines as volatile UF_6 by reaction of the fines with 5 to 15 vol.% BrF_5 in nitrogen at 300°C.

4. Plutonium fluorination: the plutonium, which is converted to nonvolatile PuF_4 during the uranium fluorination step, is recovered as PuF_6 by reaction of PuF_4 with fluorine at 300 to 550°C.

The UF_6 produced in the third step is collected in a condenser together with excess BrF_5, bromine, and volatile fission-product fluorides. The UF_6 is separated from the fission products and interhalogens by fractional distillation and sorption techniques. Plutonium hexafluoride, produced in the last step, is collected in cold traps and then revaporized and passed into a separate vessel for final purification.

Implicit in the application of the BrF_5 process to the reprocessing of spent fuel materials is the need to consider methods for the recycle of the interhalogen. Two different schemes for BrF_5 recycle are being considered. In the first scheme, represented in Fig. 1, Phase II, the liquid mixture containing bromine, BrF_5, fission-product fluorides, and UF_6 is contacted with fluorine gas during the fractional distillation step to convert the bromine component to BrF_3. The BrF_3 product is then fluorinated to BrF_5 in a separate vessel, and the BrF_5 is recycled. The second scheme involves fluorination of the bromine to either BrF_3 or BrF_5 prior to condensation of the UF_6 product.

Demonstration tests on this process are being carried out in a 2-in.-diameter fluid-bed reactor with UO_2–PuO_2 fuel containing simulated fission products. Recent experimental work[5] has concerned evaluating the use of 50 vol.% fluorine in the plutonium-recovery step instead of 90 vol.% fluorine as used previously.[6] The charge to the fluid-bed reactor consisted of 650 g of UO_2–PuO_2 fission-product pellets and 1100 g of alumina containing 0.6 g of CsF, 0.15 g of RbF, and 0.5 g of NpO_2.

The processing sequence consisted of the following: oxidation of the pellets for 4 hr at 450°C with 20 vol.% oxygen, fluorination of the uranium to UF_6 with 10 vol.% BrF_5 at 300°C for 2 hr, and recycle fluorination of the plutonium to PuF_6 with 50 vol.% fluorine for 5 hr at 300°C, 5 hr while the reaction temperature was increased from 300 to 550°C, and 5 hr at 550°C.

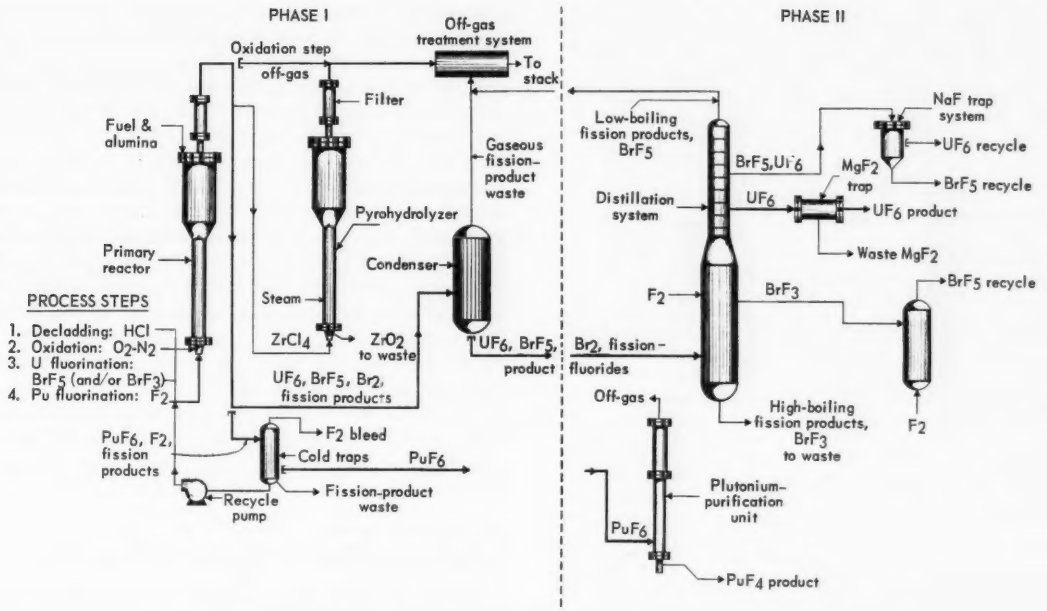

Fig. 1 Fluid-bed volatility-process interhalogen reference flow sheet.[4]

The final alumina bed contained <0.001 wt.% uranium, 0.009 wt.% plutonium, and 0.003 wt.% neptunium. Since these results are nearly identical to those obtained previously in experiments using 90 vol.% fluorine, it appears that the concentration of fluorine in the plutonium-recovery step can be varied within the range 50 to 90 vol.% in nitrogen without affecting the removal of plutonium from the alumina bed.[5]

OXIDATION OF UO_2

In connection with the plan of AEC to construct a hot engineering-scale pilot plant at Oak Ridge National Laboratory, an experimental program is under way at the Oak Ridge Gaseous Diffusion Plant (ORGDP) to determine the processing conditions and equipment requirements for optimum batch oxidation of UO_2 pellets and to obtain the information required for conceptual plan studies and engineering analyses.[7,8]

The experimental equipment consists of a fluid-bed reactor and a separate vessel for filtration and cooling of the effluent gases from the reactor (Fig. 2). In the experiments, approximately 35 kg of UO_2 pellets ($\frac{3}{8}$ in. in diameter and $\frac{3}{4}$ in. long) were charged to the reactor. The quantity of inert-alumina fluid-bed material varied from 22 to 91 kg. The UO_2 pellet bed was supported on a bed of $\frac{1}{2}$-in.-diameter refractory alumina balls.

Results from a series of 21 runs have indicated:

1. Essentially complete oxidation of UO_2 pellets to produce material of −35-mesh particle size can be accomplished under controlled conditions. The alumina-to-U_3O_8 ratio can be as low as 0.8; however, the fluidization properties of the alumina−U_3O_8 mixture are poor at this ratio.

2. The technique of oxidizing the pellet bed progressively from the top to the bottom has been effective in reducing the tendency of the pellet bed to plug or channel.

3. A minimum superficial gas velocity through the pellet bed must be maintained to keep the reacting bed free of U_3O_8 powder. The minimum velocity depends on the depth of the pellet bed. For a shallow bed (up to 1 ft), a velocity of 1 ft/sec is satisfactory. For deeper beds, a velocity greater than 2 ft/sec is required; satisfactory results have been consistently achieved at 3 ft/sec.

4. The maximum amount of uranium elutriated from the reactor to the cooler has been 32 wt.% of the uranium charge. The material transferred has contained about 92 wt.% U_3O_8.

Harrison and associates[9] have reported the results of a basic study of the oxidation of irradiated UO_2 spheres in dry air at temperatures between 320 and 380°C. The oxidation reaction was interpreted as being first order and occurring in two stages with the rate constant being higher for the second stage. Neutron irradiation up to 9 at.% burnup was not found to alter the oxidation mechanism fundamentally but did produce a general decrease in reaction rates. Thus the Arrhenius activation energy for the second stage of the oxidation reaction increased from 15

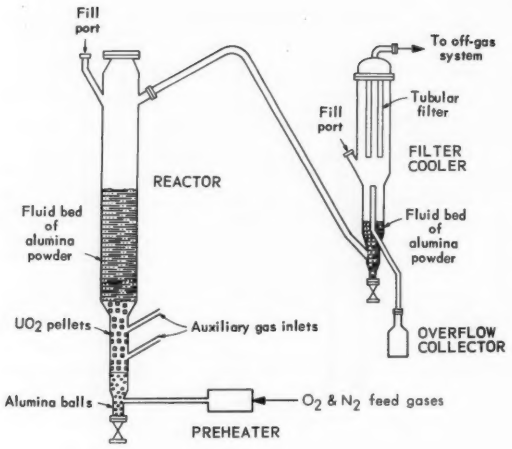

Fig. 2 Pilot-scale facility for fluid-bed oxidation of UO_2 pellets.[7]

kcal/mole for unirradiated UO_2 to approximately 25 kcal/mole at 8.5 at.% burnup.

FLUORINATION OF UO_2 FUELS WITH BrF_5

Engineering-scale studies are being performed at ANL in a 3-in.-diameter fluid-bed reactor facility to determine the effects of important process variables on the fluorination of UO_2 fuels with BrF_5. In these studies the oxide fuel is oxidized to U_3O_8 fines in a fluid bed of alumina by reaction with 19 vol.% oxygen at 450°C and the fines fluorinated with 12 or 21 vol.% BrF_5 at 225 or 300°C. In several runs,[10] a temperature excursion within the pellet bed was observed during the oxidation step. Although a portion of the pellet bed reached 590°C, no operational problems were encountered, and this behavior did not appear to affect fluorination of the oxide fines.

In an experiment in which U_3O_8 fines, produced by oxidation of 2.2 kg UO_2, were fluorinated with 21 vol.% BrF_5 for 2 hr at 300°C, it was observed[11] that the UF_6 production rate remained constant at about 130 lb UF_6/(hr)(sq ft) until about 80% of the oxide was fluorinated. A BrF_5 utilization efficiency of 40% was sustained during the constant-rate period. The final alumina bed at the end of the fluorination period contained no agglomerates or unreacted oxide and was a free-flowing material.

BEHAVIOR OF NEPTUNIUM

In the fluorination of oxidized fuel materials with BrF_5, neptunium is converted to volatile NpF_6 which accompanies the UF_6 product stream. The results of a study of the kinetics of the reaction between NpF_4 and BrF_5 to produce NpF_6 have been reported in Ref. 4. The rate of reaction was measured at 300, 325, 350, and 400°C in a boat reactor. An activation energy of 26 kcal/mole was derived from rate data obtained at the three lower temperature levels. The rate of reaction of NpF_4 is lower by a factor of about 250 than the rate of reaction of UF_4 with BrF_5.

Experiments on the chemistry of NpF_6 have shown[12] that NpF_6 is reduced to solid NpF_4 by reaction with elemental bromine (the product of reaction of BrF_5 with uranium compounds) at 30°C. Since UF_6 is not reduced by bromine, this reaction offers an attractive technique for separating uranium from neptunium in NpF_6–UF_6 mixtures. Several experiments were performed[12,13] to evaluate this reaction at 30 and 75°C. The reduction of NpF_6 by bromine proceeds slowly at 30°C; however, at 75°C the reaction is rapid and NpF_6 is completely reduced[13] to solid NpF_4 in 1 hr. Since small amounts of uranium were found in the NpF_4 product, additional treatment of the solid product may be required to obtain neptunium of high purity.

Preparation and Properties of Fluorides

An experimental determination of the equilibrium constant for the reaction $ClF_3 + F_2 = ClF_5$ at 350°C has been reported by Bougon et al.[14] The authors observed that at 350°C equilibrium is achieved within 2 hr and is not affected by prolonged heating at this temperature. An equilibrium constant $k_p = 5 \times 10^{-3}$ atm^{-1} is reported. The enthalpy of formation of ClF_5 was determined to be -57.7 ± 1 kcal/mole.

Two recent publications concerning the spectral analyses of volatile fluorides have been issued. Blanchard[15] has reported results of the infrared spectra of gaseous WOF_4 and $MoOF_4$. The infrared vibration–rotation spectra of SeF_6 and WF_6 were reported by Abramowitz and Levin.[16]

In other work, Siegel and Northrup[17] have reported the results of crystallographic studies of several transition-metal hexafluorides, and Edwards et al.[18] have determined the crystal structures of W, Mo, Re, and Tc oxytetrafluorides.

As part of a continuing investigation at ANL[19] on obtaining thermochemical data by measuring the heat of formation of fluorides by combustion in a fluorine bomb calorimeter, standard enthalpies of formation (expressed as kcal/mole) have been obtained for ThF_4, 505.2; CF_4 (g), 222.7; PF_3 (g), 228.8; ErF_3, 406; HoF_3, 406.5; and LaF_3, 415.

By employing solid-state galvanic cells that combined the fluorides of Mg, Ni, Fe, and U, Lofgren and McIver[20] were able to compute the enthalpies of formation of NiF_2, UF_4, and FeF_2. The values of ΔH_{298} were: $Ni + F_2 \rightarrow NiF_2$ (-156.7 ± 0.5 kcal/mole); $UF_3 + \frac{1}{2} F_2 \rightarrow UF_4$ (two determinations in two cells: -99.1 ± 1.0 and -97.9 ± 0.9 kcal/mole); $Fe + F_2 \rightarrow FeF_2$ (-169.9 ± 0.7 kcal/mole).

In a special issue of *Atomic Energy Review*, devoted to the physicochemical properties of plutonium com-

pounds and alloys, Rand[21] presented a compilation of the thermochemical properties of plutonium compounds. Chemical thermodynamic data for plutonium compounds have also been reviewed and assessed by Oetting.[22]

References

1. J. Schmets, G. Camozzo, R. Heremans, and G. Pierini, Reprocessing Mixed Oxide Fuels by Fluorination, paper presented at the International Atomic Energy Agency Colloquium on the Use of Plutonium as Nuclear Fuel, Brussels, March 13–17, 1967. Available in translation as USAEC Report ANL-TRANS-478, 1967.
2. Centre d'Étude de l'Énergie Nucléaire, Reprocessing of Irradiated Fuels, Quarterly Report No. 26, July 1–September 30, 1966, USAEC Report EURAEC-1832, 1967.
3. *Power Reactor Technol. Reactor Fuel Process.*, 10(1): 72-74 (Winter 1966–1967).
4. Argonne National Laboratory, Chemical Engineering Division Semiannual Report, July–December 1966, USAEC Report ANL-7325, p. 51, 1966.
5. R. M. Adams and A. Glassner (Comps.), Reactor Development Program Progress Report, April 1967, USAEC Report ANL-7329, pp. 71-72, Argonne National Laboratory, June 16, 1967.
6. *Reactor Fuel-Process. Technol.*, 10(3): 227-228 (Summer 1967).
7. S. H. Smiley, J. H. Pashley, and R. B. Schappel, ORGDP Fuel Reprocessing Studies. Summary Progress Report, July–December 1966, USAEC Report K-1717, Union Carbide Corporation Nuclear Division, Oak Ridge Gaseous Diffusion Plant, June 12, 1967.
8. S. H. Smiley, ORGDP Fuel Reprocessing Studies. Progress Report for Period Ending February 28, 1967, USAEC Report K-L-1780(Pt. 19), Union Carbide Corporation Nuclear Division, Oak Ridge Gaseous Diffusion Plant, Apr. 3, 1967.
9. K. T. Harrison, C. Padgett, and K. T. Scott, The Kinetics of the Oxidation of Irradiated Uranium Dioxide Spheres in Dry Air, British Report AERE-R-5370, February 1967, and *J. Nucl. Mater.*, 23: 121–138 (1967).
10. R. M. Adams and A. Glassner (Comps.), Reactor Development Program Progress Report, March 1967, USAEC Report ANL-7317, pp. 86-87, Argonne National Laboratory, Apr. 28, 1967.
11. R. M. Adams and A. Glassner (Comps.), Reactor Development Program Progress Report, April 1967, USAEC Report ANL-7329, p. 73, Argonne National Laboratory, June 16, 1967.
12. R. M. Adams and A. Glassner (Comps.), Reactor Development Program Progress Report, January 1967, USAEC Report ANL-7302, p. 76, Argonne National Laboratory, Feb. 24, 1967.
13. R. M. Adams and A. Glassner (Comps.), Reactor Development Program Progress Report, February 1967, USAEC Report ANL-7308, p. 73, Argonne National Laboratory, Mar. 28, 1967.
14. R. Bougon, J. Chatelet, and P. Plurien, Chlorine Pentafluoride, *Compt. Rend., Ser. C.*, 264(22): 1747-1750 (May 29, 1967).
15. S. Blanchard, Spectre Infrarouge des Oxytetrafluorures Gazeux de Tungstene et de Molybdene, French Report CEA-R-3194, 1967.
16. S. Abramowitz and I. W. Levin, Vibrational Analysis of SeF_6 and WF_6, *Inorg. Chem.*, 6(3): 538-541 (March 1967).
17. S. Siegel and D. A. Northrup, X-Ray Diffraction Studies of Some Transition Metal Hexafluorides, *Inorg. Chem.*, 5(12): 2187-2188 (December 1966).
18. A. J. Edwards, G. R. Jones, and B. R. Steventon, The Crystal Structures of Tungsten, Molybdenum, Rhenium, and Technetium Oxide Tetrafluorides, *Chem. Commun.*, (No. 9): 462-463 (May 10, 1967).
19. Argonne National Laboratory, Chemical Engineering Division Research Highlights, May 1966–April 1967, USAEC Report ANL-7350, 1967.
20. N. L. Lofgren and E. J. McIver, Thermodynamic Properties of Some Fluoride Systems, British Report AERE-R-5169, March 1966.
21. M. H. Rand, Thermochemical Properties in "Plutonium: Physicochemical Properties of Its Compounds and Alloys," *At. Energy Rev.*, 4 (Special Issue No. 1): 7-51 (June 1966).
22. F. L. Oetting, The Chemical Thermodynamic Properties of Plutonium Compounds, *Chem. Rev.*, 67(3): 261-297 (June 1967).

Compact Pyrochemical Processes

By W. E. Miller and R. K. Steunenberg

Pyrochemical processes consist in high-temperature, nonaqueous procedures for the decontamination and recovery of fissile and fertile constituents in irradiated reactor fuels. Most of the processes currently under development employ liquid metals and salts as process solvents at temperatures in the range of 500 to 800°C. Chemical separations may be effected by selective volatilization, precipitation from a solvent, liquid metal–salt extraction, or electrolysis. Pyrochemical processes are being developed for ceramic (oxide or carbide), metallic, and molten-salt fuels. Their potential economic advantages depend mainly on their capability for processing short-cooled, high-burnup fuels in compact equipment and the direct production of solid, concentrated radioactive waste streams.

Liquid Metal–Salt Extraction Processes

In several of the pyrochemical processes currently under development, the major separations of fissile, fertile, and fission-product elements depend upon differences in their partition behavior between immiscible liquid-metal and liquid-salt solvents. Alloys of magnesium with zinc, cadmium, or copper are frequently used as liquid-metal solvents. The salts are usually composed of mixtures of chlorides and fluorides of alkali and alkaline-earth metals. The partition behavior of a particular element between the salt and metal phases is governed by its relative tendencies to be oxidized by the salt and reduced by the metal. In several proposed salt–metal extraction processes, magnesium metal is the reducing agent and magnesium chloride is the oxidant.

SALT-TRANSPORT PROCESSES

At Argonne National Laboratory (ANL), the current development work on pyrochemical processes is directed mainly to flow sheets that incorporate a salt-transport step. A proposed flow sheet for the recovery of uranium and plutonium from fast breeder reactor fuels was presented in detail in an earlier issue of *Power Reactor Technology and Reactor Fuel Processing*.[1] In this process, stainless-steel cladding is first removed from PuO_2-UO_2 fuel by dissolution in liquid zinc at 800°C. The liquid zinc containing the stainless-steel constituents is separated from the oxide and either discarded directly as waste or recovered for reuse. The oxide mixture is then added to a molten halide salt, which is contacted with a liquid Cu–33 wt.% Mg alloy. Uranium, plutonium, and the noble-metal fission products are reduced to the metals and transferred to the Cu–Mg alloy, in which the uranium is precipitated and the plutonium is in solution. The alkali, alkaline-earth, and rare-earth fission products remain in the salt phase, along with the MgO that is formed as a by-product of the reduction.

The oxide-reduction step is followed by a salt-transport procedure in which the Cu–Mg alloy and a Zn–5 wt.% Mg alloy are both contacted with a $MgCl_2$-based salt at 600°C. This procedure results in selective transfer of the plutonium to the Zn–Mg alloy, which is vacuum distilled to recover a metallic plutonium product. The precipitated uranium is recovered by decanting the supernatant Cu–Mg alloy, washing with liquid magnesium to remove copper and remaining fission products, and retorting to separate residual magnesium from the uranium metal.

A laboratory experiment was performed to determine whether the zinc used for decladding could be purified for reuse by precipitating the dissolved stainless-steel constituents (iron, chromium, and nickel) as aluminum intermetallic compounds.[2] Aluminum metal was added to a liquid-zinc solution containing approximately 4 wt.% iron, 0.7 wt.% chromium, and 0.6 wt.% nickel at 800°C. The quantity of aluminum added was sufficient to precipitate 80% of these metals as $FeAl_3$, $CrAl_7$, and $NiAl_3$, respectively. The temperature was decreased from 800 to 500°C, and the liquid-zinc phase was sampled. The zinc contained 0.005 wt.% Fe, 0.0025 wt.% Cr, 0.018 wt.% Ni, and 0.9 wt.% Al. Although these results indicate excellent removal of the stainless-steel constituents, the quantity of aluminum that remained in the zinc

could be great enough to reduce a part of the oxide fuel when the zinc is reused for decladding. It may prove desirable to decrease the amount of aluminum used since the removals of iron, chromium, and nickel were greater than necessary.

A number of investigations relating to the oxide-reduction step of the process have been made. Previous studies had indicated that the progress of the reduction reaction is inhibited by the presence of MgO, which is formed as a by-product of the reaction and is essentially insoluble in the salt. Several exploratory experiments were performed to determine whether the use of an alternative reductant such as calcium, whose oxide is soluble in the salt, would increase the rate and extent of reduction.[2] Calcium metal was added to the Cu–Mg alloy in slight excess of the amount required to reduce the oxides and a $CaCl_2$–20 mole % CaF_2 mixture was used as the salt phase because of the relatively high solubility of CaO in this system. These modifications of the procedure appear to be beneficial since the reductions at 800°C and an agitator speed of 800 rpm were 98% complete in 2 hr using powdered UO_2 and over 99% complete after 4 hr using sintered UO_2 pellets.

Other studies have shown that reductions of 98 to 100% are obtained when 47.5 mole % $MgCl_2$–47.5 mole % $CaCl_2$–5 mole % CaF_2 is used as the salt phase with a Cu–33 wt.% Mg alloy.[3] However, it is desirable to use a salt of lower $MgCl_2$ content in the subsequent extraction steps of the process in order to minimize plutonium losses through back extraction. An experiment has been completed to determine the feasibility of decreasing the $MgCl_2$ content of the salt after the oxide-reduction step by adding metallic calcium and lithium to the salt–metal system at about 700°C. Magnesium oxide was added to the salt to simulate the by-product material from the reduction, and cerium was added to determine its distribution coefficient in the resultant salt–metal system. Preliminary analyses show that the chemistry of the process proceeded as expected with a resulting salt composition of about 56 mole % $CaCl_2$–15 mole % $MgCl_2$–24.6 mole % LiCl–4.4 mole % CaF_2, which should be suitable for the extraction steps.

In the process flow sheet, plutonium is separated from uranium and noble-metal fission products by a salt-transport step. The theoretical aspects of the salt-transport procedure are discussed in a recently issued report.[4] In the salt-transport step, liquid salt is contacted simultaneously or alternately with liquid-metal donor and acceptor solutions. The salt flow may be either batch or continuous. When plutonium is the transferring species, the following reaction occurs in the donor alloy–salt system:

$$\text{Pu (metal phase)} + \tfrac{3}{2}MgCl_2\ \text{(salt phase)} \rightarrow PuCl_3\ \text{(salt phase)} + \tfrac{3}{2}\text{Mg (metal phase)}$$

The reverse reaction occurs in the acceptor alloy–salt system. If the salt-transport step is carried to completion, the concentration of plutonium in the salt over the donor and acceptor alloys is the same and the ratio of plutonium concentrations in the two alloys may be represented by

$$\frac{\text{Wt.\% Pu in solution in acceptor alloy}}{\text{Wt.\% Pu in solution in donor alloy}} = \frac{K_{Pu(a)}}{K_{Pu(d)}}$$

where $K_{Pu(a)}$ and $K_{Pu(d)}$ are the distribution coefficients of plutonium between the salt phase and acceptor alloy and the salt phase and donor alloy, respectively. In the same report[4] the distribution behavior of various fuel constituents between liquid metals and molten salts is discussed.

The feasibility of the salt-transport procedure has recently been demonstrated on an engineering scale, using uranium rather than plutonium.[4] Figure 1 shows

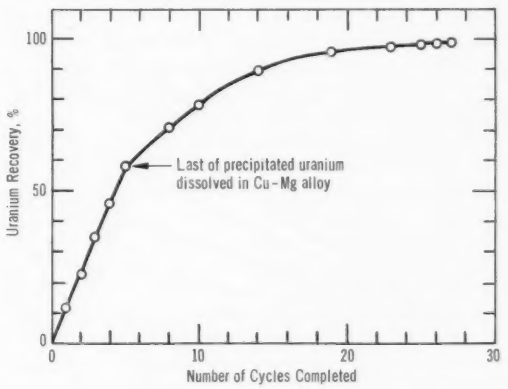

Fig. 1 Rate of uranium recovery in salt-transport experiment.[4]

System:	*Cu–Mg/$MgCl_2$/Zn–Mg*
Donor Alloy:	*Cu–5 wt.% Mg*
Acceptor Alloy:	*Mg–35 wt.% Zn*
Salt:	*100% $MgCl_2$*
Temperature:	*840°C*

the results of a run in which approximately 5 kg of uranium was transported from a Cu–5 wt.% Mg alloy to a Zn–65 wt.% Mg alloy at about 830°C, using $MgCl_2$ as the salt phase. The salt was contacted alternately with the two alloys by means of a pressure-siphoning technique. At the beginning of the run, approximately 40% of the uranium was dissolved in the Cu–Mg alloy, the remainder being present as a precipitated phase. As shown in Fig. 1, the uranium transferred at a constant rate until the fifth cycle, when the last of the precipitate in the Cu–Mg alloy had dissolved. Since the concentration of uranium in the donor alloy decreased with each succeeding cycle, the uranium transfer rate also decreased. A uranium

recovery of 99% was achieved after a total of 27 cycles. Representative inactive fission-product elements (Zr, Mo, Pd, Ru, and Nb) had been added to the donor alloy along with uranium. When the transport step was completed, the acceptor alloy was decanted from the precipitated uranium, which was then washed with additional Zn–Mg and recovered by retorting. The removals of the fission-product elements were as follows: Zr, 99.7%; Mo, 99.9%; Pd, 99.99%; Ru, 99.99%; Nb, 99.9999%.

Either batch or continuous-flow equipment can be used in plant-scale operation of the salt-transport step. If batch equipment is used, the transport rate of uranium can be maximized by operating in such a way that the donor alloy is always saturated with uranium. The uranium transport rate for a particular combination of salt and alloys will depend upon the cycle time and the volumes of the vessels in a batch process. This dependence is illustrated in Fig. 2. The

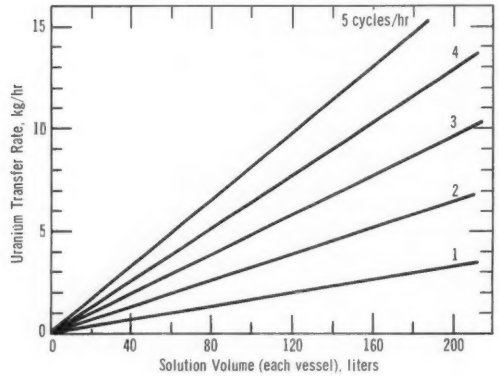

Fig. 2 Calculated rates of uranium transfer for batch-transfer system.[4]

System:	*Cu–Mg/$MgCl_2$/Zn–Mg*
Donor Alloy:	*Cu–5 wt.% Mg*
Acceptor Alloy:	*Mg–35 wt.% Zn*
Salt:	*100% $MgCl_2$*
Temperature:	*840°C*

dependence of the uranium transport rate on the rate of salt circulation and the vessel size in a continuous salt flow system is shown in Fig. 3.

In the salt-transport step for plutonium, a Cu–33 wt.% Mg solution is used as the donor alloy at a temperature of 600°C. Since the plutonium in the donor alloy will be in solution at the outset, the constant-rate period observed in the uranium experiments will not be encountered. The rate of plutonium transport will therefore depend almost entirely on its distribution coefficient and the ratio of salt to metal used in the donor system. Figure 4 shows the theoretical plutonium recoveries in a batch operation as functions of the number of cycles and the salt-to-metal ratio for the case in which the efficiency of salt transfer is 90% and the equilibration reactions are 99% complete. It is evident that over 99.9% plutonium recovery can be achieved in a few cycles if large salt-to-metal ratios are used. The percentage of plutonium recovered is independent of the quantity of plutonium involved if the solubility of plutonium in the donor alloy is not exceeded.

Investigations have continued at ANL on materials and components for pyrochemical process equipment.[5] A test[3] has recently been concluded in which a molten chloride salt at 560°C was circulated through typical equipment components for a total period of 1348 hr. No significant reaction of the wall thickness in 304 stainless steel was found. The intergranular penetration did not exceed about 0.05 mm. Earlier corrosion studies[6] had shown promising results for small specimens of niobium exposed at 750°C to a Cu–33 wt.% Mg–1 wt.% U solution, together with a molten salt consisting of 50 mole % $MgCl_2$, 30 mole % NaCl, and 20 mole % KCl. Niobium has continued to show good corrosion resistance in the same system.[3] A welded niobium crucible has shown no evidence of corrosion after 384 hr of exposure.

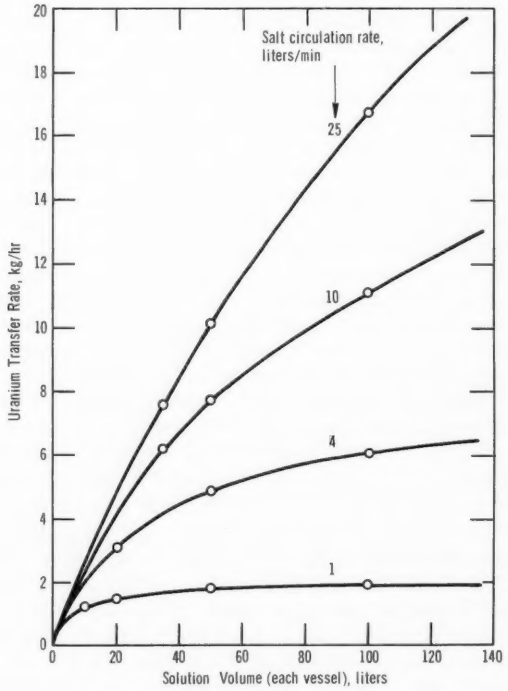

Fig. 3 Calculated rates of uranium transfer for continuous salt-transport systems.[4]

System:	*Cu–Mg/$MgCl_2$/Zn–Mg*
Donor Alloy:	*Cu–5 wt.% Mg*
Acceptor Alloy:	*Mg–35 wt.% Zn*
Salt:	*100% $MgCl_2$*
Temperature:	*840°C*

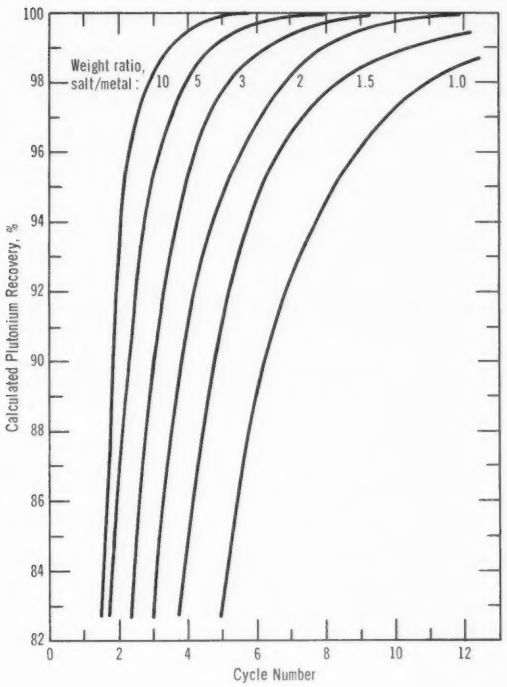

Fig. 4 Calculated rates of plutonium transport for batch-transfer systems.[4] Calculations are based on the following:

Donor Alloy:	*Cu–33 wt.% Mg*
Acceptor Alloy:	*Zn–5 wt.% Mg*
Salt:	*50 mole % $MgCl_2$, 30 mole % NaCl, 20 mole % KCl*
Temperature:	*600°C*

PROCESSES FOR MOLTEN SALT BREEDER REACTOR FUEL

Work at Oak Ridge National Laboratory (ORNL) on the application of pyrochemical processing techniques to molten salt breeder reactor (MSBR) fuel has been summarized in a recent report.[7] The MSBR is a thermal breeder reactor that is designed to operate on the Th–^{233}U fuel cycle. The fuel is a molten fluoride salt (66 mole % LiF–34 mole % BeF_2) containing ^{235}U fluoride as the fissionable material and ZrF_4 as the stabilizing agent to prevent possible uranium oxide precipitation. The objectives of reprocessing in this fuel cycle are to remove rare-earth fission products, which are neutron poisons, from the core fuel and to recover bred ^{233}Pa from the blanket as soon as possible.

Two methods of rare-earth removal are under investigation: (1) rare-earth fluorides in the molten-salt fuel may be reduced and extracted by a liquid metal, and (2) rare-earth fluorides may be precipitated from the molten salt along with UF_3 as solid solutions. Protactinium may be removed from the blanket salt by the addition of thorium metal or by oxide precipitation.

In the processing schemes proposed for the MSBR, uranium is first removed from the core fuel by fluorination. The stripped salt is then contacted with a liquid Bi–Li alloy, which reduces the rare-earth fluorides. Thus the rare earths are extracted into the alloy, and an equivalent amount of LiF enters the salt phase. Experimental results have shown that essentially all cerium, lanthanum, and neodymium, and substantial amounts of samarium and europium are removed from the salt when a Bi–2 mole % Li alloy is used as the reductant. Since isotopically pure ^{7}Li must be used in the alloy, it is desirable to minimize the amount of lithium remaining in the alloy, which becomes a waste stream. Therefore the distribution behavior of representative rare earths between the salt and metal phases was determined as a function of the lithium concentration in the metal. The results are presented in Fig. 5.

An alternative method of rare-earth removal is based on the formation of solid solutions of UF_3 and rare-earth trifluorides, which are insoluble in the molten-salt fuel. In previous experiments it had been shown that reduction of UF_4 in solution in the salt to insoluble UF_3 by zirconium metal resulted in coprecipitation[8] of the rare-earth trifluorides with the UF_3. More recent studies[7] have been conducted on the removal of rare earths from the salt through incremental additions of solid UF_3. Approximately 1 mole % CeF_3 was found in UF_3 that had been added to a 66 mole % LiF–34 mole % BeF_2 melt with an initial CeF_3 content of about 10^{-4} mole fraction. In a similar experiment with neodymium, the NdF_3 content of the UF_3 was about 0.2 mole %.

Methods of removing protactinium from the MSBR blanket salt were reviewed in the previous issue.[9] Further experiments[7] have been conducted, using relatively high protactinium concentrations of 24 to 81 ppm. Protactinium in a 73 mole % LiF–27 mole %

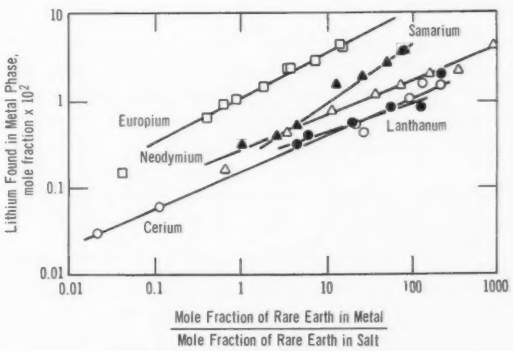

Fig. 5 Effect[7] of lithium concentration in metal phase on the distribution of rare earths between LiF–BeF_2 (66 to 34 mole %) and bismuth at 600°C.

ThF_4 melt was reduced by thorium metal and collected on steel wool. It is believed that the protactinium coprecipitates with small amounts of iron in the salt and is codeposited on the steel wool.

SLAGGING PROCESSES

These processes are conducted at high temperatures and involve the selective oxidation of the more chemically reactive fission-product elements from a liquid metal such as molten uranium or plutonium. Melt refining, an example of oxidative slagging, is used routinely to reprocess the fuel discharged from the second Experimental Breeder Reactor (EBR-II). The production performance of EBR-II fuel-reprocessing and -refabrication operations is summarized in monthly progress reports of Argonne National Laboratory.[10]

References

1. *Power Reactor Technol. Reactor Fuel Process.*, 10(1): 80 (Winter 1966-1967).
2. R. M. Adams and A. Glassner (Comps.), Reactor Development Program Progress Report, May 1967, USAEC Report ANL-7342, pp. 80-82, Argonne National Laboratory, June 30, 1967.
3. R. M. Adams and A. Glassner (Comps.), Reactor Development Program Progress Report, April 1967, USAEC Report ANL-7329, pp. 52-53, Argonne National Laboratory, June 16, 1967.
4. R. C. Vogel, M. Levenson, E. R. Proud, and J. Royal, Chemical Engineering Division Research Highlights, May 1966–April 1967, USAEC Report ANL-7350, pp. 8-20, Argonne National Laboratory.
5. R. M. Adams and A. Glassner (Comps.), Reactor Development Program Progress Report, December 1966, USAEC Report ANL-7286, pp. 32-35, Argonne National Laboratory, Jan. 26, 1967.
6. R. M. Adams and A. Glassner (Comps.), Reactor Development Program Progress Report, November 1966, USAEC Report ANL-7279, pp. 35-37, Argonne National Laboratory, Dec. 21, 1966.
7. Reactor Chemistry Division Annual Progress Report for Period Ending December 31, 1966, USAEC Report ORNL-4076, pp. 33-41, Oak Ridge National Laboratory, March 1967.
8. R. B. Briggs, Molten-Salt Reactor Program. Semiannual Progress Report for Period Ending Aug. 31, 1966, USAEC Report ORNL-4037, p. 145, Oak Ridge National Laboratory, January 1967.
9. *Reactor Fuel-Process. Technol.*, 10(3): 235-236 (Summer 1967).
10. R. M. Adams and A. Glassner (Comps.), Reactor Development Program Progress Report, March 1967, USAEC Report ANL-7317, pp. 30-32, Argonne National Laboratory, Apr. 28, 1967.

Progress in Waste-Disposal Research and Development

By Phillip Fineman

Conversion of High-Level-Activity Wastes to Solids

Pacific Northwest Laboratory (PNL) is conducting a program that will demonstrate the solidification of high-level-activity wastes by various solidification processes.[1] The processes are (1) the PNL spray-solidification process, (2) the ORNL (Oak Ridge National Laboratory) pot calcination and rising-level glass processes, and (3) the BNL (Brookhaven National Laboratory) phosphate-glass process. They will be tested on an engineering scale with plant-level-activity wastes in a multipurpose facility, known as the Waste Solidification Engineering Prototypes (WSEP). Recent PNL progress reports cover the continuing experimental work and equipment design and verification tests conducted on the spray-solidification[2] and the phosphate-glass[3] processes and present results of the first demonstration pot calcination runs[4] carried out with highly radioactive liquid wastes. These demonstration runs are discussed below.

POT CALCINATION PROCESS

In the pot calcination process, one of three pot solidification processes developed at ORNL, the calcination and solidification steps are carried out in the same vessel or pot. This vessel, which is cylindrically shaped, also serves as the permanent storage container for the solidified waste product.

Three runs were completed in which simulated PW-2 wastes* containing added radioactivity were used for feed solutions. In these runs, $NaNO_3$ and $Ca(NO_3)_2$ were added to retain the sulfate and minimize its volatilization from the calciner. In the first run, WSEP-I, the $NaNO_3$ was added to the feed, and the $Ca(NO_3)_2$ was fed as a separate stream to the calciner pot. In the other two runs, PC-2 and PC-3, both additives were introduced directly to the feed. In all runs, overall retention of fission-product activity within the processing and off-gas system was satisfactory. Although there was some ruthenium volatilization from the calciner pot, the ruthenium was effectively retained by the off-gas system.

Operating difficulties were encountered in the preparation and handling of the PW-2 waste feed which was to be used for runs PC-2 and PC-3. Solids, mostly sodium–rare-earth double sulfates,† caused plugging of the feed pump loop, feed tank sparger, and several feed transfer lines. Lowering the solids content to prevent further plugging was accomplished by reducing the sulfate concentration in the waste from 0.87*M* to about 0.6*M*.

Operation of the calciner and auxiliary processing equipment was very satisfactory throughout the three runs. The thermal liquid-level probe for controlling the feed rates to the pots performed well.

Other details for each of the three runs are presented below.

Run WSEP-I. A total of 850 liters of feed containing added 85,000 curies of mixed fission-product activity was processed in a 12-in.-OD pot fabricated of 304L stainless steel. The volume of calcine was estimated to be 105 liters, resulting in a volume reduction (feed to calcine) of about 8.

The furnace temperature was generally maintained at 850°C. However, internal heat generation in the

*PW-2 waste is a combined first- and second-cycle Purex-process waste. It is high in nitric acid (~5*M*) and contains iron and sulfate ions from the ferrous sulfamate reductant.

†Laboratory investigations[5] showed that the formation of the sodium–rare-earth double sulfate can be prevented by diluting the PW-2 from the usual 100 gal of waste produced per metric ton of uranium to 200 gal per metric ton at 4.0*M* free HNO_3. If dilution is undesirable, the caking tendency of the precipitate can be avoided by adding phosphoric acid. Less than 0.5*M* phosphoric acid is sufficient for this purpose, but the minimum concentration remains to be determined.

lower portions of the pot increased the calcine temperature to 875 to 885°C; this necessitated decreasing the furnace temperatures in these zones. Future runs at higher heat-generation rates will require forced air cooling of the pot wall during processing to prevent excessive calcine temperatures.

Run PC-2. In this run, 940 liters of feed containing added 430,000 curies of mixed fission-product activity (of which 35,000 curies was ruthenium) was processed in a 12-in.-OD calciner pot to a final calcine volume of about 105 liters for a volume reduction (feed to calcine) of about 9. This waste would be equivalent to processing 2.3 metric tons of 20,000-Mwd power-reactor fuel that had been allowed to cool for 6 years. Heat generation (1500 watts) in the calcine during calcination produced a noticeable increase in the internal pot temperature. When the pot wall temperature reached the furnace operation temperature (850°C), the furnace temperature was reduced to prevent calcine temperatures in excess of 850°C.

The self-generating heat density of the calcine product was 16.5 watts/liter. At equilibrium, with the pot in a cool furnace, the maximum centerline temperature of the pot was 485°C, and the temperature drop from the center line of the pot to its wall was 235°C. Self-pressurization in the calciner pot after sealing was less than 1 psi.

Run PC-3. In this run an 8-in.-OD pot, also fabricated of 304L stainless steel, was used for the calcination of 553 liters of feed containing added 375,000 curies of mixed fission-product activity (including 32,000 curies of ruthenium). A calcine volume of 60 liters was produced for a volume reduction of ~9. This waste would be equivalent to processing 1.4 metric tons of 20,000-Mwd power-reactor fuel that had been allowed to cool for 3.3 years. Internal heat generation (1800 watts) in the 8-in.-OD pot did not produce the increase in pot wall temperature that was experienced with the 12-in.-OD units in the other two runs.

The self-generating heat density of the calcine product amounted to 30 watts/liter. Equilibrium pot temperatures were similar to those found for the 12-in.-OD pot of run PC-2. Self-pressurization of the sealed 8-in.-OD pot was also less than 1 psi.

General

ION-EXCHANGE RECOVERY OF CESIUM FROM PUREX-PROCESS WASTES

Two recent PNL reports discuss the application of inorganic ion exchangers to the recovery of ^{137}Cs from alkaline[6] and acidic[7] wastes.

Alkaline Wastes. Acidic wastes from the Purex process at PNL are concentrated, treated with excess sodium hydroxide, and stored in underground mild-steel tanks.[6] Most of the fission products precipitate and settle to the bottom of the tanks, but cesium and sodium remain in solution. Recovery of the cesium from these wastes is accomplished by passing the alkaline supernatant directly through a bed of Decalso (an aluminosilicate-gel ion exchanger). The cesium-loaded Decalso is then shipped by rail to ORNL where the cesium is eluted, purified further, and encapsulated. Approximately 3 megacuries of cesium has been shipped to ORNL since 1961.

The initial laboratory work on this recovery process was completed in 1960. Since then, changing feed compositions in the various waste tanks at the PNL waste tank farm have required the continuation of laboratory investigations. Bray[6] has summarized the results of these investigations relative to the variables that affect the cesium-loading characteristics of Decalso:

1. *Sodium-to-Cesium Mole Ratio.* The loading of cesium is dependent on the sodium-to-cesium mole ratio. Loadings of 200 g of cesium per liter of exchanger were obtained when sodium was absent, whereas cesium loadings were only 0.8 g/liter at a mole ratio of sodium to cesium of 10,000.

2. *Temperature.* The temperature of the influent solution to the ion exchanger represents a major variable in the cesium loadings from the Purex alkaline supernatant which contains a sodium-to-cesium mole ratio of approximately 10,000. At these levels a decrease in temperature from 50°C to 25°C or 6°C increased the loading by 70 or 190%, respectively.

3. *Influent pH.* The cesium loading is also affected by the *p*H of the alkaline waste. Increasing the *p*H from 10.8 to 12, 12.5, or 13 decreased the cesium loading by 8.5, 27, or 42%, respectively. Below a *p*H of 12, earlier work[8] had shown that the loss of loading was slight.

4. *Resin Pretreatment.* Before being used, the Decalso is pretreated with NH_4NO_3. The cesium is eluted also with $5\,M$ NH_4NO_3. Thus the resin is usually in the NH_4^+ form after each loading–elution cycle. The effect of several different pretreatments on cesium loadings was determined. The loading on the Na^+-form "as-received" resin was compared with resin treated with $1\,M$ NaOH, $1\,M$ $NaNO_3$, or $1\,M$ NH_4NO_3 for a period of 24 hr. The cesium retained was 97% for NaOH-treated resin, 122% for $NaNO_3$-treated resin, and 130% for NH_4NO_3-treated resin.

5. *Flow Rate of the Influent Solution.* Cesium loadings on Decalso increase with decreasing flow rate [column volumes (CV) per hour]. The loadings at 0.5 C/C_0 show* that a flow-rate decrease from 11.4 to 0.59 CV/hr increased the loading by about 40%.

6. *Effect of Aluminum Concentration.* It was found that aluminum salts present in the waste solution precipitated and plugged the Decalso resin bed under

*C/C_0 is the ratio of the activity level in the effluent to the activity level in the influent.

certain conditions of pH, aluminum concentration, and temperature. However, diluting the alkaline supernatant with water (feed-to-water ratio of 5:1) prior to cooling was effective in preventing precipitation at temperatures as low as 6°C.

Acid Wastes. In the PNL waste-management program, the acid wastes are treated with an excess of sodium hydroxide and then stored as an alkaline waste. As noted above, an ion-exchange procedure utilizing Decalso has been developed to remove cesium from alkaline wastes. Several cation exchangers are now available that are capable of recovering cesium from highly acidic solutions. Among these are two phosphate exchangers recently introduced and studied by the Société d'Études, de Recherches et d'Applications pour l'Industrie (SERAI, Brussels, Belgium) under the registered trade name ABEDEM TiA (PhTiA) and ABEDEM Sn (PhSn).[9] Jones[7] has reported on the preliminary studies conducted to determine the cesium capacities and relative selectivities and capabilities of these two cation exchangers. Some of the results of these studies are as follows:

1. *Equilibrium Studies.* Equilibrium cesium capacities were determined for H^+-form exchangers in multi-cation systems (in the presence of Na, Ce, Sr, Fe, and hydrogen ions). Generally PhTiA exhibited a higher cesium selectivity than PhSn. The cesium capacity of the exchangers in a $1 \times 10^{-3} M$ $CsNO_3$ solution at 25°C was found to be 0.45 meq per gram of PhTiA and 0.10 meq per gram of PhSn. The variation of the cesium capacity with increased acid and cesium concentrations was investigated using a synthetic Purex acid waste (PAW).* A decreased capacity with increased acidity and increased capacity with increased cesium concentration were noted for both exchangers.

2. *Kinetic Studies.* Column studies, performed with synthetic PAW, were carried out to determine cesium column capacities as a function of acid and cesium concentrations. The same relative dependence as derived from equilibrium data was found in the kinetic studies. The PhTiA exhibited a high cesium sorption rate. It showed essentially no change in capacity at 50% breakthrough at effluent flow rates up to 16 CV/hr, and its 50% breakthrough capacities were usually about 60% of the equilibrium values.

3. *Elution Studies.* Elution studies were made on both exchangers using various eluting agents such as NH_4Cl, NH_4NO_3, NH_4OH, $(NH_4)_2CO_3$, and NH_4NO_3–HNO_3. Of the various agents tested, NH_4NO_3 was found to be the most suitable. Elution at elevated temperatures (55°C) removed cesium more efficiently than elution at room temperature. A proposed procedure for cesium removal would consist of column loading at room temperature followed by cesium elution using $5M$ NH_4NO_3 at elevated temperatures (55°C).

4. *Hot-Cell Experiment.* A hot-cell run to investigate the cesium loading of PhTiA was made using actual PAW. The results of this run indicate that a fast and efficient cesium-recovery process can be established using this exchanger.

*Purex acid waste (PAW) is high in acid ($2M$ to $4M$) and sodium ($1.5M$) and contains lesser amounts of Fe, Al, Cr, and Ni. Among the radioactive constituents present are cesium, strontium, and rare earths.

Selected Current Literature

Solvent extraction processes are being used to recover useful fission products from process solutions generated in the reprocessing of spent nuclear fuel. The solvent extraction of various fission products will be covered in a series of articles prepared for publication in *Isotopes and Radiation Technology*, one of four Technical Progress Reviews published by the AEC. The first of these articles[10] discusses in detail the solvent extraction of ^{90}Sr with di-(2-ethylhexyl) phosphoric acid diluted with kerosene.

References

1. *Reactor Fuel-Process. Technol.*, 10(3): 253-256 (Summer 1967).
2. A. M. Platt (Ed.), Research and Development Activities, Fixation of Radioactive Residues, Quarterly Progress Report, Pacific Northwest Laboratory.
   a. October–December 1966, USAEC Report BNWL-410, pp. 13-18, April 1967.
   b. January–March 1967, USAEC Report BNWL-434, pp. 12-15, June 1967.
3. A. M. Platt (Ed.), Research and Development Activities, Fixation of Radioactive Residues, Quarterly Progress Report, Pacific Northwest Laboratory.
   a. October–December 1966, USAEC Report BNWL-410, pp. 7-13, April 1967.
   b. January–March 1967, USAEC Report BNWL-434, pp. 11 and 12, June 1967.
4. A. M. Platt (Ed.), Research and Development Activities, Fixation of Radioactive Residues, Quarterly Progress Report, Pacific Northwest Laboratory.
   a. October–December 1966, USAEC Report BNWL-410, pp. 2-7, April 1967.
   b. January–March 1967, USAEC Report BNWL-434, pp. 3-11, June 1967.
5. A. M. Platt (Ed.), Research and Development Activities, Fixation of Radioactive Residues, Quarterly Progress Report, January–March 1967, USAEC Report BNWL-434, p. 2, Pacific Northwest Laboratory, June 1967.
6. L. A. Bray, Recovery of Cesium from Purex Alkaline Waste with a Synthetic Zeolite, USAEC Report BNWL-288, Pacific Northwest Laboratory, June 1967.
7. Y. V. Jones, A Preliminary Study of Cesium Sorption from Acid Waste Solutions Utilizing Phosphate Exchangers, USAEC Report BNWL-270, Pacific Northwest Laboratory, November 1966.
8. H. H. Van Tuyl and L. A. Bray, Recovery of Cesium from Purex Tank Farm Supernatant Solution by Ferrocyanide Precipitation and Absorption on Decalso, USAEC Report HW-70874, Hanford Atomic Products Operation, Oct. 18, 1961.
9. *Reactor Fuel Process.*, 9(4): 226 (Fall 1966).
10. *Isotop. Radiat. Technol.*, 4(3): 214-222 (Spring 1967).

Index

Reactor and Fuel-Processing Technology

Volume 10

Note: The page range for each of the four issues of Vol. 10 is as follows:

No. 1, pages 1 to 92
No. 2, pages 93 to 179
No. 3, pages 181 to 258
No. 4, pages 259 to 321

NUCLEAR SCIENCE ABSTRACTS

The U. S. Atomic Energy Commission, Division of Technical Information, publishes *Nuclear Science Abstracts* (*NSA*), a semimonthly journal containing abstracts of the literature of nuclear science and engineering.

NSA covers (1) research reports of the U. S. Atomic Energy Commission and its contractors; (2) research reports of government agencies, universities, and industrial research organizations on a worldwide basis; and (3) translations, patents, books, and articles appearing in technical and scientific journals.

Complete indexes covering subject, author, source, and report number are included in each issue. These are cumulated quarterly, semiannually, and annually providing a detailed and convenient key to the literature.

Availability of *NSA*

SALE *NSA* is available on subscription from the Superintendent of Documents, U. S. Government Printing Office, Washington, D. C., 20402, at $30.00 per year for the semimonthly abstract issues and $22.00 per year for the four cumulated-index issues. Subscriptions are postpaid within the United States, Canada, Mexico, and all Central and South American countries, except Argentina, Brazil, Guyana, French Guiana, Surinam, and British Honduras. Subscribers in these Central and South American countries, and in all other countries throughout the world, should remit $37.00 per year for subscriptions to semimonthly abstract issues and $25.00 per year for the four cumulated-index issues.

EXCHANGE *NSA* is also available on an exchange basis to universities, research institutions, industrial firms, and publishers of scientific information. Inquiries should be directed to the Division of Technical Information Extension, U. S. Atomic Energy Commission, P. O. Box 62, Oak Ridge, Tennessee, 37830.

TECHNICAL PROGRESS REVIEWS may be purchased from Superintendent of Documents, U. S. Government Printing Office, Washington, D. C., 20402. *Nuclear Safety* at $3.50 per year (six issues) for each subscription or $0.60 per issue; each of the other journals at $2.50 per year (four issues) or $0.70 per issue. The use of the coupon below will facilitate the handling of your order.

POSTAGE AND REMITTANCE: Postpaid within the United States, Canada, Mexico, and all Central and South American countries except Argentina, Brazil, Guyana, French Guiana, Surinam, and British Honduras. For these Central and South American countries and all other countries: add, for each annual subscription, $1.00 for *Nuclear Safety* and $0.75 for each of the other journals; for single issues, add one-fourth of the single-issue price. Payment should be by check, money order, or document coupons, and MUST accompany order. Remittances from foreign countries should be made by international money order or draft on an American bank payable to the Superintendent of Documents or by UNESCO book coupons.

order form

SUPERINTENDENT OF DOCUMENTS
U. S. GOVERNMENT PRINTING OFFICE
WASHINGTON, D. C., 20402

Enclosed:

document coupons ☐ check ☐ money order ☐

Charge to Superintendent of Documents No. _____

Please send a one-year subscription to

☐ ISOTOPES AND RADIATION TECHNOLOGY
☐ NUCLEAR SAFETY
☐ REACTOR AND FUEL-PROCESSING TECHNOLOGY
☐ REACTOR MATERIALS

SUPERINTENDENT OF DOCUMENTS
U. S. GOVERNMENT PRINTING OFFICE
WASHINGTON, D. C., 20402

(Print clearly)

_____
Name

_____
Street

_____
City, State, ZIP Code